Uniform Field Distribution Using Distributed Magnetic Structure

Jayashree Keezhanatham Seshadri

Thesis submitted to the faculty of the Virginia Polytechnic Institute and State University in partial fulfillment of the requirements for the degree of

Master of Science

In

Electrical Engineering

Approved

Paul Plassmann (Chair)

Mantu Hudiat

Disapproved

Guo Quan Lu

September 30th, 2011

Blacksburg, Virginia

Key Words: constant flux, constant-flux inductor, low temperature co-fired ceramic, low-profile magnetics, quality factor, transformer

Uniform Field Distribution Using Distributed Magnetic Structure

Jayashree Keezhanatham Seshadri

Abstract

Energy distribution in a conventional magnetic component is generally not at a designer's disposal. In a conventional toroidal inductor, the energy density is inversely proportional to the square of the radius. Thus, a designer would be unable to prescribe uniform field distribution to fully utilize the inductor volume for storing magnetic energy.

To address this problem a new inductor design, called a "constant-flux" inductor, is introduced in this thesis. This new inductor has the core and windings configured to distribute the magnetic flux and energy relatively uniformly throughout the core volume to achieve power density higher than that of a conventional toroidal inductor. The core of this new inductor design is made of concentric cells of magnetic material, and the windings are wound in the gaps between the cells. This structure is designed to avoid crowding of the flux, thus ensuring lower core energy losses. In addition, the windings are patterned for shorter length and larger area of cross-section to facilitate lower winding energy losses.

Based on this approach, a set of new, constant flux inductor/transformer designs has been developed. This design set is based on specific input parameters are presented in this thesis. These parameters include the required inductance, peak and rms current, frequency of operation, permissible dc resistance, material properties of the core such as relative permeability, maximum permissible magnetic flux density for the allowed core loss, and Steinmetz parameters to compute the core loss. For each constant flux inductor/transformer design, the winding loss and

core loss of the magnetic components are computed. In addition, the quality factor is used as the deciding criterion for selection of an optimized inductor/transformer design.

The first design presented in this thesis shows that for the same maximum magnetic field intensity, height, total stored energy, and material, the footprint area of the new five-cell constant-flux inductor is 1.65 times less than that of an equivalent conventional toroidal inductor. The winding loss for the new inductor is at least 10% smaller, and core loss is at least 1% smaller than that in conventional inductors. For higher energy densities and taller inductors, an optimal field ratio of the dimensions of each cell ($\alpha = R_i min/R_i max$) and a larger number of cells is desired. However, there is a practical difficulty in realizing this structure with a larger number of cells and higher field ratio α. To address this problem, an inductor design is presented that has a footprint area of a three-cell constant-flux inductor ($\alpha = 0.6$) that is 1.48 times smaller in comparison to an equivalent conventional toroidal inductor. For the same maximum magnetic flux density, height, material, and winding loss, the energy stored in this new three-cell constant-flux inductor ($\alpha = 0.6$) is four times larger than that of an equivalent conventional toroidal inductor.

Finally, new designs for application-specific toroidal inductors are presented in this thesis. First, a constant-flux inductor is designed for high-current, high-power applications. An equivalent constant-flux inductor to a commercially available inductor (E70340-010) was designed. The height of this equivalent inductor is 20% less than the commercial product with the same inductance and dc resistance. Second, a constant-flux inductor design of inductance 1.2 μH was fabricated using Micrometal-8 for the core and flat wire of 0.97 mm x 0.25 mm for the conductor. The core material of this inductor has relative permeability < 28 and maximum allowed flux density of 3600 Gauss. The dc resistance of this new, constant flux inductor was measured to be 14.4 mΩ.

Acknowledgement

I would like to thank my parents for their love, support, and encouragement to let me pursue my dreams.

I am very grateful to my advisor, Prof. Khai Ngo for his guidance and support. He has been a great source of inspiration and an excellent mentor. I am extremely privileged to have him as my advisor.

I would like to thank Dean DePauw, Ennis McCrery, and Dr. Plassmann for their support, help, and guidance. I would like to express my gratitude to the members of thesis committee, Dr. Lu and Dr. Hudait for their guidance.

Many thanks to all the members of the research group: Xiao Cao, Yiying Yao, Li Jiang, Craig Xiao, Tao Tao, Di Xu, Woochan Kim, Yin Wang, Jason Zheng, Jesus Calata, and Wenli Zhang. I would also like to thank Mingkai, for helping me time and again. I am grateful to all the CPES staff and students. Special thanks to Dave and David from ESM machine shop, VT.

I would like to thank my friends Ravi, Navaneeta, Nevedetha, Lakshmi, Shraddha, Siddharth, and Sridhar for their invaluable help in numerous occasions.

Special thanks to Madhumitha, Shantanu, Roshan, Vaishnavi, Sharanya, Tejaswini, and Mithila who have been a pillars of support all through the journey.

Last but not least, thanks to Vijay for his support and understanding.

Contents

NOMENCLATURE

A	Empirical exponent for frequency in Steinmetz equation
A	Ratio of minimum to maximum magnetic field in a cell (Hmin/ Hmax)
α_optimal	α for which maximum energy is stored in a constant-flux/constant-width inductor for given ncell, height
Area	Cross-sectional area of the winding
Bmax	Maximum flux density in each cell
B	Empirical exponent for magnetic flux density in Steinmetz equation
Cell	Each ring of core is defined as a cell
DCR	Dc resistance of the winding
E	Normalized height (H/R_o)
E	Energy stored in the inductor
E_{base}	Base energy for normalization
E_{norm}	Normalized energy
F	Frequency of operation
Γ	Normalized winding-window width (W_w/R_o)
H	Height of the core
H	Total height of the inductor
$H_i$min	Minimum magnetic field in i^{th} cell
Hmax	Maximum magnetic field in each cell
I	Peak current through the inductor
Irms	Root mean square (RMS) value of the current through the inductor
K	Steinmetz parameter
Ku	Clearance factor between the turns of the winding
ku_2	Clearance factor for the winding in the winding-window width
length	Length of conductor in the constant-flux inductor
L	Inductance of the inductor
Ll	Leakage inductance of a transformer

Lm	Magnetizing inductance of a transformer
N	Total number of turns (seen by outer most cell)
N_c	Number of turns in conventional toroidal inductor
ncell	Total number of cells in the magnetic component
Ne	Effective turns ratio
n_i	Number of turns between i^{th} and $i\text{-}1^{th}$ cell
N_i	Number of turns enclosed by i^{th} cell
ρ	Resistivity of the conductor
Ploss	Winding loss (I^2R loss)
$Ploss_{base}$	Base winding Loss
$Ploss_{norm}$	Normalized winding loss
Pcore	Core loss
$Pcore_{base}$	Base core loss
$Pcore_{norm}$	Normalized core loss
Q	Quality factor
$R_1,R_2\ldots R_{ncell}$	Radii of the cells of the inductor (1- outermost cell, ncell-innermost cell)
$R_i$max	Maximum radius of the i^{th} cell
$R_i$min	Minimum radius of the i^{th} cell
R_o	Outer radius of inductor (used to compute footprint area)
R_{in}	Inner radius of inductor
tcu	Thickness of conductor
μ	Permeability of the core material
Width	Width (of the core) in each cell
W_w	Width of the winding window between two cells of the constant-flux inductor

1 INTRODUCTION

Power inductors and transformers are essential components in power supplies such as dc-dc converters. During the on-period of the switch in these circuits, the power inductors store energy in the form of magnetic flux, and during the off-period this stored energy is supplied to the load. A common situation is that the current through the magnetic components in these circuits is generated by a high dc bias voltage that includes high frequency ac ripple [1]. Because of hysteresis and eddy currents in the core, some of the power transferred by the magnetic component is lost for this situation. This inefficiency forms the "core loss." An important property of this effect is that an increase in the frequency of operation results in an increase in the core loss.

A constraint in the design of an inductor is that the core of the magnetic components cannot saturate or heat up and should provide the required inductance for a given current rating. The I^2R power loss in the winding causes heating of the winding and constitutes the "winding loss." With an increase in operating frequency, the effective cross-sectional area of the current carrying conductor is reduced due to skin effect, which results in an increase in the winding loss. Furthermore, these magnetic components often have the largest footprint area on the power supply circuit board. The footprint of magnetic components can be reduced; however, with an increase in the frequency of operation, there is a trade-off of an increase in power loss because of this winding loss property [2]. To address the problem of decreasing the footprint of magnetic components on these circuits, there is a demand for low-profile, high-power density, low-loss magnetic components that can store maximum energy in the least volume.

1.1 Flux Density Distribution

When current flows through the inductor windings of an inductor, energy is stored in the form of magnetic flux in the inductor's core. In an ideal inductor, a uniform flux distribution in

the core implies uniform energy distribution. However, in conventional, real-world magnetic cores, the magnetic flux distribution is not uniform [3-5].

Based on Ampere's law, in a conventional toroidal inductor, the energy density is inversely proportional to the square of the radius. As a result, a higher energy density is achieved near the inner radius when compared to that near the outer radius. Thus, the inductor volume is not equally utilized to store the magnetic energy. Fig. 1 (a) shows a commercial toroidal inductor, and in Fig. 1(b) we illustrate a cross-section of a model of this inductor where the cross-section is taken to be orthogonal to the direction of the flow of current in the inductor's windings.

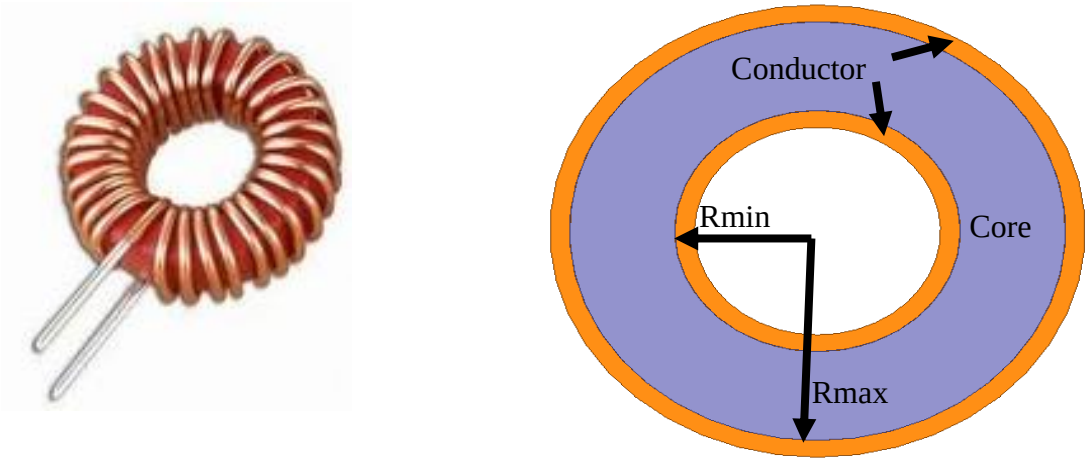

(a) (b)

Fig. 1. (a) Commercial conventional toroidal inductor; (b) Cross-section (orthogonal to direction of current flow) of a toroidal The model parameters for the commercial inductor shown in (a) are Rmax = 12.5 mm, Rmin = 7.2 mm, and height = 0.5 mm.

Consider a toroidal inductor of outer radius Rmax, inner radius Rmin, number of turns of the conductor $N_{c,}$ and carrying current I. Using Ampere's law, the magnetic field at any radius r in the toroidal core, H(r), can be solved for as follows.

$$\oint H(r).\,dl = N_c I \tag{1}$$

$$H(r) * 2\pi r = N_c I \tag{2}$$

$$H(r) = \frac{N_c I}{2\pi r} \tag{3}$$

Thus, when the radius varies in this formula for H(r) from Rmin to Rmax, the magnetic field decreases from Hmax to Hmin, where these values are computed as follows.

$$\mathrm{Hmax} = \frac{\mathrm{N_c I}}{2\pi \mathrm{Rmin}} \tag{4}$$

$$\mathrm{Hmin} = \frac{\mathrm{N_c I}}{2\pi \mathrm{Rmax}} \tag{5}$$

The energy and energy density within the core can also be computed. With H(r) as the magnetic field at any radius r in the core, B(r) as magnetic flux density at radius r in the core with outer radius Ro of the inductor (inclusive of the winding thickness wrapping the core), inner radius Rin of the inductor (inclusive of winding thickness wrapping the core), and μ as the permeability of the material, the energy stored in the magnetic component can be computed as follows.

$$\mathrm{E} = \int_{R_{in}}^{R_o} \frac{1}{2} \mathrm{B(r).H(r)} dv \tag{6}$$

$$\mathrm{B} = \mu \mathrm{H} \tag{7}$$

$$\mathrm{E} = \int_{R_{in}}^{R_o} \frac{1}{2} \mu . \mathrm{H(r)}^{\,2} dv \tag{8}$$

$$\mathrm{E} = \int_{R_{in}}^{R_o} \frac{1}{2} \mu . \left(\frac{\mathrm{N_c I}}{2\pi \mathrm{r}}\right)^{2} dv \tag{9}$$

From equation (9) and Fig. 2(b), we note that the energy density is inversely proportional to the square of the radius, r. As such, the capability of the magnetic core material to store magnetic energy is not fully utilized because the energy density is not constant throughout the core. This variation in magnetic field and energy density is illustrated in Fig. 2 (a) and (b).

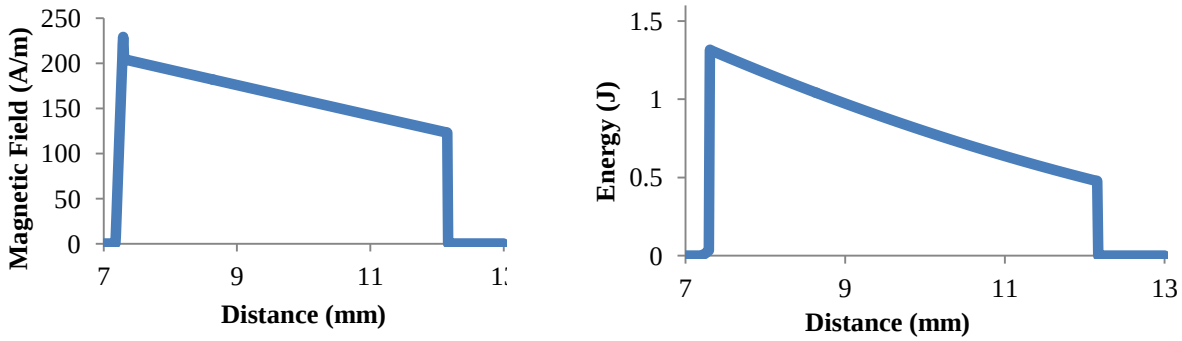

(a) (b)

Fig. 2 (a) Distribution of magnetic field as a function of r based on equation (3); (b) Distribution of energy within the core as a function of r based on equation (9). The equation parameters used are based on a conventional toroidal inductor with Rmax = 12 mm, Rmin = 7.2 mm, height = 0.5 mm, I = 1 A, N_c = 10, and relative permeability = 30.

In order to achieve uniform flux distribution and to accommodate the winding, manufactured toroidal cores tend to be relatively "thin." However, this thinness degrades the overall power density: the power density could be improved by decreasing the inner radius of the toroid. However, if one does this, the magnetic field distribution is no longer uniform, with flux crowding near the inner radius. This situation is illustrated in Fig. 3. As shown in this illustration, the crowding of the magnetic flux means loss of energy density not only in the high-flux region (near inner radius) owing to reduced permeability, but also in the low-flux region (near outer radius), which is not fully utilized. Flux crowding also generates hot spots/zones, further reducing the effectiveness of the core. As a result of these problems, there is a demand for an inductor design that enables a uniform distribution of the magnetic field and energy in the core without flux crowding.

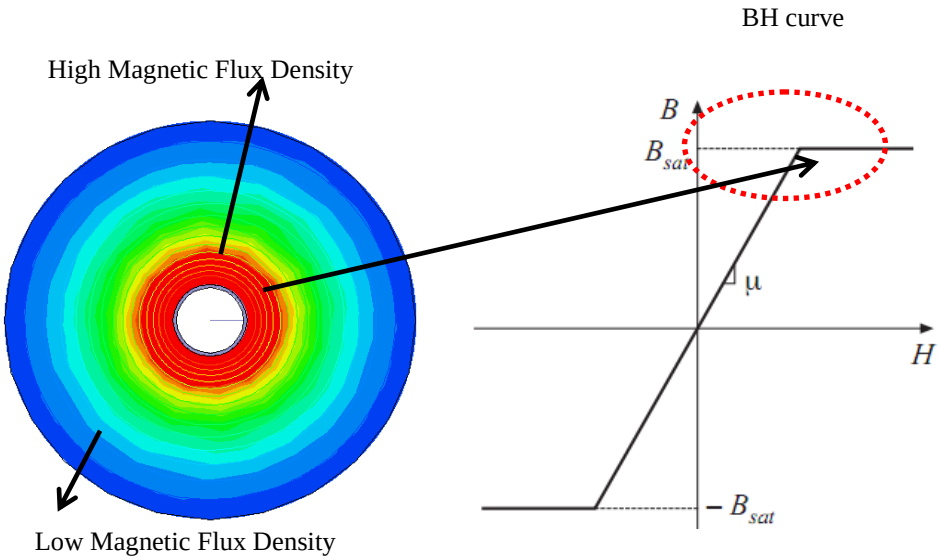

Fig. 3. High magnetic flux density near inner radius of "thick" toroidal inductor causes core saturation of the magnetic field.

To address these problems, one approach is to use multiple identical magnetic cores in the form of a "matrix core." For example, the matrix core illustrated in Fig. 4, as discussed in [6-11], consists of multiple identical magnetic cores with the winding connecting these elemental cores. Advantages of this structure include a low profile, good heat dissipation, and high efficiency. However, disadvantages of this approach include a high flux density around the conductor in each element and low flux density among elements, along with high winding loss due to the inter-element interconnections.

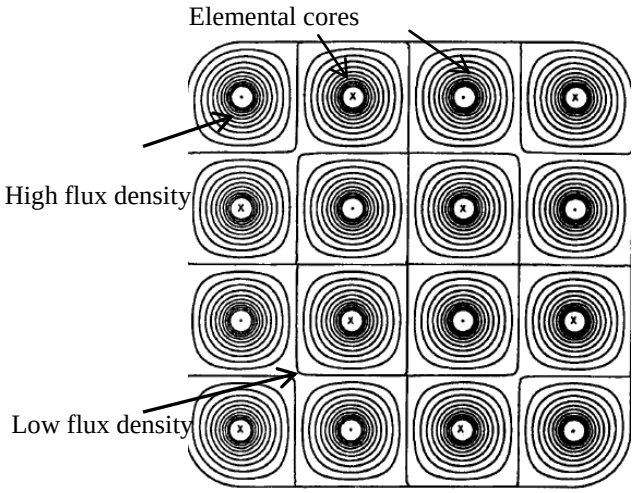

Fig. 4. A 4x4 matrix core structure. A disadvantage of this structure is the high flux density around the conductor in each element and the low flux density in between elements [9].

1.2 Losses in the Magnetic Component

As discussed earlier, the energy losses in an inductor/transformer arise from two main sources: core loss and winding loss. Core loss of the magnetic component largely depends on the material properties: the flux density distribution in the core and the frequency of operation. At low operating frequencies, hysteresis loss is the main loss source. As the operating frequency increases, loss due to eddy currents in the core begins to dominate. The specifics of these losses are dependent on the core material. Thus, the proper choice of material is essential to operate efficiently at high frequency [12-14].

Winding loss depends on the winding arrangement and consideration of eddy current effects by the designer. A number of different structures have been proposed in the past to reduce the winding loss in the windings. Improvement of winding on the surface and reduction of losses in the slots of toroidal inductors is described in [15, 16]. A meandering coil structure to reduce the length of coil and leakage flux to improve quality factor is shown in [17]. Low-profile inductor designs are described in [18]. Work done in [19-21] use thin film technology to develop low-profile inductors. Work done in [22, 23] use thick film technology, while the work in [12, 24-30]

use low-temperature co-fired ceramic (LTCC) to design low-profile, high-frequency inductors with high quality factor. An effective design to distribute windings in the core and slots to reduce winding loss is essential in order to keep the overall losses low.

1.3 Constant-Flux/Constant-Width Magnetic Component

There is a continuing strong demand in the marketplace for high-power density, low-profile magnetic components. One of the goals of this thesis is to develop a method to distribute magnetic flux relatively uniformly throughout the core and hence, avoid crowding of flux and reduce core volume. The approach we consider in this thesis is to employ a constant-flux/constant-width toroidal inductor/transformer design.

A constant-flux/constant-width toroidal inductor/transformer consists of a distributed core and winding structure. The distributed core is composed of concentric magnetic cells. The windings are wound in the gaps between the cells. The dimensions (inner and outer radius) of the cell and number of ampere-turns in each cell are decided such that there is no crowding of flux (at the inner radius). The maximum value of the magnetic flux density is such that the core loss is within the permissible limit for that material. In the winding structure, all turns start/end from the outermost circumference but can end/start at the slots other than the one at the innermost circumference. The mixture of short and long conductors helps reduce the winding loss. The number of cells in the inductor depends on the amount of energy or inductance required.

1.4 Thesis Outline

The remainder of this thesis consists of the following material. Chapter 2 introduces the concept of a distributed inductor consisting of concentric cells of magnetic material. Example designs of a constant-flux/constant-width inductor are presented and compared with an equivalent conventional toroidal inductor (ECTI). Energy and loss of a constant-flux inductor are derived in Chapter 3. Chapter 4 describes the process flow and algorithm used to design these

inductors. Chapter 5 summarizes the steps for the fabrication of a constant-flux inductor using low-temperature, co-fired ceramic (ESL-40010) material and Micrometal-8. Chapter 6 demonstrates the proof of concept for the magnetic structure and compares it with a commercial product for a high-current, high-power application. Chapter 7 introduces the concept of a constant-flux transformer. This chapter includes the procedure used for designing a transformer for a given magnetizing and leakage. A design example based on this procedure is also given in this chapter. The thesis work is summarized in Chapter 8 and is followed by suggestions for future work in Chapter 9.

2 DISTRIBUTED INDUCTOR

A distributed inductor (DI) consists of a distributed core and winding. The distributed core and winding are structured to achieve desirable distribution of the magnetic field and thus, energy. The core of the DI is made of concentric cells of magnetic material. The windings are wound in the gaps between the cells. These gaps form the slot for the conductor to pass through. Fig. 5(b) shows the cross-section of a DI with four concentric cells and slots between the cells filled with conductor, while Fig. 5(a) shows the fabricated DI with four cells of the core with a thin wire wound in the slots/gaps in between the cells.

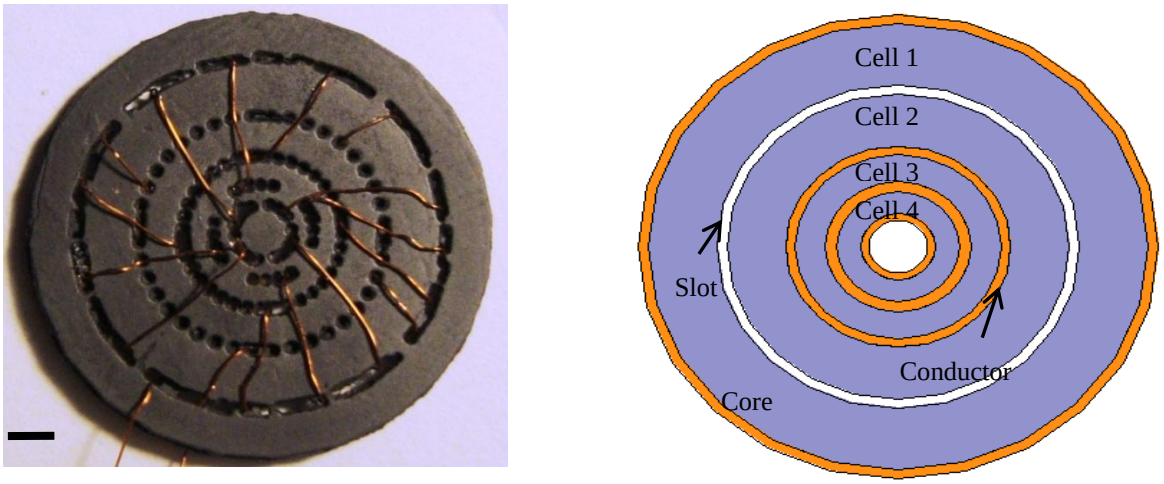

(a) (b)

Fig. 5 (a) Constant-flux inductor with four cells; (b) Cross-section (orthogonal to current flow) of constant-flux inductor with four cells showing conductor and slots.

The winding distribution for a conventional toroidal inductor and DI are shown in Fig. 6(a) and Fig. 6 (b). In the DI, the winding can start from the outermost cell. It goes on one surface of the core and through a slot in one of the inner cells. It returns along the other surface of the core and terminates at the next slot of the outermost cell. The next turn starts from this slot and continues in a similar fashion. Thus, the winding length may vary from one turn to another and depends on the inner cell to which the turn goes.

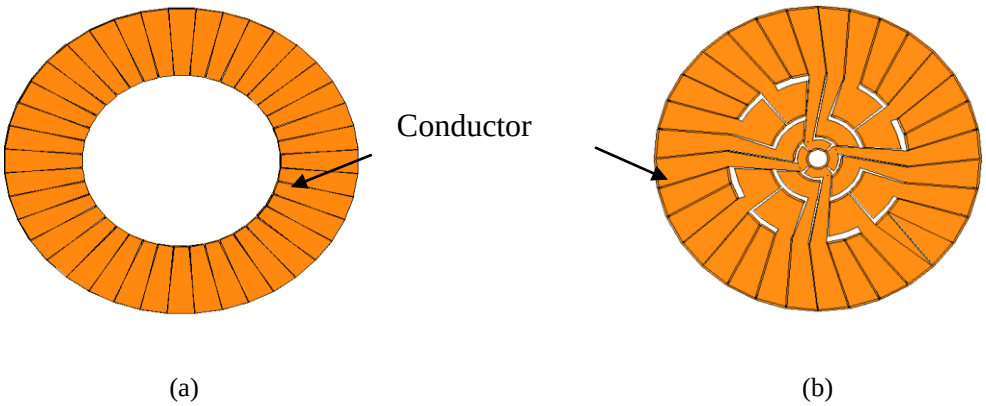

Fig. 6. Non-uniform conductors spread on the surface and in slots of a (a) Conventional core; (b) Distributed core. Only the winding distribution is shown here (not the core).

Fig. 7 shows the flow of current in a DI. A few turns of the winding is shown in the figure. Current flows from top to bottom in the conductor on the outermost cell while it flows from bottom to top in the conductor in the inner cells.

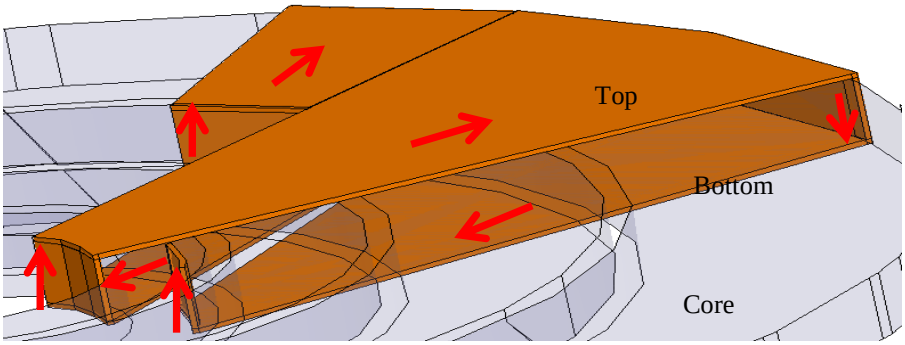

Fig. 7. Flow of current in the distributed winding in the slot and on top and bottom surfaces in a constant-flux inductor with three cells.

The lengths of the turns (of the windings) in a DI are not equal. As not all the turns in the DI span the entire width of the core (as in the conventional case), the resistance is lower. In addition, the diameter/width of the wire in the constant-flux inductor is larger than that in the conventional inductor (since the former is limited by the outermost circumference, whereas the latter is limited by the innermost circumference), further reducing the winding resistance. In order to reduce the core loss, the flux density needs to be reduced. This will also reduce the

fringing field and the associated winding loss. In addition, if the wire length could be shortened, the winding loss would be reduced naturally to compensate for the additional losses expected from proximity and fringing effects.

In order to reduce the magnetic flux density, the area of the magnetic path needs to be increased. This could be achieved by reducing the inner core diameter. The reduction is feasible since the rather large hole in the center of the toroid is underutilized. However, a core with a large radius ratio (outer radius/inner radius) would suffer from flux crowding, loss, and thermal issues near the inner radius. In the constant-flux inductor/transformer, the innermost radius and number of ampere-turns at that radius is defined by the maximum magnetic field the inductor can have for the permissible core loss. The maximum magnetic field Hmax of an inductor depends on the core material. A larger magnetic field and, thus, a larger magnetic flux density is desired to store higher energy in the core. However, with an increase in the magnetic flux density, the core loss increases for a given frequency of operation.

For a given core loss density and frequency of operation, maximum magnetic flux density Bmax can be determined. Hmax is set by the Bmax for a given material from the hysteresis curve of the material. In the linear region of the hysteresis curve of the material, well before saturation, permeability is the slope of the B-H curve:

$$\mathrm{Hmax} = \frac{\mathrm{Bmax}}{\mu} \tag{10}$$

Starting from the innermost cells (all parameters for the innermost cell are denoted by subscript ncell), the magnetic field goes down from Hmax to H_{ncell}min following Ampere's law:

$$\mathrm{Hmax} = \frac{n_{ncell} I}{2\pi R_{ncell} min} \tag{11}$$

$$H_{ncell}\mathrm{min} = \frac{n_{ncell} I}{2\pi R_{ncell} max} \tag{12}$$

When the field goes down to H_{ncell}min, it picks up more turns at almost the same radius R_{ncell}max, such that the maximum magnetic field in the second cell is equal to that of the first cell:

$$\mathrm{Hmax} = \frac{(n_{ncell} + n_{ncell-1})I}{2\pi R_{(ncell-1)}min} \tag{13}$$

$$H_{ncell-1}\mathrm{min} = \frac{(n_{ncell} + n_{ncell-1})I}{2\pi R_{(ncell-1)}max} \tag{14}$$

Thus, the R_1min can be found from R_1max. Similar formulae apply to each cell. The winding thickness (plus clearance) needs to fit between the two cells:

$$R_i\mathrm{min} - R_{i+1}\,\mathrm{max} = W_w \tag{15}$$

The ampere turns (n_iI) between $R_i$min and R_{i+1}max are given by the following formula.

$$n_iI = 2\,\pi\,\mathrm{Hmax}(R_i\mathrm{min} - R_{i+1}\mathrm{max}) \tag{16}$$

Thus, by choosing an appropriate n_i, Hmax can be maintained to be a constant in each cell. By choosing an appropriate $R_i$max, the maximum radius of each cell, $H_i$min can be set to the required value.

Number of cells ncell in the DI depends on the required inductance or energy.

$$N_i = \sum_{1}^{ncell} n_i \tag{17}$$

$$L_i = \frac{\mu * h}{2\pi} * \left[N_i{}^2 * \ln\left(\frac{R_i\mathrm{max}}{R_i\mathrm{min}}\right)\right] \tag{18}$$

$$L = \sum_{1}^{ncell} L_i \tag{19}$$

$$E = \frac{1}{2}LI^2 \tag{20}$$

Given an outer radius, the distributed core can be constructed in several ways. Two of these ways, a constant-flux distributed core and a distributed core of constant width, are discussed in sections 2.1 and 2.2.

2.1 Constant-Flux Distributed Core

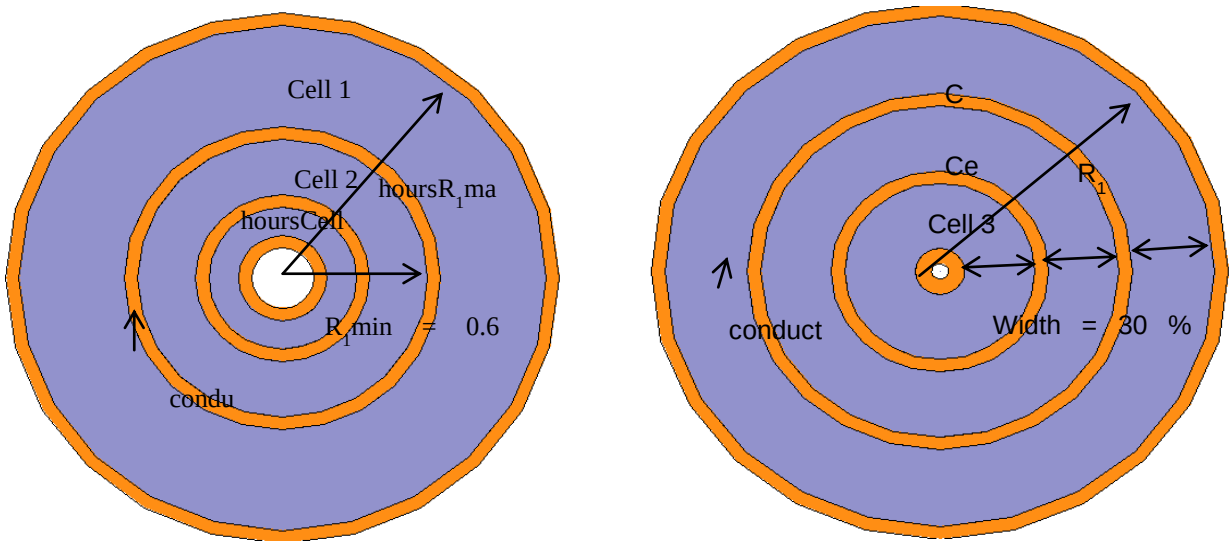

(a) (b)

Fig. 8 Comparison of constant-flux and constant-width inductors with equal footprint area/volume, energy, and core material properties. (a) Three cells of constant-flux inductor with $\alpha = 0.6$. (b) Three cells of constant-width inductor of width = 30% outer radius.

A constant-flux inductor (CFI) has a distributed core and winding structure such that the flux in each cell is uniformly distributed. This DI is also referred to as the distributed inductor with constant flux.

In this case, illustrated in Fig. 8[a], the maximum and minimum magnetic field intensities are kept constant in each cell, resulting in uniform field ratio α (ratio of minimum-to-maximum magnetic field intensity) across the cells. The magnetic field intensity is allowed to fall by α across each cell. A non-uniform field is implied by α of 0 while a uniform field is implied by α of 1.

$$\alpha = \frac{H_i min}{Hmax} = \frac{R_i min}{R_i max} \tag{21}$$

For designing a one-turn DI with constant flux, the following relations are obtained.

$$N = 1 \tag{22}$$

For a given core loss density and relative permeability of the core, Bmax is set from the data sheet of the magnetic material. Thus, Hmax for each cell is obtained from the hysteresis curve of the material in the linear region as follows.

$$Hmax = \frac{Bmax}{\mu} \tag{23}$$

In the constant-flux inductor, Hmin in each cell is equal, as Hmax and field ratio α are equal in all cells, thus we have the following relationship.

$$H_i min = Hmin = Hmax * \alpha \tag{24}$$

Given the footprint area or outermost radius R_1max, for the CFI, the minimum radius of the first cell (outermost) is given by the following formula.

$$R_1 min = R_1 max * \alpha \tag{25}$$

Assuming the winding-window width to be zero, the outer radius of the next inner cell is equal to the inner radius of the immediate outer cell. Thus, we have the following relations.

$$R_2 max = R_1 min = R_1 max * \alpha \tag{26}$$

$$R_2 min = R_2 max * \alpha = R_1 max * \alpha^2 \tag{27}$$

Generalizing these relations to the i^{th} cell (counting from the outermost cell) we have the following.

$$R_i max = R_{i-1} min = R_1 max * \alpha^{i-1} \tag{28}$$

$$R_i min = R_i max * \alpha = R_1 max * \alpha^i \tag{29}$$

The number of ampere-turns in each cell is computed using the fact that Hmax is equal in all cells:

$$\frac{N_i I}{2\pi R_i \min} = \frac{N_{i-1} I}{2\pi R_{i-1} \min} \tag{30}$$

$$N_i = N_{i-1} \frac{R_i \min}{R_{i-1} \min} = N_{i-1} \alpha \tag{31}$$

Thus, the number of ampere-turns from the center seen by the i^{th} cell is given by

$$N_i = N\alpha^i \tag{32}$$

For the one-turn design, we have the following relationship.

$$N_i = \alpha^i \tag{33}$$

2.2 Distributed Core of Constant Width

In this case, illustrated in Fig. 8(b), the core cells have uniform width. The number of ampere-turns in each cell is such that the maximum magnetic field intensity in each cell is constant. The minimum field need not be equal in each cell as α in this case is not a constant in each cell. α is higher for the outer cells, and as the radii decreases, α decreases.

For designing a one-turn DI of constant width, the following steps are observed.

$$N = 1 \tag{34}$$

For a given core loss density and relative permeability of the core, Bmax is set from the data sheet. Thus, Hmax for each cell is given by

$$\text{Hmax} = \frac{\text{Bmax}}{\mu} \tag{35}$$

Given the footprint area or the outermost radius R_1max, for the DI of constant width, the minimum radius of the cell can be obtained from R_1max

$$R_i \min = R_1 \max - \text{ width} \tag{36}$$

Assuming zero winding-window width, the outer radius of the next inner cell is almost equal to the inner radius of the immediate outer cell:

$$R_{i-1}max = R_i min = R_1 max - width \tag{37}$$

$$R_{i-1}min = R_{i-1}max - width = R_1 max - 2 * width \tag{38}$$

Thus, generalizing for any i^{th} cell (counting from the outer most cell), $R_i max$ and $R_i min$ are given by

$$R_i max = R_{i-1}min = R_1 max - (i-1) * width \tag{39}$$

$$R_i min = R_i max - width = R_1 max - i * width \tag{40}$$

For the number of ampere-turns, Hmax is equal in all cells:

$$\frac{N_i I}{2\pi R_i min} = \frac{N_{i-1} I}{2\pi R_{i-1} min} \tag{41}$$

$$N_{i-1} = \frac{N_1 * R_{i-1} min}{R_1 min} \tag{42}$$

Inductance of the one-turn DI of constant width for a material with permeability μ and height h is given by

$$L_i = \frac{\mu * h}{2\,\pi} * \left[{N_i}^2 * \ln\left(\frac{R_i max}{R_i min}\right)\right] \tag{43}$$

$$L = \sum_{1}^{ncell} L_i \tag{44}$$

$$E = \frac{1}{2} L I^2 \tag{45}$$

The maximum number of cells in a DI with constant width depends on the maximum outer radius and width. The minimum radius of the innermost cell should be greater than zero.

$$width * \ Cell\_max \leq R_1 max \tag{46}$$

$$Cell\_max \leq \frac{R_1 max}{width} \tag{47}$$

3 CALCULATIONS

This section describes the theoretical calculations of energy, core loss, and winding loss in a constant-flux inductor (CFI) or a distributed inductor of constant flux, discussed in section 2.1

3.1 Energy Stored in a Constant-Flux Inductor

Consider an ncell CFI of core material with permeability μ, height h, outer radius R_o of the inductor (inclusive of the thickness of the winding [tcu] wrapping the outermost cell), inner radius R_{in} of the inductor (inclusive of the thickness of the winding [tcu] wrapping the inner most cell), and Bmax being the maximum magnetic flux density in each cell. Energy stored in a conventional toroidal inductor is given in (6). Total energy stored in the CFI is the sum of the energy stored in each cell. Integrating the energy stored in each cell in (7) and summing it up for total energy of the inductor:

$$E = \frac{Bmax^2 \pi h}{\mu} \sum_{i=1}^{ncell} R_i min^2 \int_{R_i min}^{R_i max} \frac{dr}{r} = \frac{Bmax^2 \pi h}{\mu} \sum_{i=1}^{ncell} R_i min^2 \ln\left(\frac{R_i max}{R_i min}\right) \quad (48)$$

Minimum and maximum radii of any cell are computed in terms of outermost radius R_o by using (15) and (21) recursively:

$$R_1\,max = R_o - W_w$$

$$R_1\,min = \alpha R_1\,max = \alpha(R_o - W_w)$$

$$R_2\,min = \alpha R_2\,max = \alpha(R_1\,min - W_w) = \alpha(\alpha(R_o - W_w) - W_w)$$
$$= \alpha^2 R_o - (\alpha^2 + \alpha)\,W_w$$

$$R_i\,min = \alpha^i R_o - \left(\alpha^i + \alpha^{i-1} + \cdots + \alpha\right) W_w$$

$R_i$min can be simplified using summation of i terms in a geometric series[12]:

$$R_i \min = \alpha^i R_o - \alpha \frac{(1-\alpha^i)}{1-\alpha} W_w \tag{49}$$

The total height of the inductor is the sum of the height of the core and twice the thickness of the conductor (one for conductor wound below the core and one for the conductor wound above the core). Normalizing the winding-window width W_w, the total height of the inductor H, and the height of the core h with respect to the outermost radius of the CFI:

$$\gamma = \frac{W_w}{R_o} \tag{50}$$

$$\varepsilon = \frac{H}{R_o} \tag{51}$$

$$\frac{h}{R_o} = \frac{H}{R_o} - \frac{2W_w}{R_o} = \varepsilon - 2\gamma \tag{52}$$

Thus, rewriting the total energy (48) stored in a CFI in terms of γ, R_o, and α using (49), (50), (51), and (52):

$$E = \frac{Bmax^2\ \pi\ h\ R_o^2}{\mu} \ln\left(\frac{1}{\alpha}\right) \sum_{1}^{ncell} \left(\alpha^i - \alpha \frac{(1-\alpha^i)}{1-\alpha}\gamma\right)^2 \tag{53}$$

The total energy stored in the CFI is normalized with respect to the energy stored in a block of dimensions R_o x R_o x R_o and made of the same material and having a uniform flux density distribution Bmax throughout the core.

$$E_{base} = \frac{2\pi Bmax^2\ R_o^3}{2\mu} \tag{54}$$

$$E_{norm} = \frac{E}{E_{base}} = \frac{h}{R_o} \ln\left(\frac{1}{\alpha}\right) \sum_{1}^{ncell} \left(\alpha^i - \alpha \frac{(1-\alpha^i)}{1-\alpha} \gamma\right)^2$$

$$= (\varepsilon - 2\gamma)\ \ln\left(\frac{1}{\alpha}\right) \sum_{1}^{ncell} \left(\alpha^i - \frac{\alpha(1-\alpha^i)}{1-\alpha} \gamma\right)^2 \quad (55)$$

Fig. 9 is a plot of normalized energy stored in the CFI versus α for different winding-window widths. This plot shows that the amount of energy stored peaks for a particular α. A DI with a large α would need too many cells, and a DI with a small α would require a larger footprint or height to store the same amount of energy as the DI with optimal α for a given footprint, height, winding-window width, and number of cells. The smaller the winding-window width, the higher the energy stored for the same number of cells as there is more core material to store more energy. Optimized α needs to be chosen to store the maximum amount of energy in a CFI for a given number of cells and W_w (which depends on the thickness of the conductor).

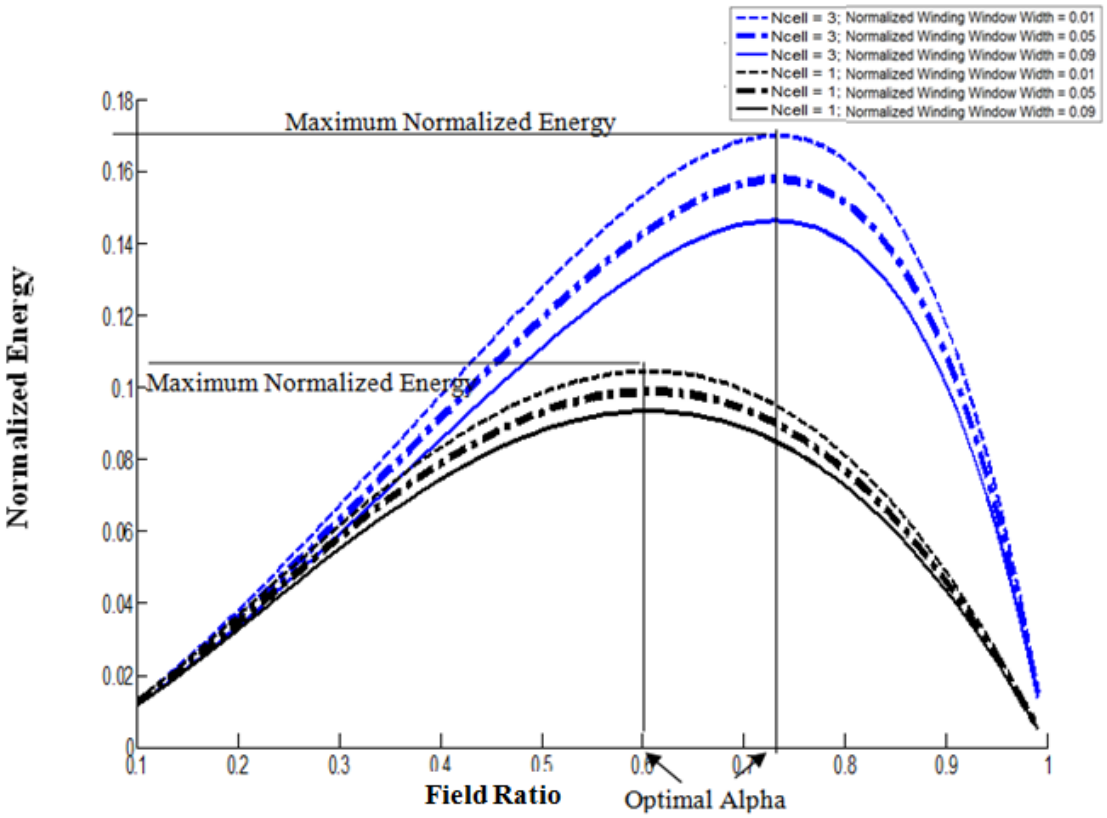

Fig. 9. Normalized energy (55) in a one-cell and a three-cell constant-flux inductor versus field ratio α for normalized winding-window width γ = 0.01, 0.05, 0.09 and normalized height ε = 0.5.

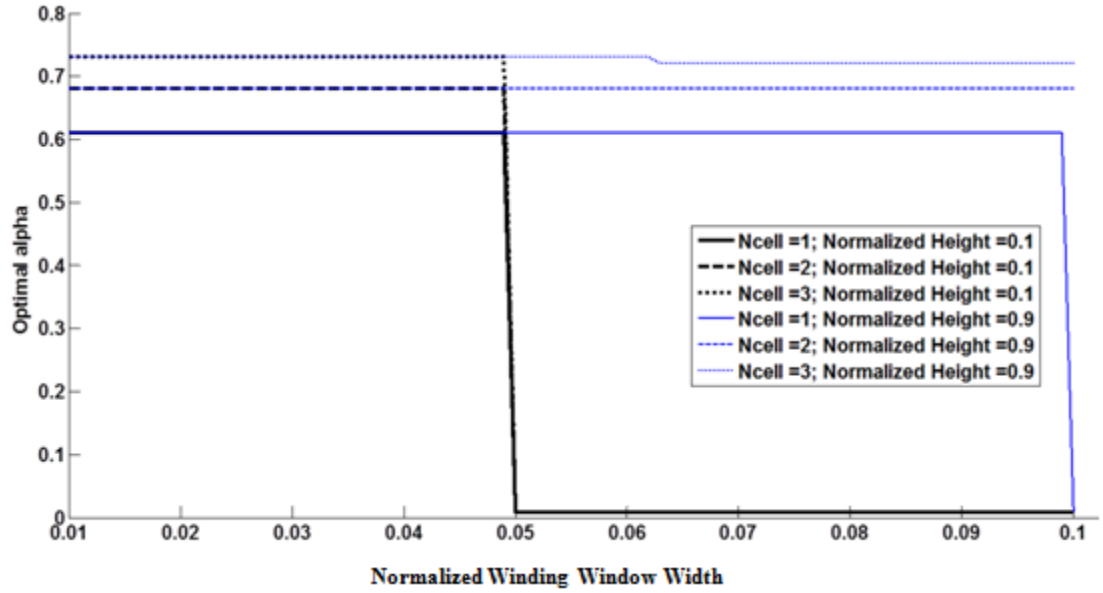

Fig. 10. Optimal field ratio at which maximum energy is stored in a DI. Optimal field ratio α for a DI varies depending on height, winding-window width, and number of cells.

Maximum normalized energy is the energy stored at α_optimal for a given number of cells, height, and winding-window width of the inductor. In Fig. 11, the maximum normalized energy is plotted against the normalized height and normalized winding-window width for CFI of ncell = 1, 2, and 3. Maximum normalized energy increases with an increase in the height of the core for a given number of cells of the inductor. Maximum normalized energy increases with an increase in ncell for a given height of the inductor. With an increase in the number of cells and an increase in the height of the core, maximum normalized energy increases as there is more core material to store more energy.

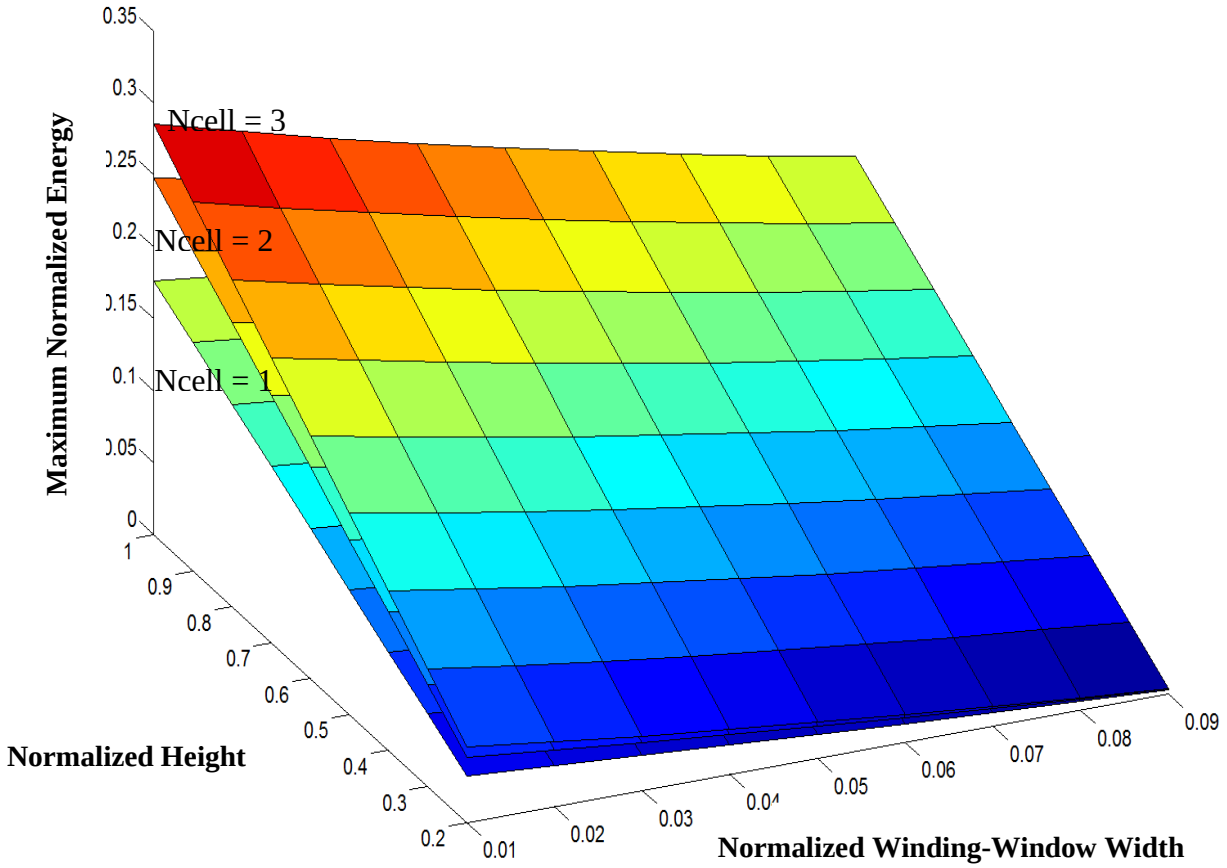

Fig. 11. Maximum normalized energy in a one, two, and three cell CFI with Bmax as maximum flux density in the core, outer radius R_o, and α_optimal. W_w and height are normalized with respect to the outer radius of the CFI as in (50) and (52). Energy is normalized with respect to the energy stored in a block of dimensions R_o x R_o x R_o made up of same material and with uniform maximum flux density Bmax throughout the core according to (55).

Maximum normalized energy of the inductor decreases with an increase in normalized winding-window width for a given number of cells of the inductor, as shown in Fig. 12. With an increase in the gap between the cells of the DI of the same footprint, the core material to store energy is reduced.

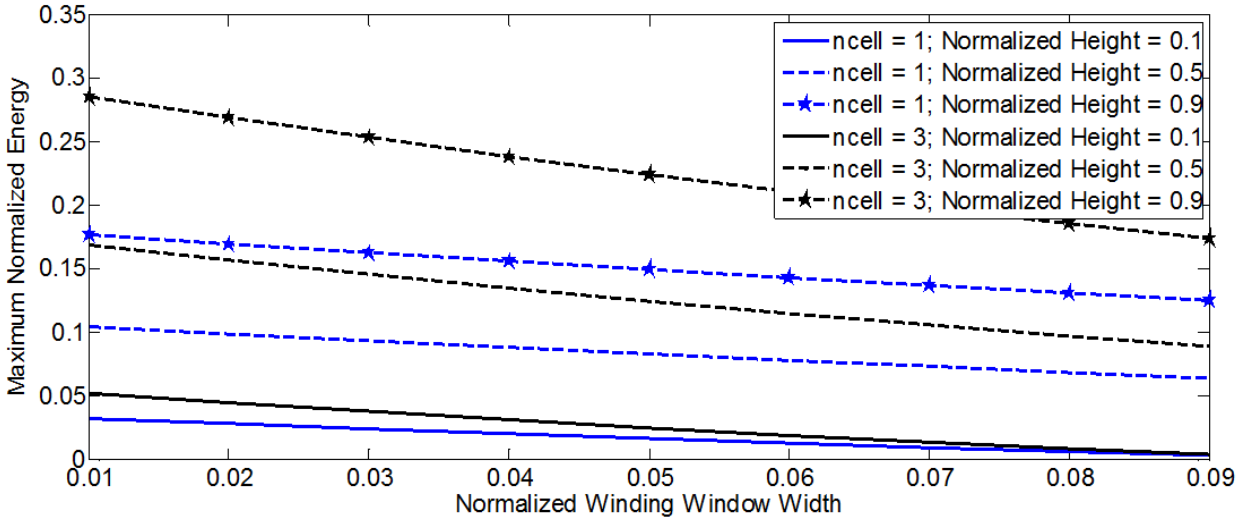

Fig. 12. Plot of maximum normalized energy in a one, two, and three cell constant-flux inductor with different normalized heights versus normalized winding-window width. W_w and height h are normalized with respect to the outer radius of the CFI as in (50) and (52). Energy is normalized with respect to the energy stored in a block of R_o x R_o x R_o made up of same material and with uniform maximum flux density Bmax throughout the core according to (55).

Thus, to store maximum energy in a distributed inductor for a given outer radius, inner radius, and number of cells, α optimal should be chosen such that the energy peaks at that field ratio α. Normalized winding-window width should be small such that it is just enough to wind the conductor (and clearance) through the slot. The maximum allowed thickness of core should be chosen such that the height of the inductor (height of the core and twice the thickness of the conductor) meets the specification.

3.2 Core Loss in a Constant-Flux Inductor

Calculation of core loss density depends on the material properties of the magnetic material under consideration. Core loss density is given by the Steinmetz equation [1]:

$$\text{Pcore}_{\text{density}} = \text{k}f^{a}B^{\beta} \tag{56}$$

where a, β, k are properties of the material and $\text{Pcore}_{\text{density}}$ in kW/m^3, f in MHz, B in mT.

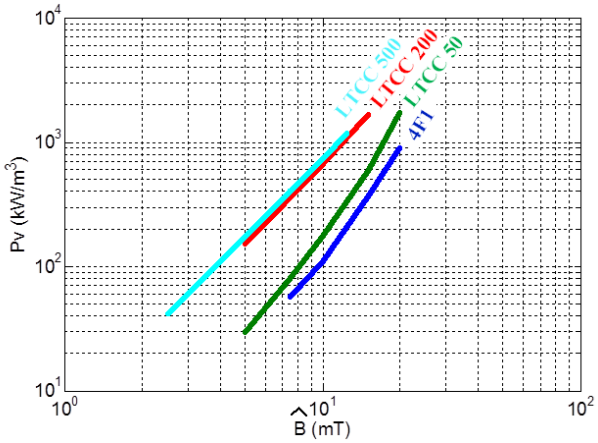

Fig. 13. Core loss density comparison of LTCC-50,200,500, and 4F1 material at 3MHz [31] for the cores immersed in oil bath at 100°C.

A plot of the core loss density versus the magnetic flux density in LTCC -50, 200, 500 and 4F1 [31] is shown in Fig. 13, and the Steinmetz parameters are listed in TABLE I.

TABLE I

Curve Fit Steinmetz Equation Parameters for LTCC-50, 200, 500 and 4F1

Material	**k**	**a**	**β**
4F1	0.0292	1.599	2.902
LTCC 50	0.1094	1.296	2.715
LTCC 200	0.3948	2.127	2.255
LTCC 500	0.3312	2.447	2.203

Magnetic flux density distribution is not uniform throughout a constant-flux core as well. Integrating the core loss throughout the volume of each cell where magnetic flux density is a function of radial distance and summing the loss in each cell for the two cases when $\beta = 2$ and $\beta \neq 2$:

if $\beta = 2$

$$\text{Pcore} = \sum_{i=1}^{\text{ncell}} \text{kf}^{a} * 2 * \pi * h * (\text{Hmax} * \mu * R_i\text{min})^2 \left(\ln\left(\frac{R_i\text{max}}{R_i\text{min}}\right)\right) \tag{57}$$

If $\beta \neq 2$

$$\text{Pcore} = \sum_{i=1}^{\text{ncell}} \frac{\text{kf}^{a} 2 * \pi * h * (\text{Hmax} * \mu * R_i\text{min})^{\beta}}{2-\beta} [(R_i\text{max}^{2-\beta} - R_i\text{min}^{2-\beta})] \tag{58}$$

Simplifying and rewriting $R_i$min, $R_i$max in terms of γ, R_o, and α using (49), (50), (51), and (52):

if $\beta = 2$

$$\text{Pcore} = \sum_{i=1}^{\text{ncell}} \text{kf}^{a} 2\pi h\, \text{Bmax}^2\, R_o^2 \left(\alpha^i - \frac{\alpha(1-\alpha^i)}{1-\alpha}\gamma\right)^2 \left(\ln\left(\frac{1}{\alpha}\right)\right) \tag{59}$$

if $\beta \neq 2$

$$\text{Pcore} = \sum_{i=1}^{\text{ncell}} \frac{\text{kf}^{a} 2\pi h \text{Bmax}^{\beta}}{(2-\beta)} R_o^2 \left(\alpha^i - \frac{\alpha(1-\alpha^i)}{1-\alpha}\gamma\right)^2 (\alpha^{\beta-2} - 1) \tag{60}$$

Normalizing the core loss with respect to core loss in a block of dimensions R_o x R_o x R_o, made of same material, having a uniform flux density distribution of Bmax throughout the core:

if $\beta = 2$

$$\text{Pcore}_{\text{base}} = \frac{2\pi \text{kf}^{a} \text{Bmax}^2\, R_o^3}{2} \tag{61}$$

if $\beta \neq 2$

$$\text{Pcore}_{\text{base}} = \frac{2\pi \text{kf}^{a} \text{Bmax}^{\beta}\, R_o^3}{2} \tag{62}$$

Thus, normalizing the core loss in (59) and (60):

$$\text{if } \beta = 2$$

$$\text{Pcore}_{\text{nom}} = \sum_{1}^{\text{ncell}} (\varepsilon - 2\gamma)\left(\alpha^{i} - \frac{\alpha(1-\alpha^{i})}{1-\alpha}\gamma\right)^{2} \left(\ln\left(\frac{1}{\alpha}\right)\right) \tag{63}$$

$$\text{if } \beta \neq 2$$

$$\text{Pcore}_{\text{norm}} = \sum_{1}^{\text{ncell}} \frac{(\varepsilon - 2\gamma)}{(2-\beta)}\left(\alpha^{i} - \frac{\alpha(1-\alpha^{i})}{1-\alpha}\gamma\right)^{2} (\alpha^{\beta-2} - 1) \tag{64}$$

Fig. 14 shows that the normalized core loss (for $\beta = 2$) versus α for different γ follows the plot for the normalized energy versus α (Fig. 11). Core loss peaks at α_optimal. Fig. 15 and Fig. 16 show plots of maximum normalized core loss versus normalized winding-window width and normalized height for $\beta = 2$ and $\beta \neq 2$. Maximum normalized core loss is the core loss at the α_optimal, which is α for which normalized energy peaks for a given normalized winding-window width, normalized height, and number of cells.

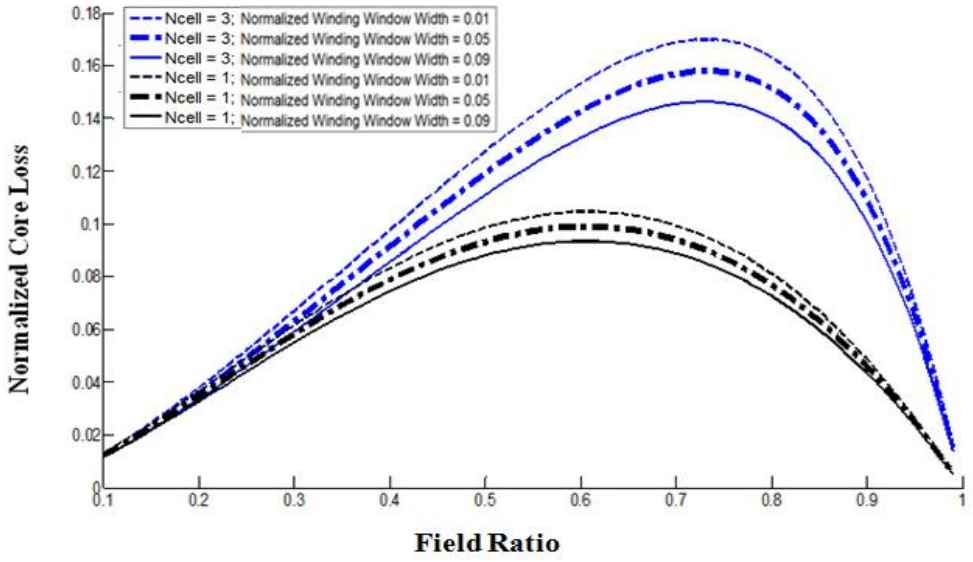

Fig. 14. Normalized core loss in a one-cell and three cell CFI with Bmax as maximum flux density in the core, outer radius R_o, $\beta = 2$ versus α for normalized height $\varepsilon = 0.5$ and normalized winding-window width $\gamma = 0.01$, 0.05, and 0.09. W_w and height are normalized with respect to the outer radius of the CFI as in (50) and (52). Core loss is

normalized with respect to the loss in a block of R_o x R_o x R_o with uniform maximum flux density Bmax throughout the core and with same material properties of the core as the CFI (a, β, k) according to (63).

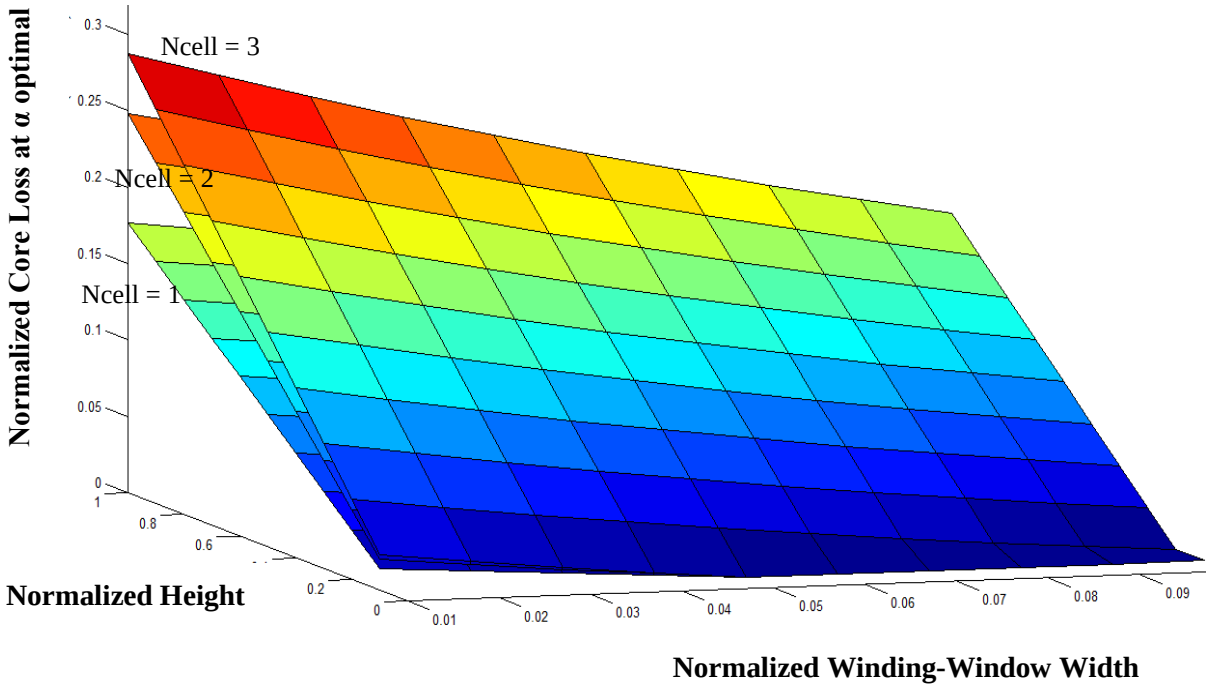

Fig. 15. Maximum normalized core loss in a one, two, and three cell CFI with Bmax as maximum flux density in the core, outer radius R_o, α_optimal, β = 2 versus normalized winding-window width and normalized height. W_w and height are normalized with respect to the outer radius of the CFI as in (50) and (52) Core loss is normalized with respect to the loss in a block of R_o x R_o x R_o with uniform maximum flux density Bmax throughout the core and same material properties of the core as the CFI (a, β, k) according to (63).

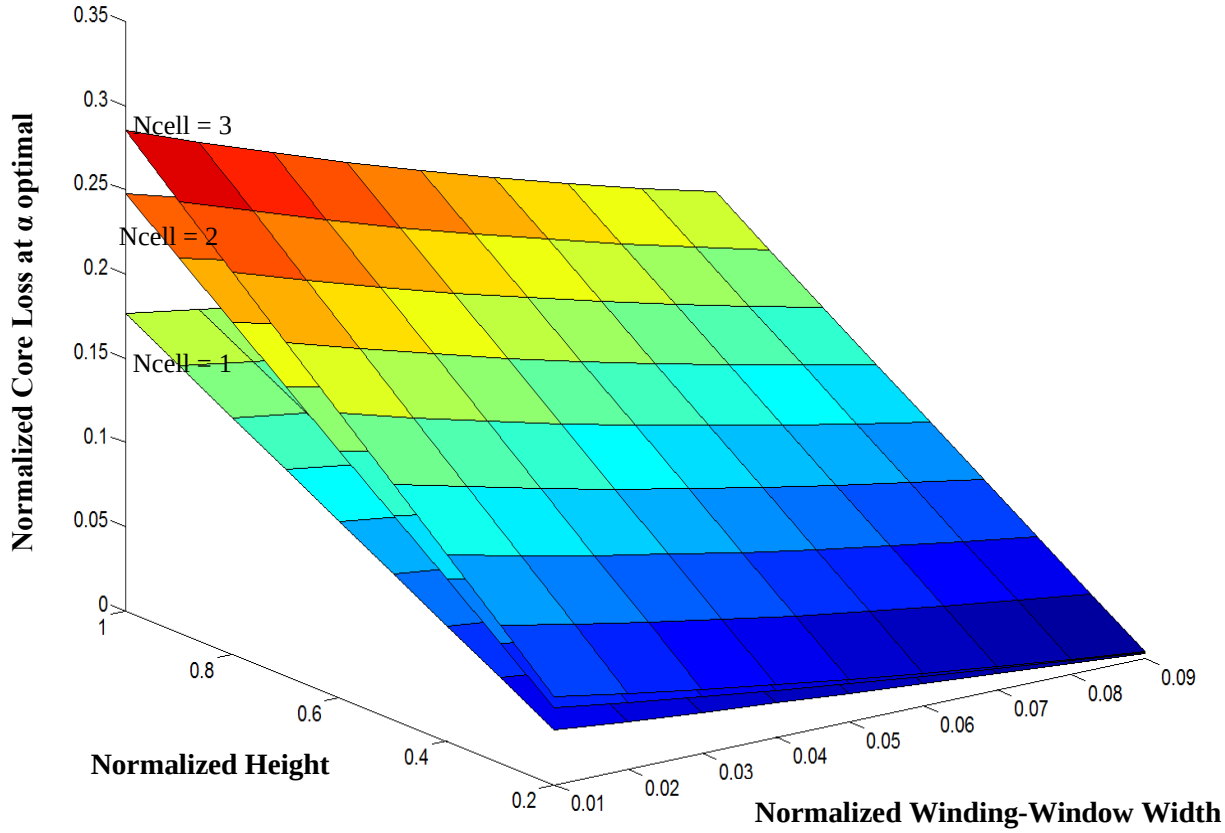

Fig. 16. Maximum normalized core loss in a one, two, and three cell CFI with Bmax as maximum flux density in the core, outer radius R_o, α_optimal, β = 2.92 versus normalized winding-window width and normalized height. W_w and height are normalized with respect to the outer radius of the CFI as in (50) and (52) Core loss is normalized with respect to the loss in a block of R_o x R_o x R_o with uniform maximum flux density Bmax throughout the core and same material properties of the core as the CFI (a, β, k) according to (64).

These plots (Fig. 14, Fig. 15, and Fig. 16) show that the maximum core loss increases with an increase in the number of cells for the same normalized height and normalized winding-window width. For an increase in the normalized height with a constant γ, maximum core loss increases. For an increase in γ with a constant core height, maximum core loss decreases. Thus, the trend of increase or decrease of core loss of a given CFI is very similar to the energy. Thus, the more the energy that is stored in the core, the more the core loss in the CFI.

3.3 Winding Loss in a Constant-Flux Inductor

The given fixed height of the inductor is shared between the height of the winding (or thickness of the winding) and the height of the core in a core-inside structure, as shown in Fig. 17.

$$H = 2 * tcu + h \tag{65}$$

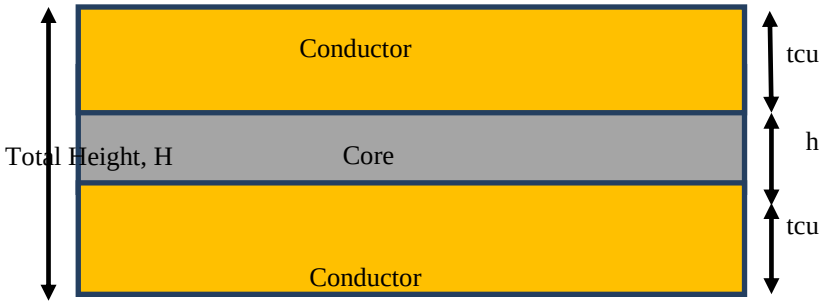

Fig. 17. Side view of an inductor with total height shared by the winding and the core.

At a high frequency of operation, the thickness of the conductor used depends on the skin depth of the conductor at that frequency. Skin depth of a conductor is given by

$$\delta = \sqrt{\frac{2\rho}{2\pi f \mu}} \tag{66}$$

Where μ, ρ are permeability and resistivity of conductor.

Skin depth of copper at 3 MHz is 30 μm. Thus, the thickness of conductor chosen is 2* skin depth i.e. 60 μm.

$$\text{tcu} = 2 * \delta \tag{67}$$

Dc Winding loss of the windings is given by

$$\text{DCR} = \frac{\rho \text{ length}}{\text{Area}} \tag{68}$$

$$\text{Winding loss} = \text{Irms}^2 \text{DCR} \tag{69}$$

Ideally, winding is spread on the surface and in the winding window. Winding loss of the distributed windings is divided into winding loss due to winding on the surfaces of the core and due to winding in the winding window along the height of the core. Assuming that conductors cover the entire surface, the outermost cell would have the windings going/coming from all the inner cells totaling N ($N_1 = N$) turns. For the next inner cell, there would be N_2 turns covering the surface and so on.

The length of the conductor is given by summing up the conductor length across each cell. The length of the conductor in terms of R_o, γ, α using (49), (50), (51), and (52) is given by

$$\begin{aligned} \text{length} &= \sum_{i=1}^{\text{ncell}} [(R_o - R_{i+1}\text{max} + h)2n_i] \\ &= \sum_{i=1}^{\text{ncell}} \left[\left(R_o - \alpha^i R_o + \frac{(1-\alpha^{i+1})W_w}{1-\alpha} + h\right)2n_i\right] \end{aligned} \tag{70}$$

Number of turns n_i of the winding seen by the i^{th} cell is given by

$$n_i = N_i - N_{i+1} = \frac{N}{R_{1\text{min}}}\,(R_i\text{min} - R_{i+1}\text{min})$$

Rewriting $R_i$min using (49) and simplifying for n_i:

$$\begin{aligned} n_i &= \frac{N}{R_1\text{min}}\left(R_o\alpha^i - \frac{\alpha(1-\alpha^i)W_w}{1-\alpha} - R_o\alpha^{i+1} + \frac{\alpha(1-\alpha^{i+1})W_w}{1-\alpha}\right) \\ &= N\frac{R_o}{R_1\text{min}}(\alpha^i - \alpha^{i+1} + \alpha^{i+1}\gamma) \end{aligned} \tag{71}$$

Thus, length (70) can be written as

$$\text{length} = \sum_{i=1}^{ncell} \left[\left(1 - \alpha^{i} + \frac{\left(1 - \alpha^{i+1}\right)\gamma}{1 - \alpha} + \varepsilon - 2\gamma \right) \frac{N\, R_o^2}{R_1 \min} \left(\alpha^{i} - \alpha^{i+1} + \alpha^{i+1}\gamma\right) \right] \tag{72}$$

The entire surface of the outer most cell is covered by the windings. Thus, the width of the winding depends on the circumference of the outermost cell and total number of turns in the CFI design.

$$\text{width} = ku * \frac{2\pi R_i \min}{N_i} = ku \frac{2\pi R_1 \min}{N} \tag{73}$$

Clearance between the turns is given by ku which is between 0 and 1.

Substituting for length (72), width (73) in (68) and (69), and using (49), (50), (51), and (52) dc resistance and winding loss are given by:

$$DCR = \frac{\rho 2N^2\, R_o^2}{2\pi R_1^2 \min\, ku\, tcu} \sum_{i=1}^{ncell} \left[\left(1 - \alpha^{i} + \frac{\left(1 - \alpha^{i+1}\right)\gamma}{1 - \alpha} + \varepsilon - 2\gamma \right) \left(\alpha^{i} - \alpha^{i+1} + \alpha^{i+1}\gamma\right) \right] \tag{74}$$

$$Ploss = \frac{\rho 2N^2\, I^2}{2\pi ku\, ku_2\, \gamma\, (\alpha - \gamma\alpha)^2 R_o} \sum_{i=1}^{ncell} \left[\left(1 - \alpha^{i} + \frac{\left(1 - \alpha^{i+1}\right)\gamma}{1 - \alpha} + \varepsilon - 2\gamma \right) \left(\alpha^{i} - \alpha^{i+1} + \alpha^{i+1}\gamma\right) \right] \tag{75}$$

where thickness of conductor is a factor of the winding-window width, such that winding can be wound around the core. Value of ku_2 varies between 0 and 1.

$$tcu = ku_2\, W_w \tag{76}$$

For normalization, we consider a R_o x R_o x R_o box made of same material as the conductor. Resistance and winding loss of this box is given by:

$$R_{base} = \frac{\rho}{R_o} \tag{77}$$

$$Ploss_{base} = N^2 I^2 \frac{\rho}{\pi R_o} = \frac{\mu^2 N^2 I^2 \, 4\pi^2 \rho R_o^2}{4\pi^2 R_o^2 \, \mu^2 R_o} = \frac{Bmax^2 4\pi^2 \rho R_o}{\pi \mu^2} \tag{78}$$

Thus, normalized winding loss expressed in terms of normalized height ε, normalized winding-window width γ, field ratio α, and outermost radius R_o:

$$Ploss_{norm} = \frac{1}{ku \, ku_2 \, \gamma(\alpha - \gamma\alpha)^2} \sum_{i=1}^{ncell} (\alpha^i - \alpha^{i+1} + \alpha^{i+1}\gamma)(1 - \alpha^i + \frac{\alpha(1-\alpha^i)}{1-\alpha} \gamma + \varepsilon - 2\gamma) \tag{79}$$

Fig. 18 shows that the normalized conductor loss decreases for increase in α. Conductor loss also decreases with an increase in winding-window width. An increase in W_w implies that the thickness of the conductor can be increased, thus, lowering the resistance of the conductor.

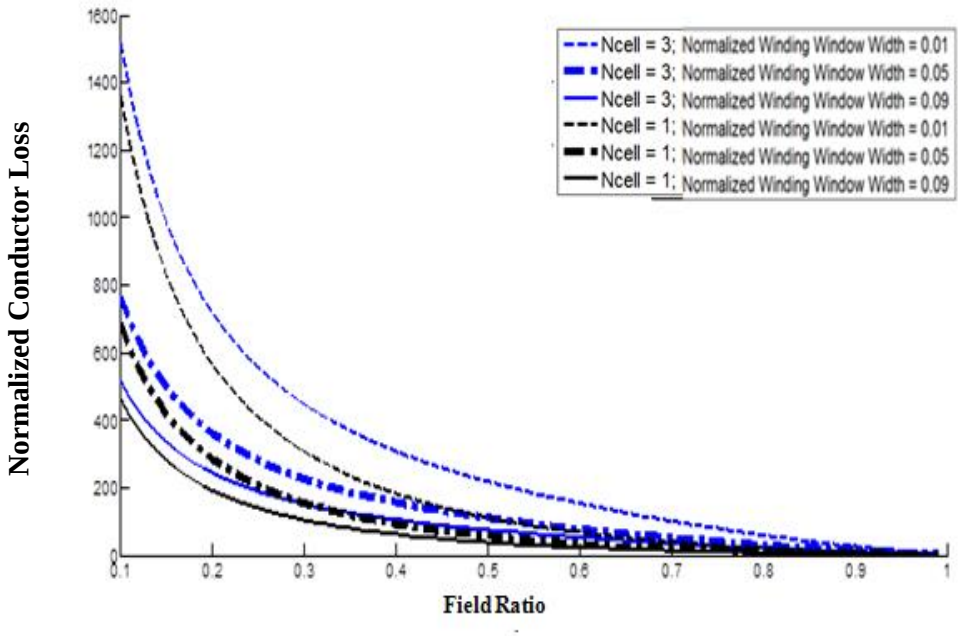

Fig. 18. Normalized conductor loss in a one cell and three cell distributed inductor versus α for normalized height $\varepsilon = 0.5$ and normalized winding-window width $\gamma = 0.01$, 0.05, and 0.09 according to (79)

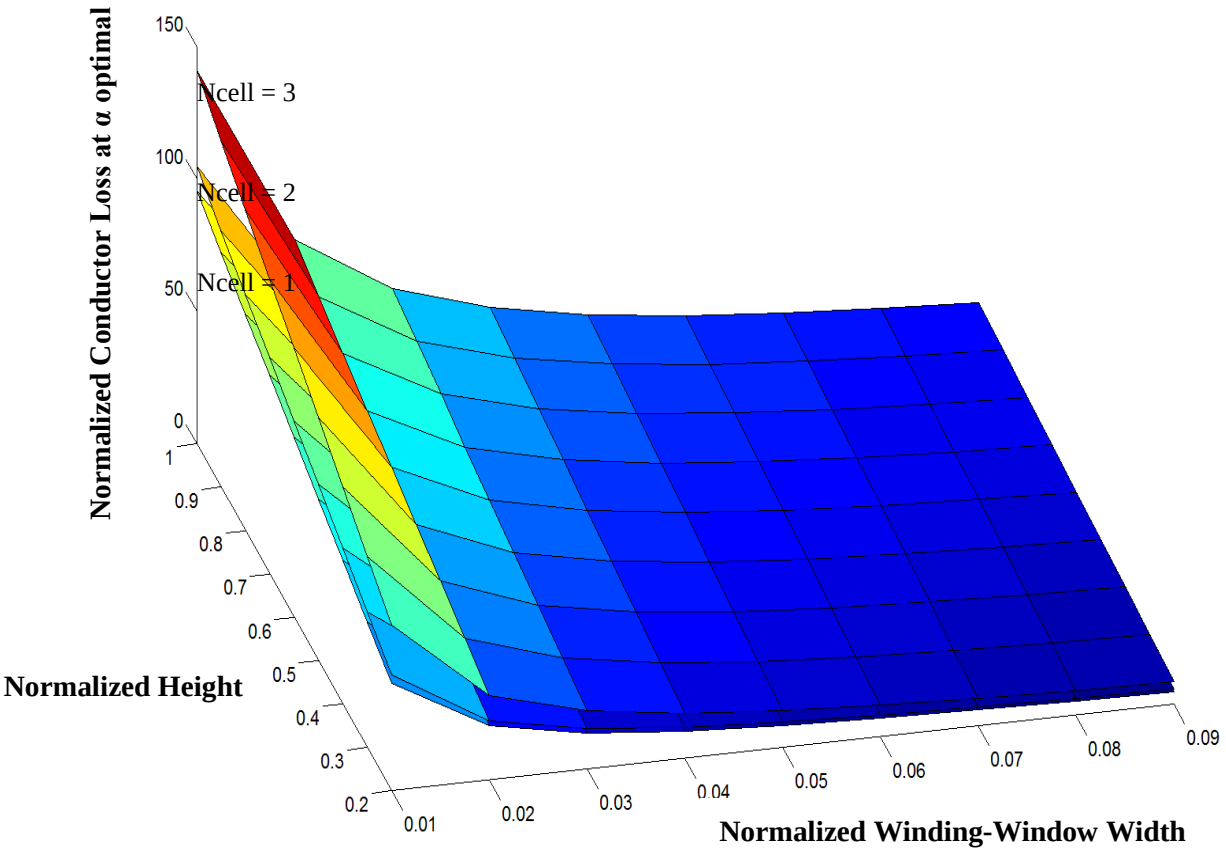

Fig. 19. Normalized conductor loss (79) in a one, two, and three cell CFI with Bmax as maximum flux density in the core, outer radius R_o, α_optimal versus normalized winding-window width and normalized height. W_w and height are normalized with respect to the outer radius of the CFI as in (50) and (52). Winding loss is normalized with respect to the loss in a block of R_o x R_o x R_o made of same material as the conductor of CFI.

The total normalized loss is the loss in the inductor due to the winding and core loss. Fig. 20 shows the total loss in the one, two, and three cell inductor for α_optimal.

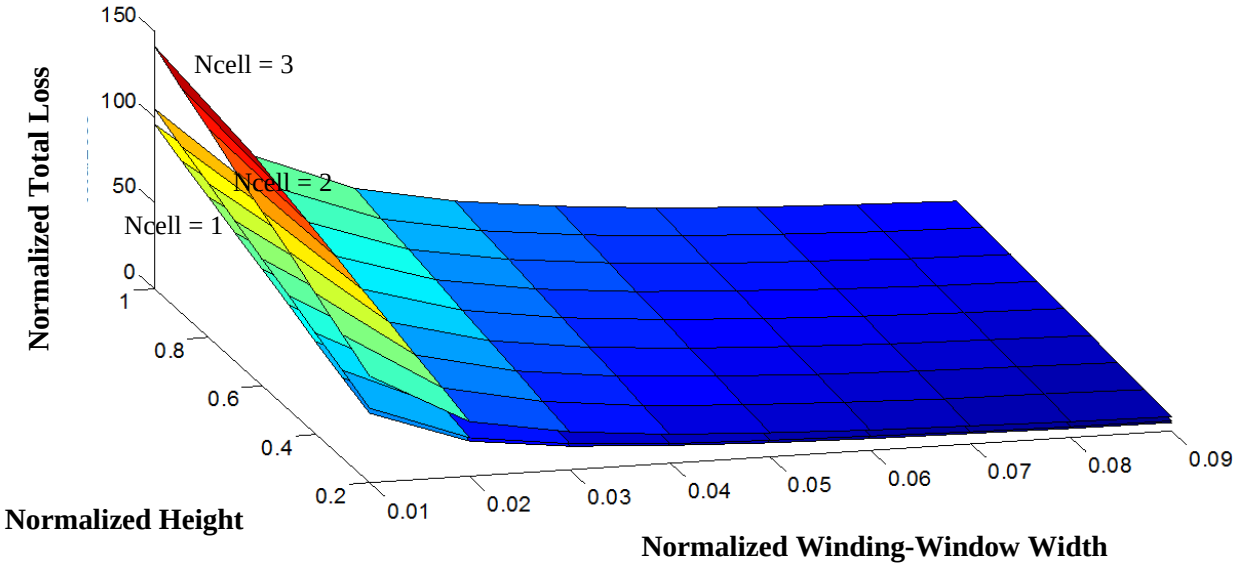

Fig. 20. Total normalized loss in a one, two, and three cell distributed inductor with Bmax as maximum flux density in the core, outer radius R_o, α_optimal β = 2 versus normalized winding-window width and normalized height.

Quality factor is the ratio of the energy stored in the inductor to the losses in the inductor. Quality factor should be considered as the deciding criterion for designing an optimized distributed inductor. Fig. 21 shows the plot of the quality factor versus the normalized height and winding-window width. Thus, depending on the ratio of allowed core loss and conductor loss in a particular design, field ratio, ncells, winding-window width, and height can be chosen. Larger winding-window widths imply lesser energy but less core and winding loss. Larger height implies more energy but more conductor and core loss. Thus, the design of a distributed inductor with constant-flux depends on the input parameters and permissible conductor and core loss limits individually or combined.

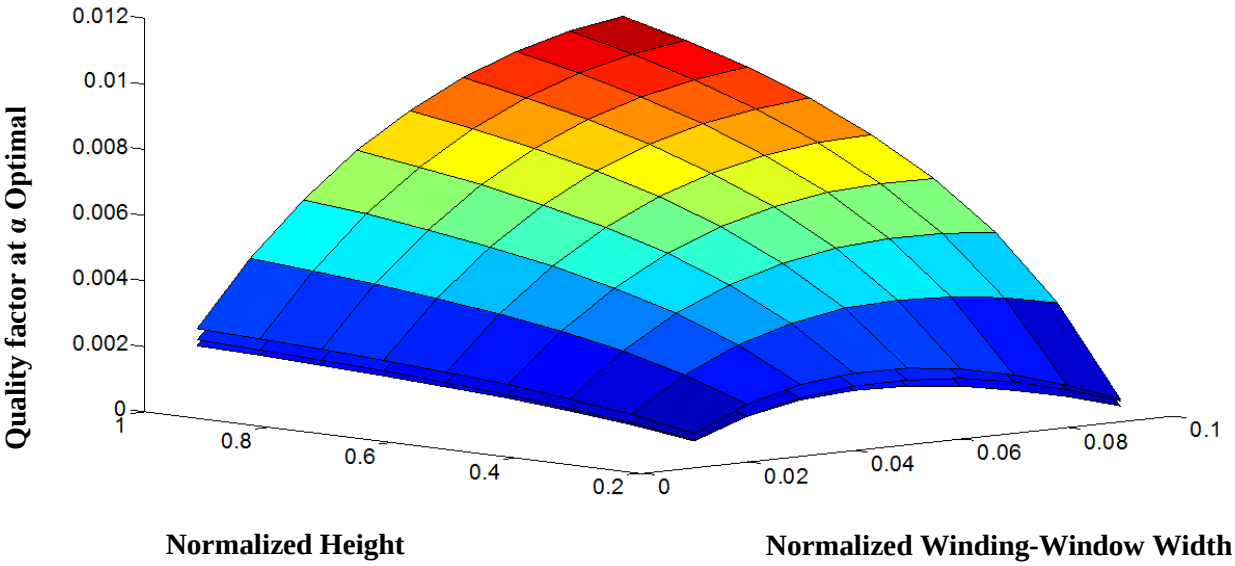

Fig. 21. Quality factor in a one, two and three cell distributed inductor with Bmax as maximum flux density in the core, outer radius Ro, α_optimal (Maximum normalized energy), β = 2 versus normalized winding-window width and normalized height.

To summarize, energy and losses of the CFI depends on the number of cells, W_w, height, and α of the inductor. Optimal α must be chosen to store maximum energy for a given number of cells, height, and W_w of the inductor. Quality factor should be considered as the deciding criterion to store maximum energy with minimum loss.

Similar expressions can also be written for the constant-width inductor. TABLE II summarizes the ratio of footprint area, length of conductor and core loss for constant-flux inductor for α = 0.6 and equivalent constant-width inductor and ECTI.

TABLE II.
Comparison of Constant-Flux Inductor, Constant-Width Inductor and Equivalent Conventional Toroidal Inductor

	Constant-Flux Inductor	Constant-Width Inductor	ECTI
	α = 0.6	Width = 30% Rmax	α = 0.56
Number of cells	3	3	1
Normalized Energy	1	1.01	1.03
Number of turns	1	1.15	1.15
Normalized length of conductor	1	1.1	1.13
Normalized Core loss	1	1.03	1.01
Normalized footprint area	1	1	1.48
Normalized Volume	1	1	1.48

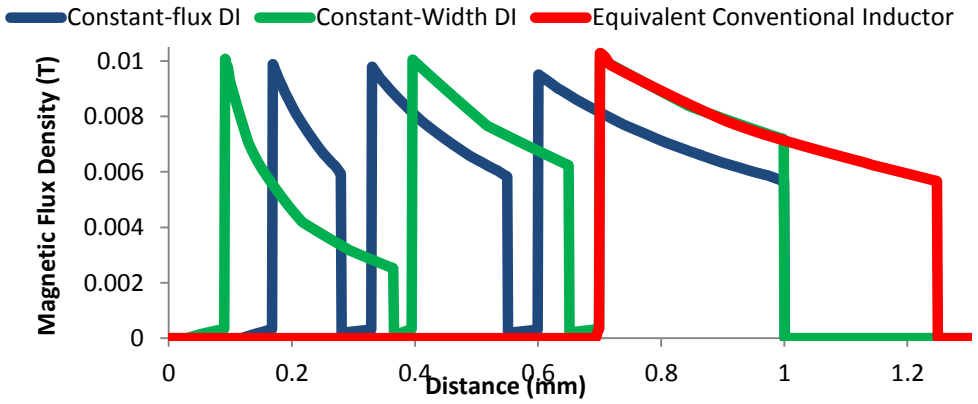

Fig. 22. Comparison of Line plot of magnetic flux density in constant-flux inductor with α = 0.6, constant-width inductor with width = 30% of outer radius and equivalent conventional toroidal inductor of equal energy, height and core material properties.

Fig. 22 shows that for the same Hmax in each cell, the same total energy, and the same material properties of the core, the footprint area of ECTI is larger than the distributed inductors by a factor of 1.48. Uniform distribution of energy in the DI is shown in Fig. 23. For the constant-width DI, the inner cell has α of 0.5 compared to α of nearly 0.9 in the outer cells. Thus, the minimum energy in the inner cell is smaller than the minimum energy in the outer cell. The length of conductor representing the winding loss and core loss for these designs are with 10% of each other and ECTI.

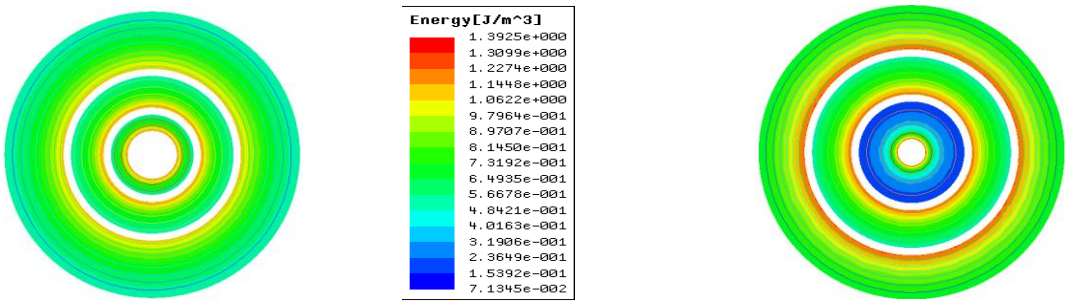

(a) (b)

Fig. 23. Uniform energy density distribution in (b) constant-flux inductor with α = 0.6 and (b) constant-width inductor of width = 30% of outer radius of equal energy, height and core material properties.

Three-cell CFI in comparison with a conventional toroidal inductor of same footprint area, made of same material, having same maximum flux density, and having same dc resistance in the winding has four times larger energy storage. The equivalent toroidal inductor, toroidal inductor with same footprint area/volume and constant-flux inductor are compared in Fig. 24 and TABLE III.

TABLE III
Comparison of CFI with Conventional Toroidal Inductor of Equal Energy and Conventional Toroidal Inductor of Equal Footprint Area

Parameter	Toroidal Inductor Of Equal Footprint Area	Constant-Flux inductor	Toroidal Inductor Of Equal Energy
Inductance (μH)	0.55	2.2	2.2
DCR (mΩ)	6	6	6
Ratio of Volume	1	1	1.48
Number of Ampere-turns	6	18	21
Ratio of Energy stored	0.25	1	1

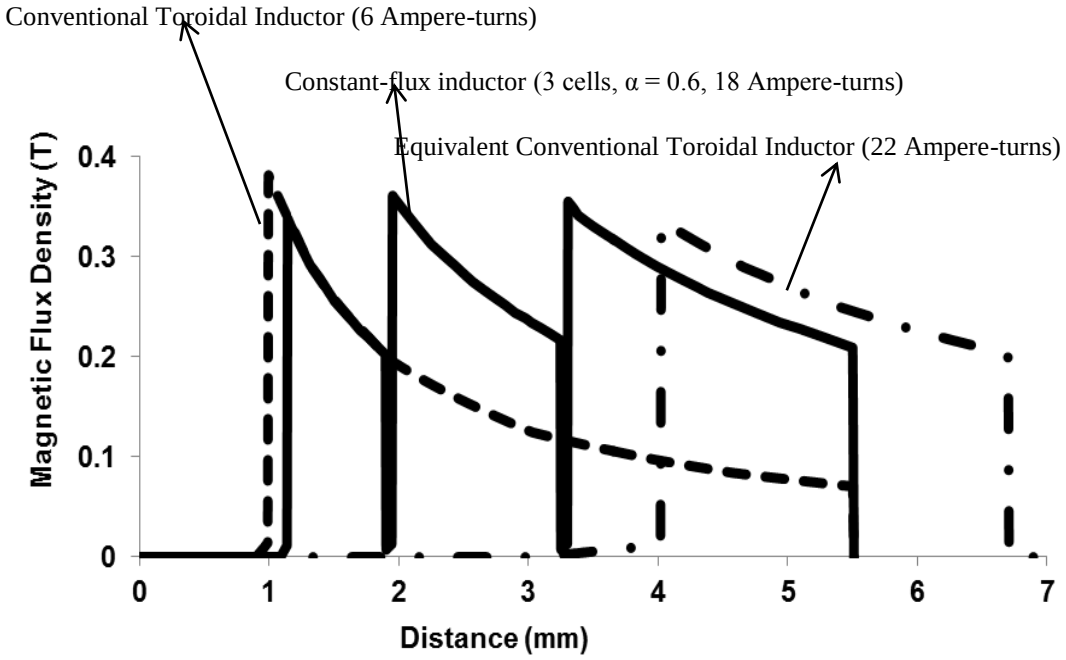

Fig. 24. Comparison of magnetic flux density along the radius of a toroidal inductor of same footprint area/volume as the constant-flux inductor of α=0.6 and a toroidal inductor of equal energy as the constant-flux inductor.

When comparing a CFI (with α = 0.9) with an ECTI, the footprint area of the CFI is 2.45 times smaller than that of the ECTI (Fig. 25). As the number of cells in the CFI decreases, the ratio of the footprint area of ECTI to CFI decreases. For α = 0.9 and 5 cells, the least ratio of the footprint area is 1.665, for α = 0.6 and 5 cells, the least ratio of footprint area is 1.6. For the constant width case, the ratio of the footprint area decreases with an increase in width.

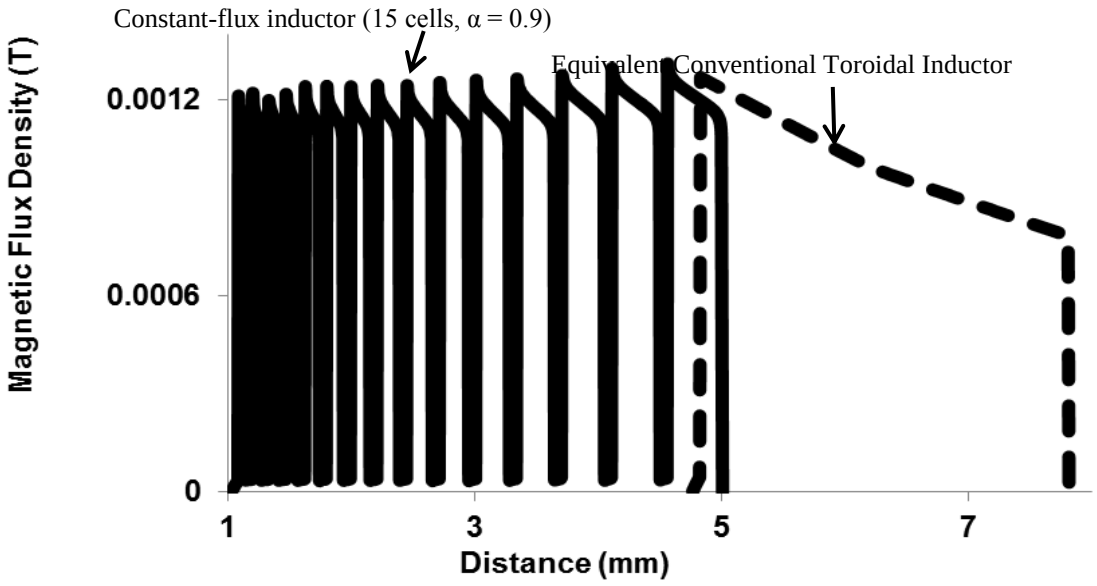

Fig. 25. Magnetic flux density distribution in a constant-flux inductor with 15 cells and α = 0.9 in comparison with equivalent conventional toroidal inductor with 2.45 times larger footprint area.

To summarize, the energy and losses of the DI of constant flux and constant width depend on the number of cells, winding-window width, height, and α/width of inductor. Optimal field ratio α must be chosen to store maximum energy for a given number of cells, height, and winding-window width of the inductor. Quality factor should be considered as the deciding criterion to store maximum energy with minimum loss.

4 PROCESS FLOW

In this chapter we present an algorithm for the design of the CFI. There are a large number of input parameters to such a design. These input parameters include: required inductance, permissible dc resistance, thickness of the conductor, maximum height of the inductor, maximum footprint area, properties of the core such as relative permeability, maximum magnetic flux density for the given core loss density (from a data sheet), and Steinmetz parameters for computing core loss. By sweeping the independent parameters: α, height of the core, outer radius; the desired output parameters such as dimensions of cells, ampere-turns in each cell, core loss, conductor loss, inductance, and finally energy are computed.

Various designs of the CFI would satisfy the given set of parameters. In order to choose the best possible design, the quality factor of the inductor is considered [18, 32]. For computing the quality factor of the inductor, energy stored and losses in the inductor need to be calculated.

$$\text{Quality Factor } Q = \frac{2\pi f E}{(Pcore + Pwinding)} \tag{80}$$

For a given outermost radius, the subsequent radii of the inner cells are determined using α or width depending on constant-flux or constant-width core. For the given material properties, Bmax and μ, Hmax is determined. Using Ampere's law, the number of ampere-turns in each cell is computed by using the Hmax, the peak current and the inner radii calculated for each cell. For each cell added from the outermost radii, energy and thus inductance are calculated and checked if it is within 5% of the required inductance. If the inductance is not met, then more cells are added, and inductance is calculated again for addition of each cell. The number of ampere-turns calculated is not necessarily an integer. But for practical reasons, the number of ampere-turns is rounded off to the nearest integer. The Hmax in each cell will not be exactly equal now.

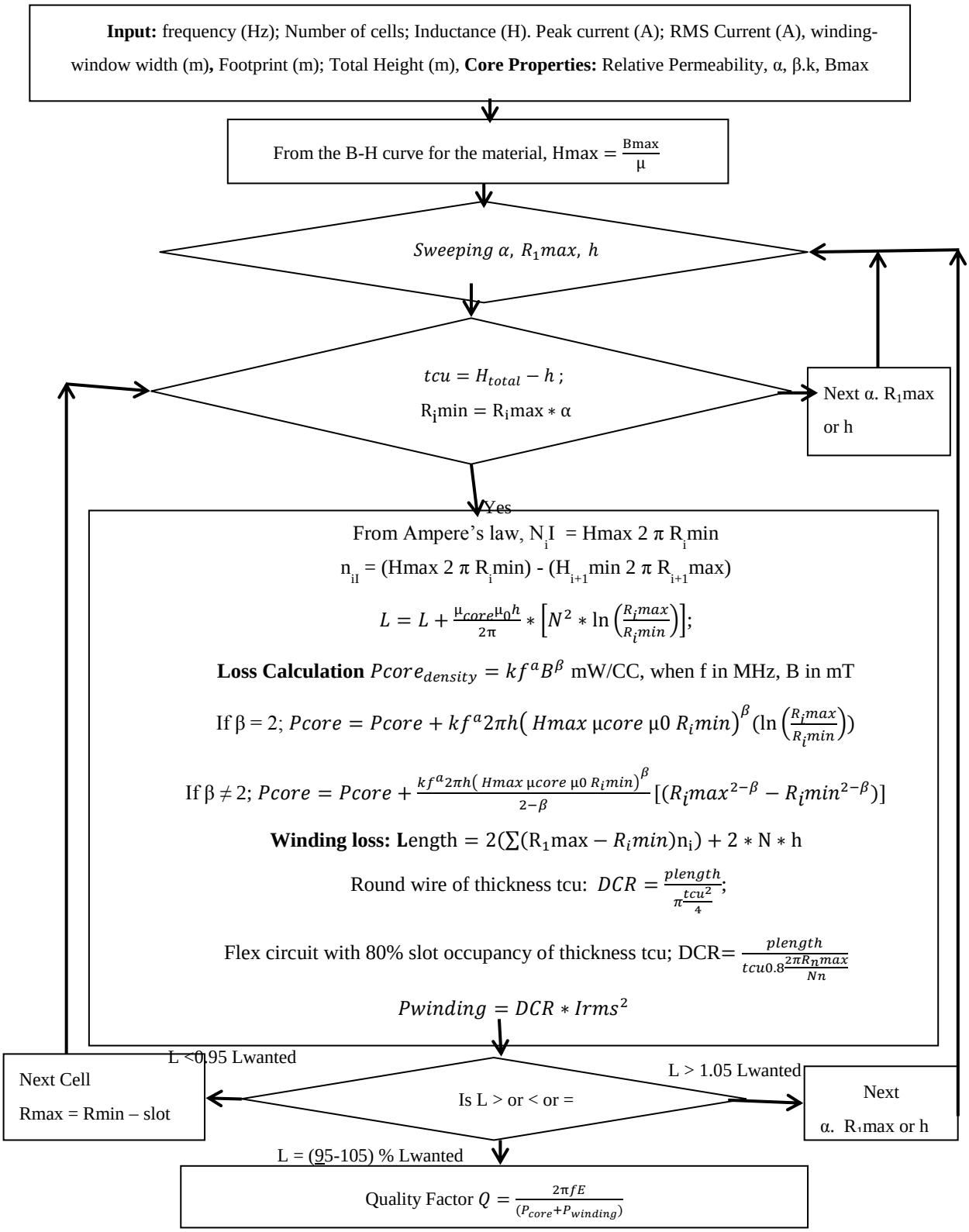

Fig. 26. Flowchart for designing a constant-flux inductor.

For the given thickness of the conductor (assuming a round conductor), DCR is computed. In the case of the flat conductor, the width of the conductor is computed using the number of ampere-turns and the minimum radius of the cell. For the required DCR and with the computed width of the flat conductor, the thickness of the conductor is calculated. The height and footprint of the inductor are computed by adding the thickness of the conductor to the core dimensions.

4.1 MATLAB Program

The program following the algorithm was written using MATLAB. The graphical user interface takes the inputs and prints the dimensions and required design parameters for the CFI with constant α. It also calculates the dimensions of ETCI.

The GUI is shown in Fig. 27. The input parameters are entered in the space provided. When "calculate" is pressed, the program runs the algorithm and designs the optimized CFI. In the output segment, it displays the dimensions of the CFI and the equivalent toroidal inductor for comparison. The red box denotes the input parameters to be entered by the user. The green box denotes the electrical properties of the CFI. The brown box denotes the mechanical properties, such as dimensions and ampere-turns of the CFI. The yellow box represents the properties of ECTI.

Fig. 27. Input and output sections of the GUI for designing constant-flux inductor

Fig. 28 shows the GUI of input parameters for a design of a CFI with powder iron material of inductance of 2.2 µH, peak to peak current of 3 A, dc current of 10 A, maximum allowed outer radius of 12 mm, maximum allowed height of 3.3 mm, frequency of operation of 3 MHz, maximum dc resistance to be less than 7 mΩ. If any material other than LTCC-50 or 4F1 is to be used, then the user must specify the value for the maximum allowed magnetic flux density and relative permeability of the material after entering "0" in the box for "other" material. In this example design, "0" is entered in the material box and relative permeability of "28" and Bmax of "0.36 T" are filled in the space provided. If core loss is an essential parameter for the inductor, then the user should enter "1" in the box for core loss, and if the material is "other," they should enter the Steinmetz parameters of the material. If no winding thickness is specified, 2* skin depth is taken as the winding thickness. The user could also input the maximum and minimum

number of cells in the CFI, along with the specified range for α. By default α is swept between 0.6 and 0.99.

The angle between each slot is calculated by dividing 360deg equally among all turns.

$$\text{SlotAngle} = \frac{360}{\text{N}} \tag{81}$$

Angle of symmetry refers to the angle of symmetry maintained for the slots in the core for the winding to pass through in each cell. An angle of symmetry of 90^o denotes symmetry in every quadrant. The angle of symmetry is used in the case of a transformer when there is a particular turns ratio maintained between the primary and secondary windings. For example, for a turns ratio of 1:4 between primary and secondary windings, 4 windings of the secondary windings can be laid in parallel on every quadrant of primary winding. This arrangement ensures tight coupling between the two windings. Thus, the angle of symmetry for the primary is 90^o.

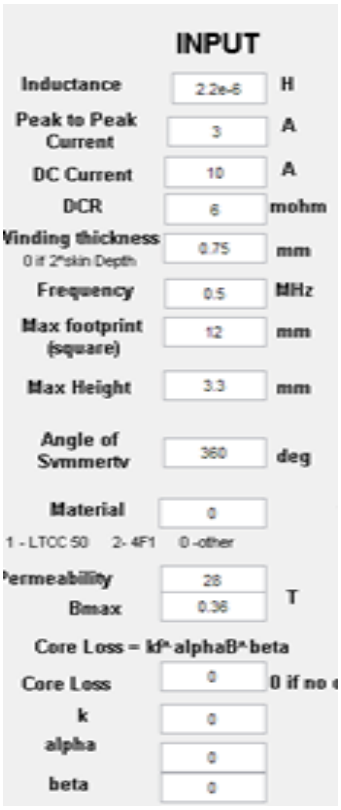

Fig. 28. Input section of GUI for the design of a constant-flux inductor of Inductance 2.2 µH for a rated current of 11.5 A.

Fig. 29 shows the GUI of the output section. The violet box displays the dimensions and number of ampere-turns in each cell. This design has 3 cells with the outermost cell having Rmax = 5.5 mm and Rmin = 3.3 mm and number of ampere-turns, n = 7. The yellow box on the bottom displays the dimensions of the ECTI. For this design, the footprint area of ECTI is at least 1.4 times larger than the CFI. The orange box denotes the dimensions of the LTCC tape that needs to be cut to account for 20% shrinkage on the x-y axis.

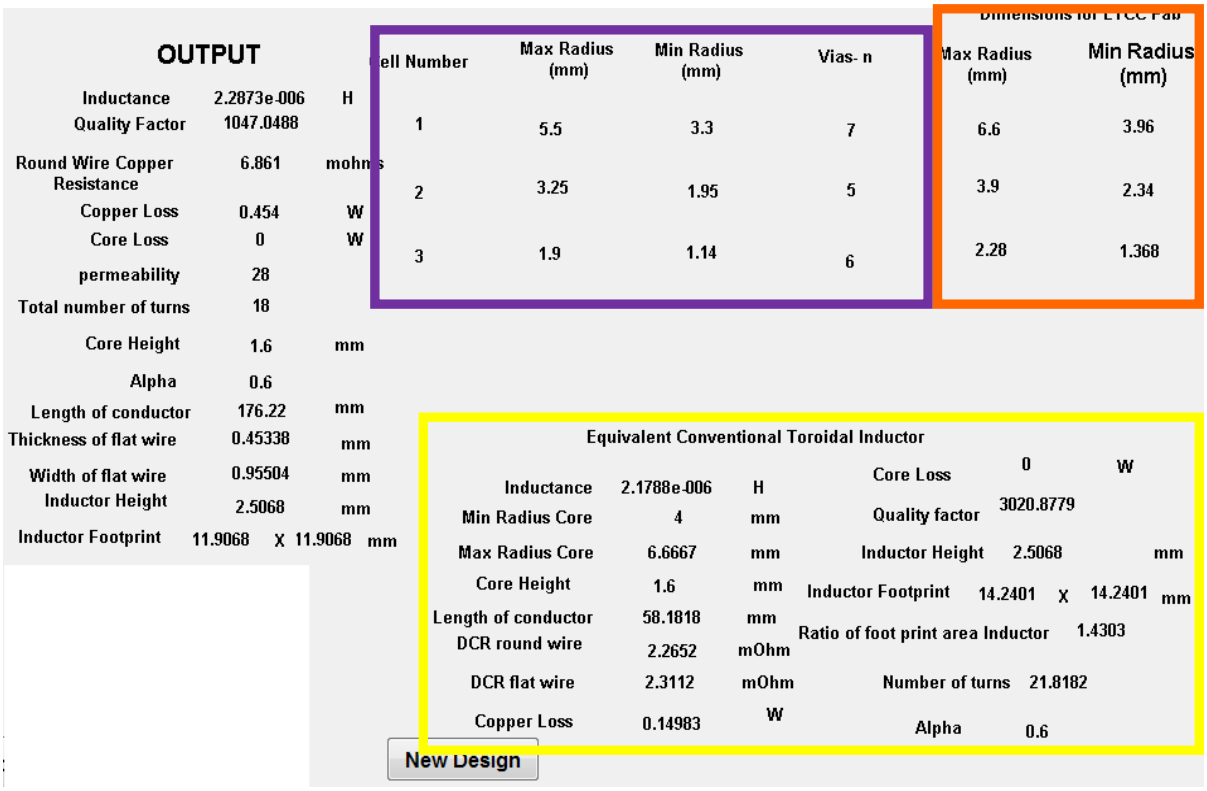

Fig. 29. Output section of the GUI displaying mechanical and electrical parameters for design of constant-flux inductor for inductance of 2.2 µH, rated current of 11.5 A.

Fig. 30 shows the angular distribution of slots for the designed CFI. The blue dots denote the current going to the slot, while the red dots denote the return path of the current in the outermost cell. The slot angle is 20 deg for this design.

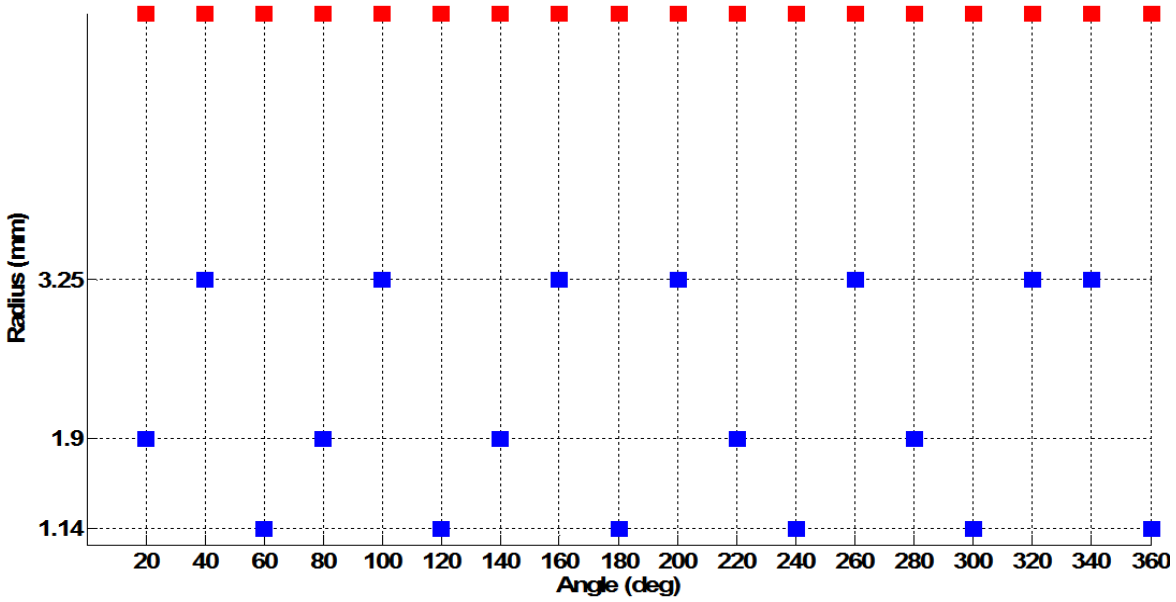

Fig. 30. Angular distribution of slot in a constant-flux inductor. The blue dots denote the current going to the slot in inner cells while red dots denote the return path of the current in the outermost cell.

In the case when there is no design available for the given input parameters, the GUI displays "no design was found" and would request the user to review the input parameters. This is illustrated in Fig. 31.

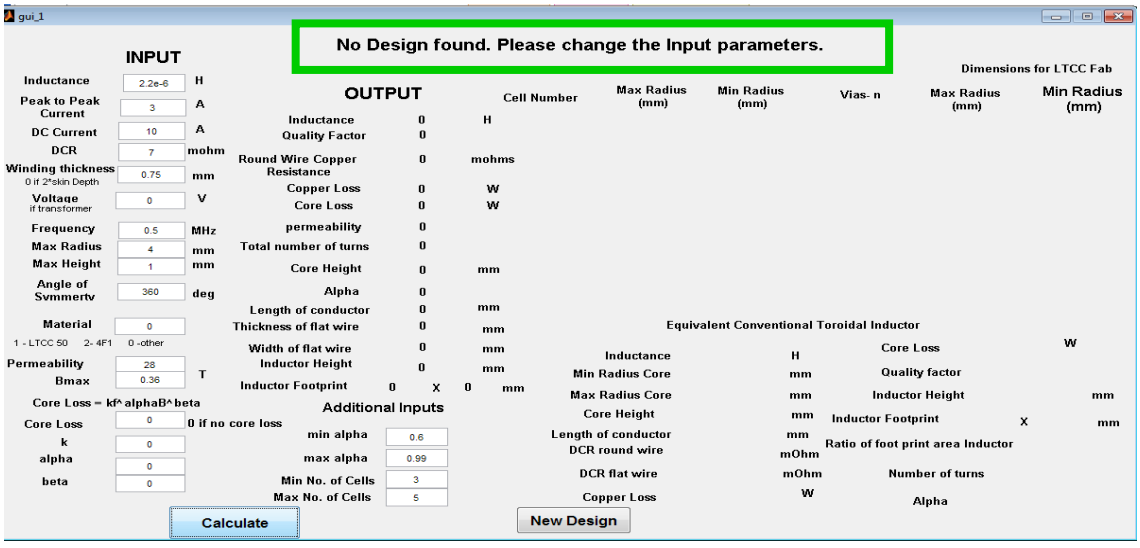

Fig. 31 GUI requesting user to review the input parameters.

5 FABRICATION PROCEDURE

This section describes the steps followed in the fabrication of the CFI using Micrometal-8 and low-temperature, co-fired ceramic (LTCC) [25-30, 33, 34] as the core materials. The dimensions and the number of ampere-turns in each cell were chosen using the algorithm described in section 2.2.

5.1 Fabrication Procedure for Constant-Flux Inductor with Micrometal-8

a. Core and winding for the CFI was drawn using Ansoft Maxwell, as shown in Fig. 32**.**

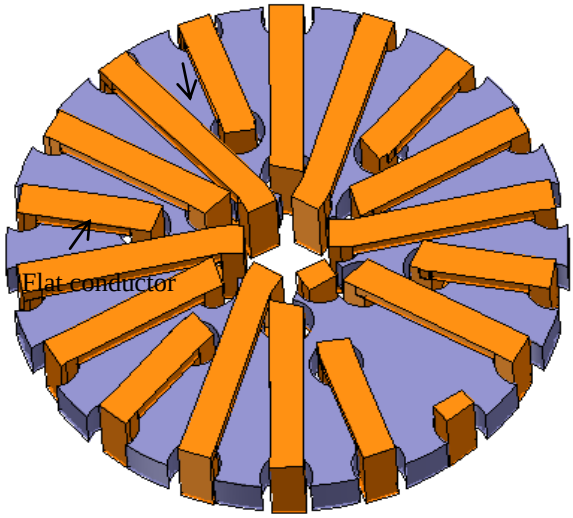

Fig. 32. Constant-flux inductor with core (12.6 mm x 12.6 mm x 1.6 mm) and winding with 18 turns is drawn using Ansoft Maxwell 12.

b. TABLE IV lists the materials used in the fabrication process.

TABLE IV. Materials Used in Fabrication of Constant-Flux Inductor

Material	**Part Number**	**Company**	**Purpose**	**Specification**
Powder Iron	Micrometal Material Mix no 8	Micrometal	Core	Relative permeability < 35
Flat Copper Wire	N/A	N/A	Conductor	Thickness – 0.25 mm Width – 1mm

c. The angular positions of the slots are as shown in the Fig. 33.

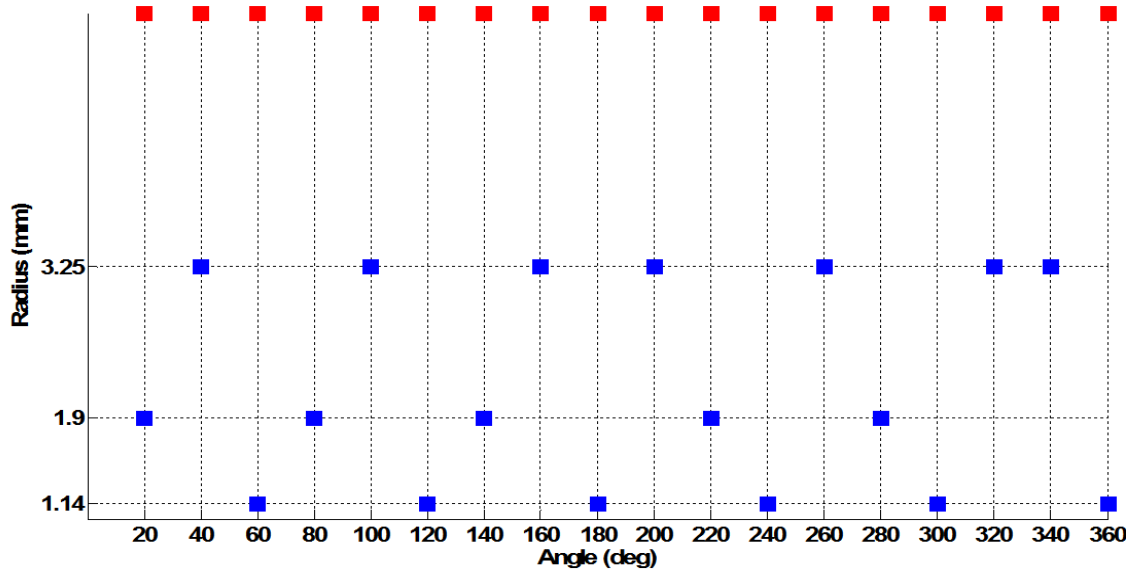

Fig. 33. Angular positions of the slots in the core for the constant-flux inductor with 18 turns and three cells. Blue dots denote the current going to the slot in inner cells while red dots denote the return path of the current in the outermost cell.

d. The 3D-drawing of the core is exported to AUTOCAD as a 2D, as shown in Fig. 34.

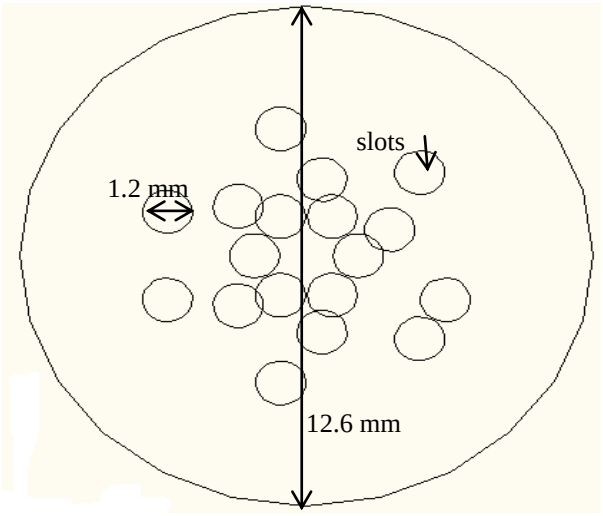

Fig. 34. 2D drawing of core with slots of constant-flux inductor.

e. Material is available in cylindrical blanks of a diameter of 12.6 mm and a height of 38 mm. The cylindrical blanks are sliced to a thickness of 1.6 mm.

f. The AutoCAD file is converted to a Gerber file with a keep-out layer and drill file for slots to be drilled. Using the Quick Circuit machine and with a drill bit of 1.2 mm, holes are drilled, as shown in Fig. 35(b). Powder iron is very brittle. The speed of the drill bit is set to a high value so that it does not crack the core.

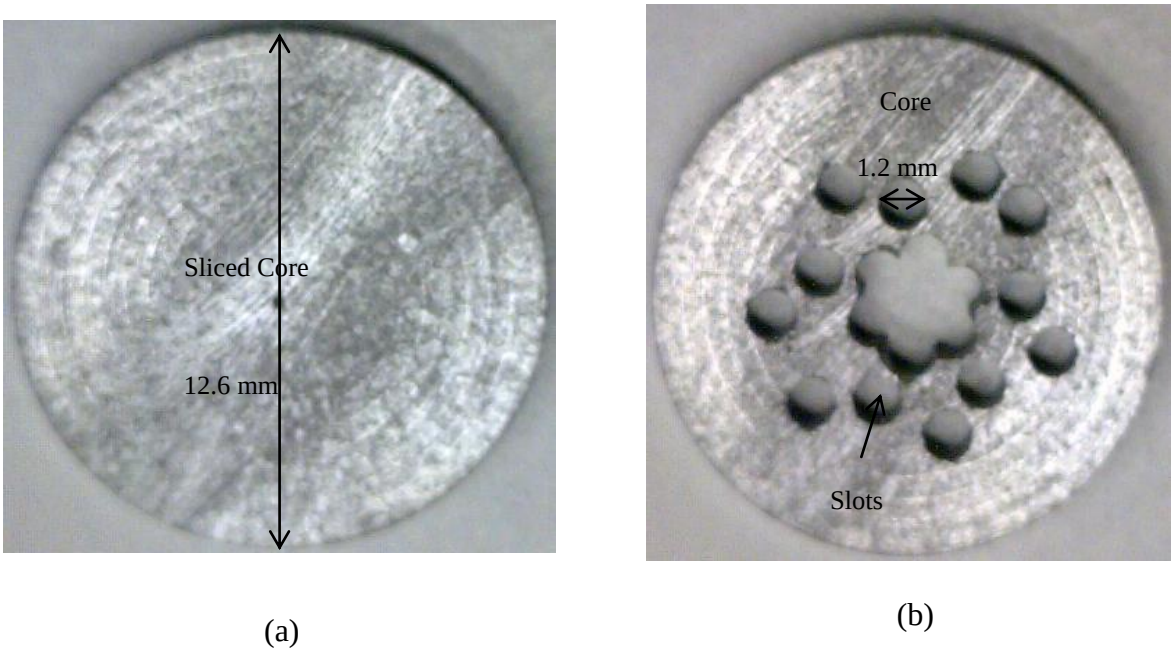

Fig. 35. (a) Sliced blank (12.6 mm x 12.6 mm x 1.6 mm) from the cylindrical blank of Micrometal-8; (b) Constant-flux inductor core with 18 slots with each of 1.2 mm diameter.

g. Flat copper conductor of thickness 0.25 mm and width 0.97 mm is wrapped with kapton tape on both sides. The kapton prevents shorting between the adjacent turns. The flat wire is then wound through the slots to form the inductor. The fabricated CFI is shown in Fig. 36.

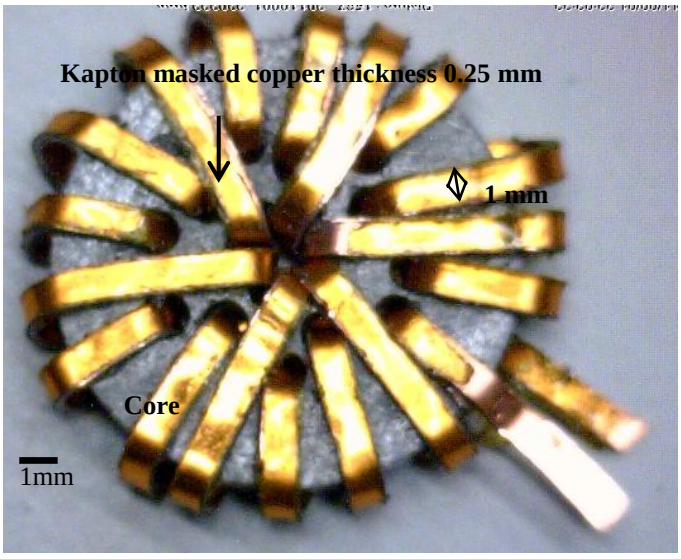

Fig. 36. Constant-flux inductor (14 mm x 14 mm x 2.5 mm) with Micrometal-8 core (12.6 mm x 12.6 mm x 1.6 mm) and flat wire copper conductor (0.25 mm x 0.97 mm) of 18 turns

5.2 Fabrication Procedure for LTCC

a. The core and winding for the CFI are drawn using Ansoft Maxwell, as shown in Fig. 37. TABLE V lists the materials used in the fabrication process.

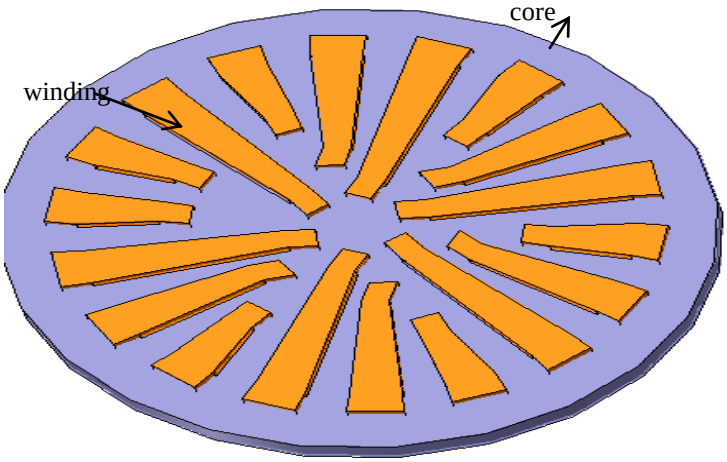

Fig. 37. Constant-flux inductor with core (12.6 mm x 12.6 mm x 1.6 mm) and winding with 32 turns drawn using Ansoft Maxwell 12.

TABLE V
Materials Used in Fabrication of 3-Cell Constant-Flux Inductor

Material	**Part Number**	**Company**	**Purpose**	**Specification**
Low Temperature Co-Fired Ceramic Tape (LTCC)	ESL – 40010	Electroscience Lab(ESL)	Core	Relative permeability > 50; Thickness of tape - 65-75 um Shrinkage % x, y = 17% ; z = 14%;
Porous Alumina	ESL 42520	Electroscience Lab	Substrate to aid burn out process	40% nominal Porosity
Silver paste	DuPont-7740 [19]	DuPont	Conductor	Sheet Resistance = 0.38 mΩ/sq Fired thickness = 0.55 µm

b. Due to the shrinkage of the tape after sintering, the size of the inductor is enlarged before sintering by 20% along x and y axis.

c. Stack of 32 layers of ESL40010 Low Temperature Co-fired Ceramic tapes from ESL with permeability of 50 are cut. Each layer is 20 mm x 20 mm. The layers are laminated under Hydraulic pressure of 1500 psi at 70^{o}C for 20 minutes using CARVER hydraulic press.

d. Ferrite tape is mounted on porous alumina ceramic substrate (ESL42520**)**. Porous alumina aids in the burnout process when the binders leave the ferrite. LASER power also partially sinters the green tape. Thus, porous alumina helps scrape out the core after the LASER cut. Alumina powder is also sprinkled on the substrate to further aid the process.

e. Using a LASER, the pattern is cut into the core using the parameters in TABLE VI, as shown in Fig. 38.

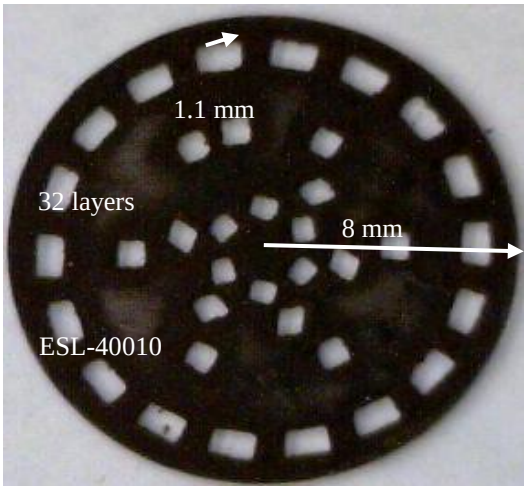

Fig. 38. Thirty two layers of ESL-40010 green tape is LASER drilled for 36 slots.

f. Mask (Fig. 39[a]), made of kapton is placed on top of the LASER-cut LTCC tape. Silver paste (7740) is filled in the slots and also on the surface. The paste is allowed to dry at 75^{o}C for 2 hours. The slots are re-filled with the paste. This process is repeated three times (Fig. 39[b]).

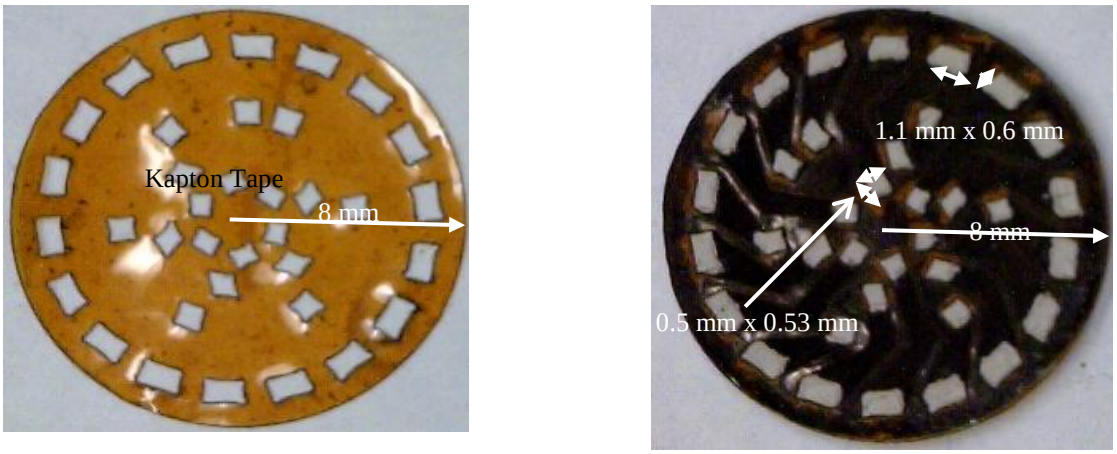

(a) (b)

Fig. 39. Kapton mask used as a guide to fill slots of the LTCC tape in (Fig. 38) with DuPont Silver paste (7740), (b) LTCC tape filled with silver paste.

g. The sintering profile is set in Vulcan 3-550 sintering oven, as shown Fig. 40. The LTCC tape with silver is placed in the sintering oven on porous alumina substrate.

h. A constant-flux inductor with DuPont silver paste on the surface and in the slots is shown in Fig. 41.

TABLE VI.
Parameters for LASER Cutting LTCC Green Tape

Pulse Spacing	0
Rep rate	1
Frequency	1
Power	32(number of layers of green tape stacked)
Pulse spacing	60
Piercing point	0
Drill Cycle	0

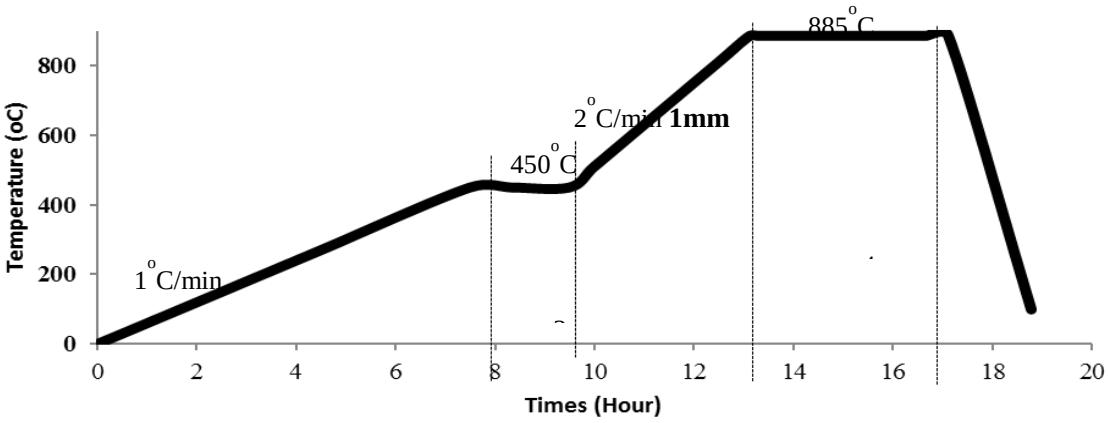

Fig. 40. Sintering profile for co-firing DuPont silver paste (7740) and ESL-40010.

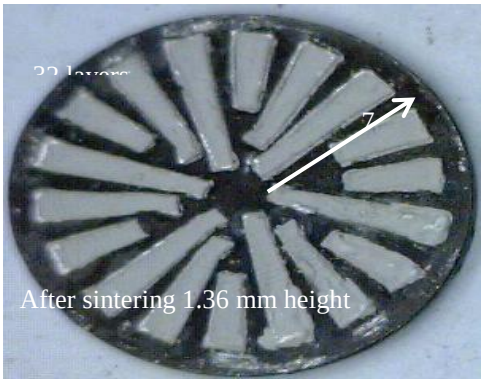

Fig. 41. Constant-flux inductor with LTCC core and DuPont Silver paste with 18 turns, 14 mm x 14 mm x 1.32 mm.

6 RESULTS AND DISCUSSIONS

This section discusses results from three different analyses. Firstly, to verify the concept of CFI, discrete toroidal inductors were used, and round copper wire was wound around them. Secondly, a CFI of high-power, high-current was designed and compared with a commercial product. Thirdly, for a set of specifications, a CFI was designed and fabricated using Micrometal-8 and design procedures mentioned in the earlier section.

6.1 Case 1: Proof of Concept

With the available cores from Micrometal, a CFI with 2 cells using discrete toroidal cores was built. TABLE VII summarizes the specification for the CFI.

Fig. 42(a) shows the CFI with two cells and eight Ampere turns. Fig. 42(b) and (c) show the uniformity in the energy distribution and magnetic flux density when the number of ampere-turns in the first and second cell is equal.

TABLE VII.
Specifications of Constant-Flux Inductor with Discrete Cores

Parameters	Values From Datasheet	Measured Values
Part Number	T90-52; T50-52D	
Relative Permeability	75	62
Radii (mm)	R_3 = 3.5 mm R_2 = 6.35 mm R_1 = 11.45 mm	R_3 = 3.78 mm R_2 = 6.35 mm R_1 = 11.49 mm
Height (mm)	9.53 mm	9.779 (T90), 9.906 (T50);

.

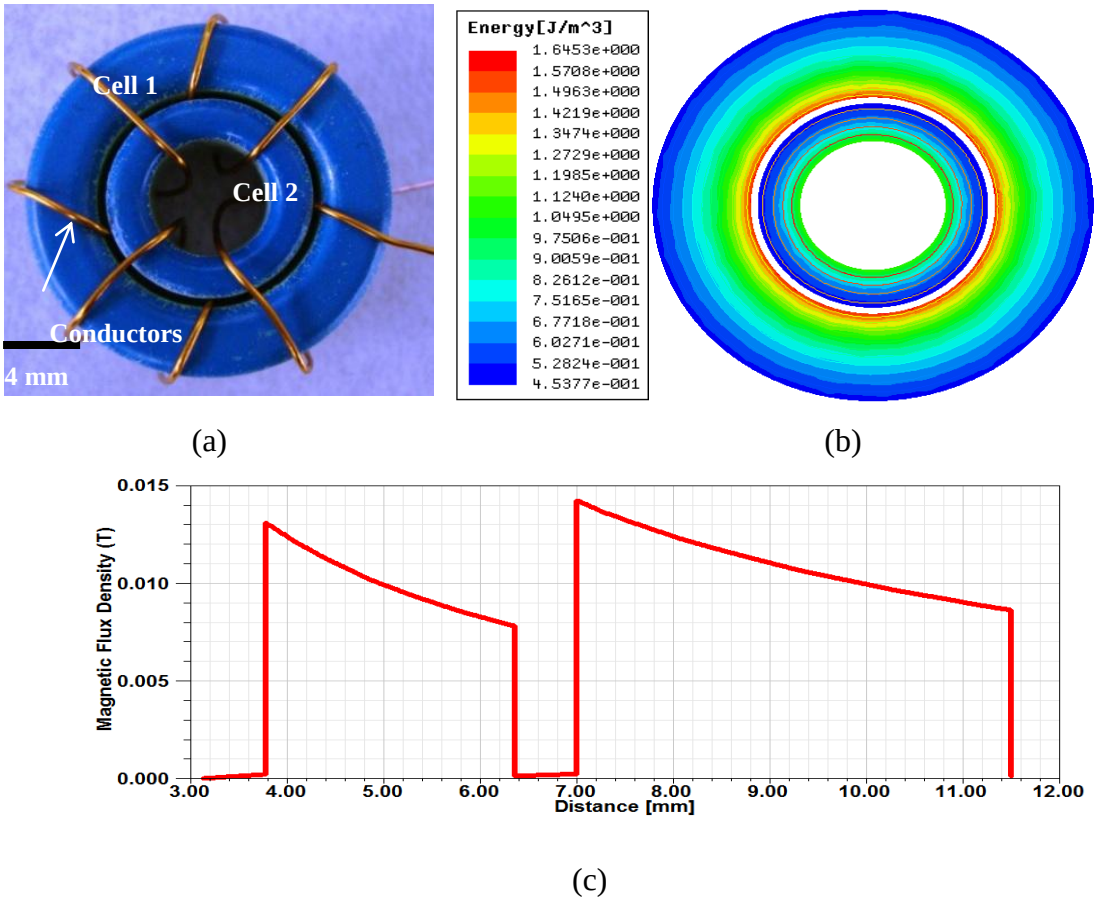

Fig. 42. (a) Distributed Micrometal inductor; (b) Energy density distribution in the core; (c) Magnetic flux density distribution in the core.

For n1 = 4, n2 = 4, the following results were obtained. TABLE VIII summarizes and compares the measured value of inductance with calculated and simulated values. Inductance has been measured using Agilent 4294A [20].

TABLE VIII
Results of the Constant-Flux Micrometal Inductor

	Calculation	**Simulation**	**Measurement**
Inductance (μH)	5.007	4.91	5.116

6.2 Case 2: Constant-Flux Inductor for High-Power Application

A constant-flux inductor is designed for a high-current, high-power application at 20 kHz. The material used for the application is Kool Mu from Magnetics Inc [23]. TABLE IX lists the

input parameters for the design, while TABLE X summarizes the mechanical and electrical parameters for input parameters for designing a CFI for high-current, high-power application.

TABLE IX.
Input Parameters for the Design of Constant-Flux Inductor for High-Current, High-Power Application

Input Parameter	**Value**
Frequency	20 KHz
Relative Permeability of core material	26
Rated Current	180 A
Peak Flux Density	1 T
Inductance	10 µH

When round wire is used in a constant-flux inductor, the winding-window width should be at least 5 mm to allow the conductor to pass through. However, use of flat wire of the same cross-sectional area reduces the thickness of the conductor to 3 mm. The conductor can be spread on the surface to meet the DCR. This results in a smaller winding-window width in the core and thus, lesser inductor volume for same amount of energy.

TABLE X.
Comparison of Output Parameters of Constant-Flux Inductor and Equivalent Conventional Toroidal Inductor for High-Power Application

	Constant-Flux Inductor	Commercial Product E70340-010 [21]	Equivalent Toroidal Inductor
Length of conductor	751 mm		788 mm
Flat wire (3.4 x 5 mm)	0.75 mΩ	0.75 mΩ	0.81 mΩ
Dimensions (mm^3) Flat wire (3.4 x 5 mm)	44.8 x 44.8 x 23.6	44.5 x 44.5 x 30	54 x 54 x 23.6
Volume ratio	1	1.3	1.45

6.3 Case 3: Fabrication of Integrated Constant-Flux Inductor

CFI is designed and fabricated for the specifications listed in the TABLE XI.

TABLE XI.
Parameters for the Design of Constant-Flux Inductor

Parameters	**Commercial Inductor**
Permeability	35
Bmax (T)	0.35
Frequency (KHz)	550
Inductance (μH)	2.2
DCR	6 mΩ

The mechanical and electrical parameters for the equivalent CFI are listed in TABLE XIII. The material used for the design is Micrometal mix 8 [22]. This material has relative (initial) permeability of 35. The material does not saturate for 3500 Gauss, and there is no drop in permeability with frequency till 1 MHz. For DCR of 6 mΩ, length of the conductor, diameter of round wire, width and thickness of flat wire are tabulated in TABLE XII.

TABLE XII
Dimensions Of Flat and Round Wire for Constant-Flux Inductor of Inductance 2.2 μH and 6 mΩ DCR with Varying Number of Cells

Cells	Permeability	Rmax (mm)	flux	Total Number of Turns	Height (mm)	Inductance (μH)	Length (mm)	Flat wire		Round wire diameter (mm)
								Width (mm)	Thickness (mm)	
3	35	6	0.73	20	1.43	2.19	172	1.173	0.421	0.79
2	35	6	0.68	18	1.67	2.10	161	1.162	0.396	0.77
1	35	6	0.61	16	2.3	2.09	151	1.149	0.376	0.74

A toroid is fabricated using this material. Due to the fabrication procedure, the permeability of the material dropped from 35 to 28 for the toroidal inductor. Thus, for calculation, the permeability is assumed to be 28 instead of 35. The line plot of magnetic flux density shown in Fig. 43 shows the uniform distribution of flux density and energy in the CFI.

Using Ansoft Maxwell, 3D of the CFI is drawn and simulated. The CFI is fabricated using the steps described in section 2.3. The inductor is fabricated using round wire and flat wire. The length of wire in both the cases should be 176 mm. From the calculation, the diameter of the round wire should be 0.75 mm to have the DCR < 6 mΩ. The wire is too thick and hence, does

not bend sharply. This results in bulging of the wire with a corresponding increase in length of the wire and height of the inductor.

Two wires of smaller diameter (0.6 mm) are wound in parallel to avoid the problem faced with thicker wire. Due to overlapping of the wires, the height of the inductor is increased. The DCR is low in this case. To further reduce the DCR to 8 mΩ, thinner wire of AWG 27 is wound in parallel. The overall height is increased to 4.45 mm.

TABLE XIII.
Parameters of Equivalent Constant-Flux Inductor

Parameters	**Constant-Flux Inductor**		
Permeability	< 28		
Bmax (Gauss)	3500		
Frequency (KHz)	500		
Radii (mm)	Cell no	Rmax	Rmin
	1	6.3	3.3
	2	3.25	1.95
	3	1.9	1.14
Ampere turns (A)	Cell No	nI	
	1	7*11.5	
	2	5*11.5	
	3	6*11.5	
Field ratio α	0.6		
Inductance (μH)	2.18e-6		
Core Height (mm)	1.6 mm		
Area of cross-section of Round Wire	0.4418 mm^2		
Length of conductor	176 mm		
DCR Round wire	6.69 mΩ		
Width of flat wire	0.955 mm		
Thickness of flat wire	0.53 mm		
Height of Inductor (with flat conductor)	2.66 mm		

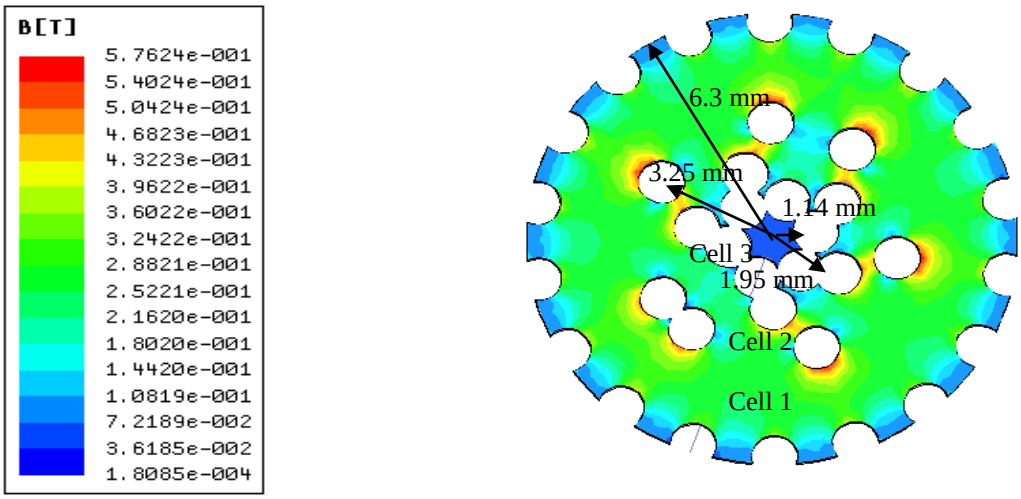

(a)

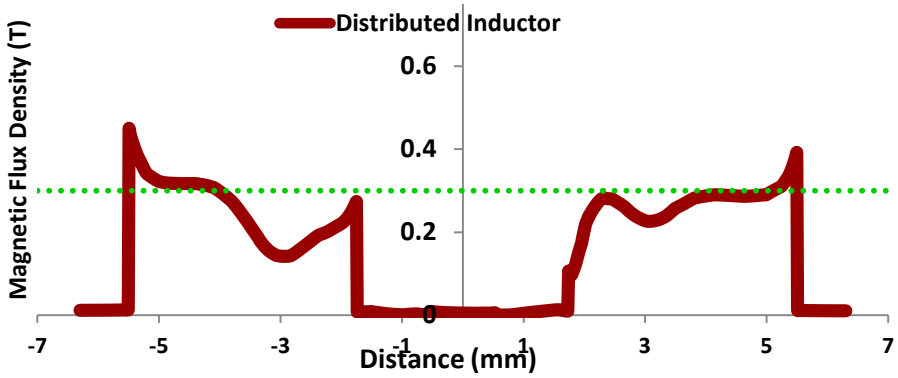

(b)

Fig. 43 (a) Cross-sectional view of magnetic flux density distribution (b Line plot of magnetic flux density distribution in constant-flux inductor of (12.6 mm x 12.6 mm x 1.6 mm) made of Micrometal-8.

Flat wire of a width of 0.97 mm and a thickness of 0.24 mm is used. The thinner wire enhances the ease of winding without bulging. Thus, the height of the inductor is reduced to 2.5 mm, while the DCR is 14.4 mΩ. The calculated resistance is 14 mΩ. The two cases are summarized in TABLE XIV.

TABLE XIV.
Comparison of Constant-Flux Inductor with Round and Flat Copper Wire

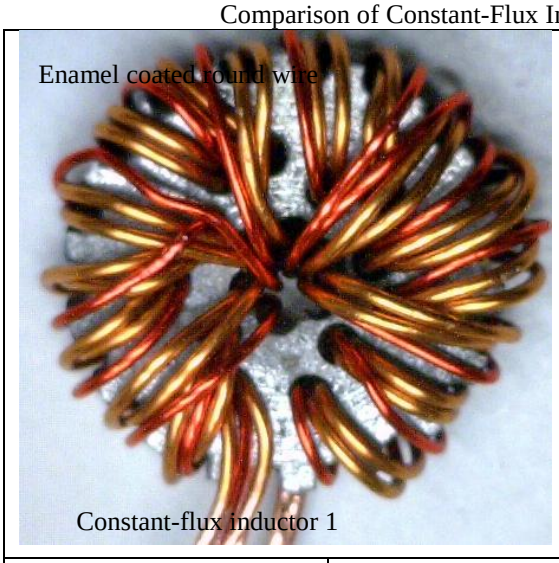

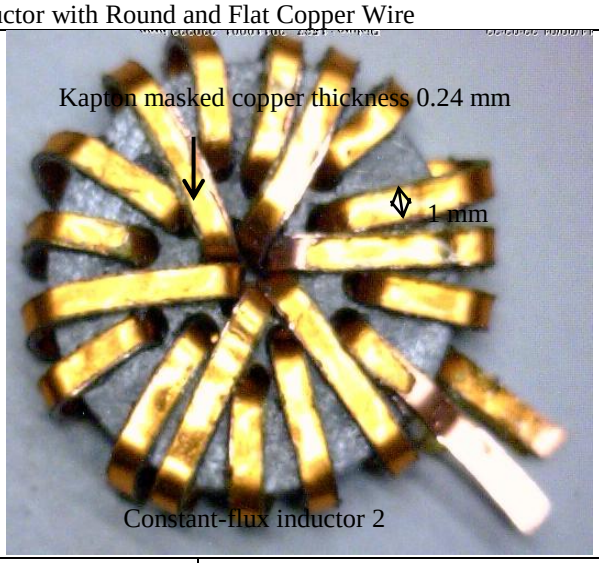

	Constant-Flux inductor -1	**Constant-Flux inductor -2**
Wire	Round wire	Flat Wire
Wire Size	2 strands – AWG -22 (0.644 diameter); 1 strand – AWG 27 (0.36 mm diameter)	Thickness : 0.24 mm Width :0.97 mm
Dimensions	13.6 x 13.6 x 4.45 mm	14 x 14 x 2.5 mm
Length of wire	~ 340 mm	~ 200 mm
Calculated Resistance	7.7 mΩ	14 mΩ
Measured Resistance	8 mΩ	14.4 mΩ

6.4 Difficulties and Solution in the Fabrication Process

The shrinkage control of LTCC tape is obtained by rotating each layer in the stack by 90^{o}. This allows an isotropic shrinkage in x-y axis.

During LASER cutting, the LTCC tape tends to sinter at the areas of cut. This makes the tape hard to remove from the substrate after cut. To enhance ease of removal of tape, porous alumina substrate with alumina powder sprinkled on it must be used.

Paralleling conductors and thicker conductors help in reducing the DCR. Owing to the thick conductor and overlapping of conductors, the length increases. The overlapping or bulging of the conductors increases the overall height of the inductor also.

7 CONSTANT-FLUX TRANSFORMER

The concept of CFI can be extended to a constant-flux transformer. In a power transformer, for a given leakage and magnetizing inductance, an inductance matrix is computed, as shown in TABLE XV, for the equivalent circuit shown in Fig. 44.

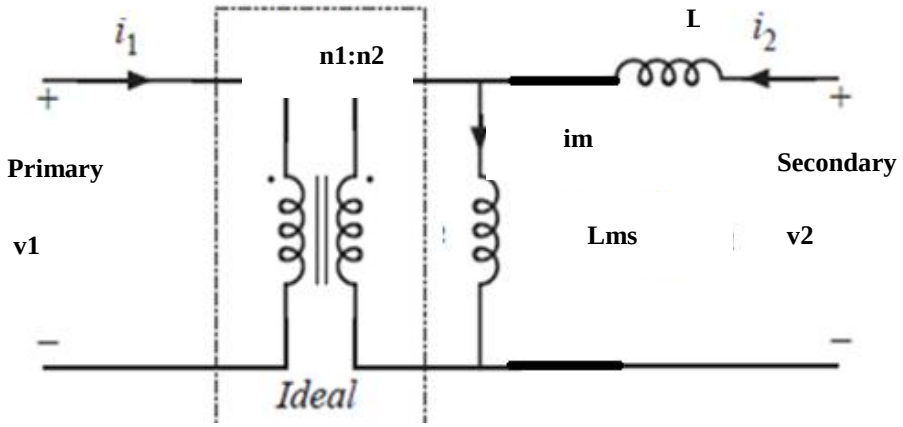

Fig. 44. Equivalent circuit of transformer with leakage and magnetizing inductances on the secondary side.

TABLE XV.
Inductance Matrix of a Transformer Showing Self and Mutual Inductances

Inductance Matrix	Primary Winding	Secondary Winding
Primary Winding	L11 (self-inductance)	L12 (Mutual inductance)
Secondary Winding	L12 (Mutual inductance)	L22 (self-inductance)

$$\begin{matrix}\mathrm{n1} - \text{number of turns on primary side;}\\ \mathrm{n2} - \text{number of turns on secondary side}\end{matrix} \tag{82}$$

$$\text{effective turns ratio, ne} = \sqrt{\frac{\mathrm{L11}}{\mathrm{L22}}} \tag{83}$$

$$\text{magnetizing Inductance (on primary side), Lm} = \frac{\mathrm{n1}}{\mathrm{n2}}\mathrm{L12} \tag{84}$$

$$\text{Leakage inductance on primary side, Ll1} = \mathrm{L11} - \frac{\mathrm{n1}}{\mathrm{n2}}\mathrm{L12} \tag{85}$$

$$\text{Leakage inductance on secondary side, Ll2} = \mathrm{L22} - \frac{\mathrm{n2}}{\mathrm{n1}}\mathrm{L12} \tag{86}$$

$$\text{Total Leakage inductance on secondary side Ll} = \mathrm{Ll2} + \frac{\mathrm{Ll1}}{\mathrm{n_e^2}} \tag{87}$$

$$\text{Mutual Inductance on Secodary side, Lms} = \frac{\mathrm{Lm}}{\mathrm{n_e^2}} \tag{88}$$

From the inductance matrix, the primary and secondary side self-inductances are computed. The primary and secondary sides are designed as two separate CFIs for the calculated self-inductances. They share the distributed core.

In order to have a good coupling between the primary and secondary windings, the primary and secondary conductors are placed one on top of the other on the surface of the core and one behind the other in the slots, as shown in Fig. 45.

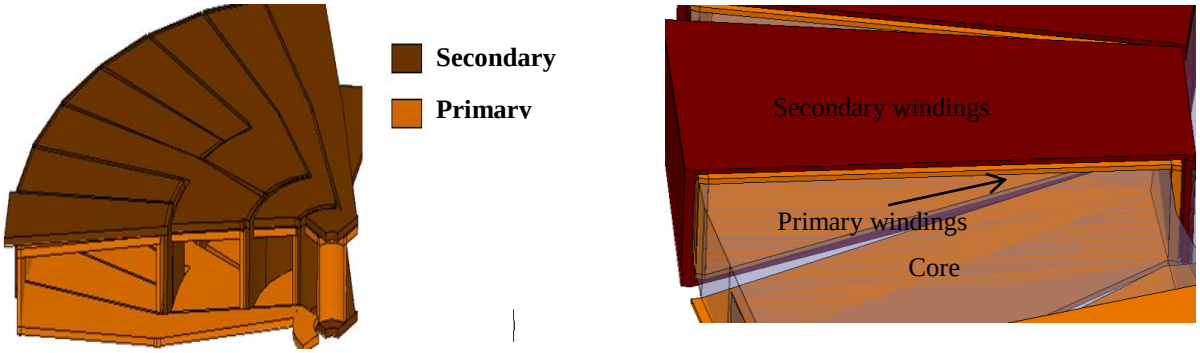

Fig. 45. Winding distribution in quarter of a constant-flux transformer with secondary winding wrapping the primary winding on the surface and in the slots.

7.1 Magnetic Material between Windings to Introduce Leakage

In this case, the secondary winding is wound around the primary winding for maximum magnetic coupling, as shown in Fig. 45. As shown in Fig. 47, the leakage inductance can be controlled by placing a magnetic material in between the primary and secondary windings. Fig. 48 shows the magnetic flux density distribution in the core when one winding is excited and the other winding is kept open.

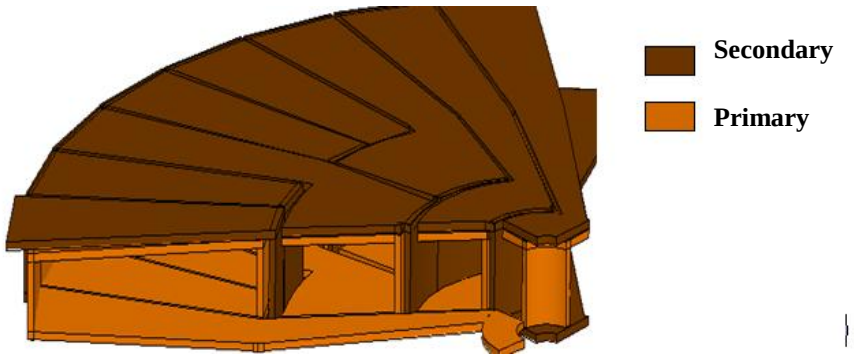

Fig 46. Winding distribution in a quarter of a constant-flux transformer with 4 cells.

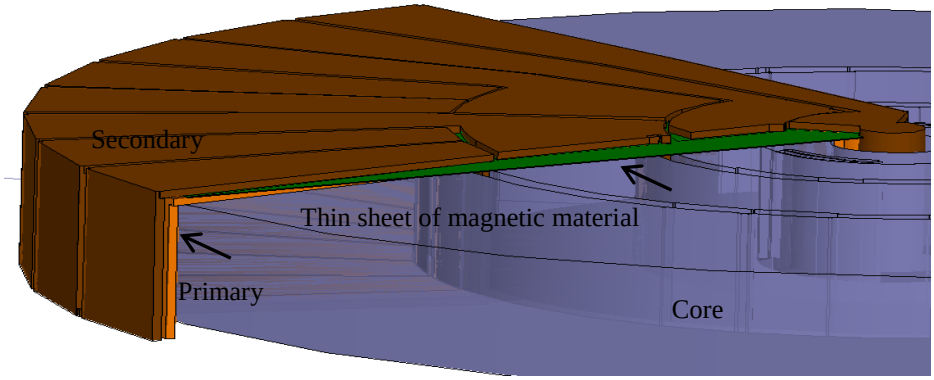

Fig. 47. Thin sheet of magnetic material sandwiched between the primary and secondary windings of a constant-flux transformer with four cells.

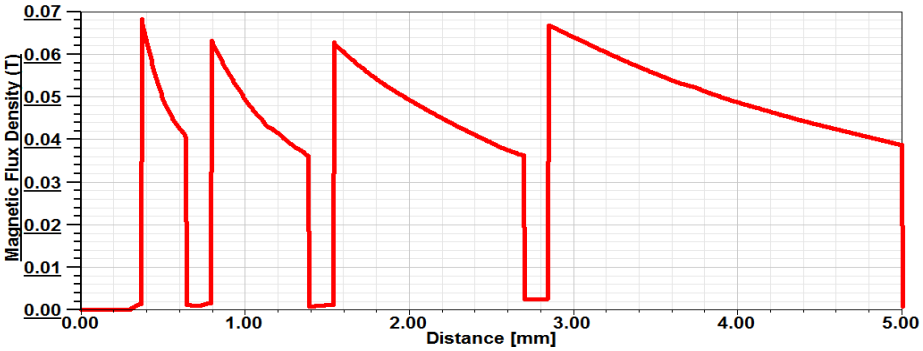

Fig. 48. Magnetic flux density distribution in the core of the constant-flux transformer with four cells.

From the matrix of self and mutual inductance obtained from the simulation results, leakage and magnetizing inductance for the transformer is calculated. With a thin layer of magnetic material of μ=60 between the primary and secondary windings on one side, magnetizing and leakage inductances were obtained. For a leakage inductance of 600 nH, the thickness of the sheet has to be varied. The thin layer of material with a lower permeability can be sandwiched between the windings on the top and bottom to obtain the desired inductances. TABLE XVI summarizes the specifications for the transformer, and TABLE XVII summarizes the inductances obtained from the simulation.

TABLE XVI.
Specifications of Distributed LTCC Transformer

Parameters	**Value**
Turns Ratio	4 :1
Number of turns	32 on the primary; 8 on the secondary
Magnetizing Inductance	600 nH (on the secondary)
Leakage Inductance	100 nH (on the secondary)
Peak Magnetizing current	2.45 A (on the secondary)
Core Height	1 mm
Footprint area	10 mm X 10 mm
Relative Permeability	50

TABLE XVII.
Results from Simulation of Constant-Flux Transformer

Parameter	**Value**
Relative permeability of the thin sheet	60
Thickness of the thin sheet	8 μm
Magnetizing inductance (on the secondary) per thickness of thin sheet	86.13 nH/μm
Leakage Inductance per unit thickness of thin sheet on the secondary	2.29 nH/ μm
Thickness of thin sheet for Ll= 100nH	43 μm

7.2 Example Design of a Constant-Flux Transformer

For a magnetizing and leakage inductance of 600 nH and 100 nH on the secondary side, respectively, primary and secondary self-inductances are 9.6 μH and 700 nH. Inductance of 700 nH on the secondary side is split into 600 nH and 100 nH. Leakage inductance is 100 nH. The leakage inductance can be assumed as an inductor with inductance of 100 nH in series with the secondary winding of the transformer. Leakage inductance is introduced by having the

primary/secondary by itself in a slot or on surface. The specifications of the transformer are listed in TABLE XVIII.

TABLE XVIII.
Specifications of Distributed LTCC Inductor Transformer

Parameters	**Value**
Turns Ratio	4 :1
Magnetizing Inductance (nH)	600 (on the secondary)
Leakage Inductance (nH)	100 (on the secondary)
Peak Magnetizing current (A)	1.1 (on the secondary)
DCR of primary windings (mΩ)	100
DCR of secondary windings (mΩ)	30
Core loss Density for Maximum magnetic flux density of 450 Gauss (mW/cc)	300

TABLE XIX.
Parameters for the Constant-Flux Transformer

Parameters	**Secondary Side**		
Material	LTCC		
Permeability	50		
Bmax (T)	0.015		
Frequency (MHz)	3		
Radii (mm)	Cell no	Rmax	Rmin
	1	20	13.2
	2	12.8	8.5
	3	8.04	5.3
	4	4.92	3.24
	5	2.84	1.87
Ampere turns (A)	Cell No	nI	
	1	6.9	
	2	4.6	
	3	2.3	
	4	2.3	
	5	2.3	
α	0.66		
Footprint area	40.8 mm x 40.8 mm		
Inductance (μH)	654		
Total Height (mm)	1.94		
DCR (mΩ)	5		

The secondary winding is laid on top of the primary winding on the top surface of the core, and the secondary winding is laid on the bottom of the primary winding on the bottom surface of the core such that the secondary winding wraps the primary winding. In the slot, the primary and

secondary are in parallel with respect to the center. The magnetic core material is between the primary and secondary windings in the outermost slot and innermost slot for a thickness of 0.1 mm. For every quadrant, there is one unaccompanied primary winding. These two reasons induce leakage between the two windings.

The ratio of number of turns in the primary and secondary is not always 1:1. Thus, to facilitate good coupling between the windings, one of the windings is paralleled [6, 7, 9, 11]. For a design with turns ratio being 1:4, 4 sets of secondary windings are paralleled, as shown in Fig. 45. Each set is placed on top/below $1/4^{th}$ of the primary windings on the surface. This ensures tight coupling between the windings.

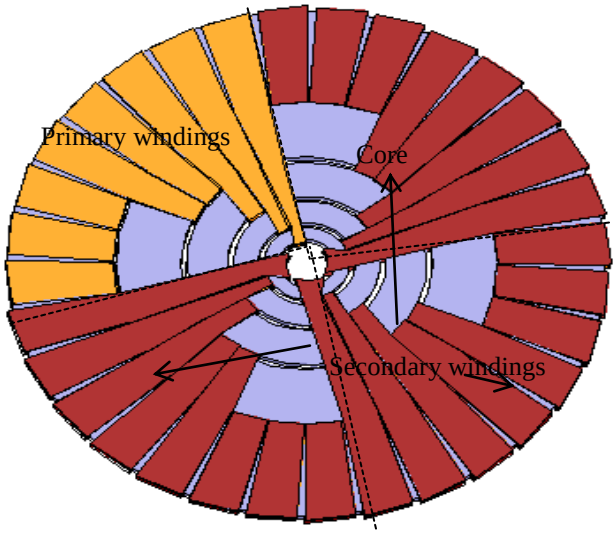

Fig. 49. Constant-flux transformer with four sets of secondary winding paralleled and placed on top of the primary winding.

Paralleling of one of the windings reduces the coupling between each set of the windings. This, in turn, reduces the overall self-inductance. The voltage across the 4 sets of secondary windings, s1, s2, s3, and s4, is Vs, and current through each is one fourth of secondary current (is). The inductance matrix is modified to accommodate for the mutual inductances of each set of secondary windings.

$$Vs1 = Vs2 = Vs3 = Vs4 = \frac{Vs1 + Vs2 + vs3 + Vs4}{4} = Vs \tag{89}$$

$$\mathrm{is1} = \mathrm{is2} = \mathrm{is3} = \mathrm{is4} = \frac{\mathrm{is}}{4} \tag{90}$$

$$\begin{pmatrix} \mathrm{Vp} \\ \mathrm{Vs1} \\ \mathrm{Vs2} \\ \mathrm{Vs3} \\ \mathrm{Vs4} \end{pmatrix} := \begin{pmatrix} \mathbf{Lpp} & \mathrm{Lps1} & \mathrm{Lps2} & \mathrm{Lps3} & \mathrm{Lps4} \\ \mathrm{Lps1} & \mathrm{Ls11} & \mathrm{Ls12} & \mathrm{Ls13} & \mathrm{Ls14} \\ \mathrm{Lps2} & \mathrm{Ls12} & \mathrm{Ls22} & \mathrm{Ls23} & \mathrm{Ls24} \\ \mathrm{Lps3} & \mathrm{Ls13} & \mathrm{Ls23} & \mathrm{Ls33} & \mathrm{Ls34} \\ \mathrm{Lps4} & \mathrm{Ls14} & \mathrm{Ls24} & \mathrm{Ls34} & \mathrm{Ls44} \end{pmatrix} \cdot \frac{\mathrm{d}}{\mathrm{dt}} \begin{pmatrix} \mathrm{ip} \\ \mathrm{is1} \\ \mathrm{is2} \\ \mathrm{is3} \\ \mathrm{is4} \end{pmatrix} \tag{91}$$

$$\begin{pmatrix} \mathrm{Vp} \\ \mathrm{Vs} \end{pmatrix} := \begin{pmatrix} \mathbf{L11} & \mathrm{L12} \\ \mathrm{L12} & \mathrm{L22} \end{pmatrix} \cdot \frac{\mathrm{d}}{\mathrm{dt}} \begin{pmatrix} \mathrm{ip} \\ \mathrm{is} \end{pmatrix} \tag{92}$$

$$\mathrm{Vp} = \mathrm{Lpp}\ \mathrm{ip} + (\mathrm{Lps1} + \mathrm{Lps2} + \mathrm{Lps3} + \mathrm{Lps4}) * \frac{\mathrm{is}}{4} \tag{93}$$

$$\mathrm{Vs} = \mathrm{L12}\ \mathrm{ip} + \mathrm{L22}\ * \mathrm{is} \tag{94}$$

$$\mathrm{L12} = \frac{(\mathrm{Lps1} + \mathrm{Lps2} + \mathrm{Lps3} + \mathrm{Lps4})}{4} \tag{95}$$

$$\mathrm{L22} = \frac{(\mathrm{Ls11} + \mathrm{Ls22} + \mathrm{Ls33} + \mathrm{Ls44})}{16} + \frac{(\mathrm{Ls12} + \mathrm{Ls13} + \mathrm{Ls14} + \mathrm{Ls23} + \mathrm{Ls24} + \mathrm{Ls34})}{8} \tag{96}$$

For the example design, using TABLE XX, the primary and secondary self, leakage and magnetizing inductances are computed.

TABLE XX.
Inductance Matrix for the Transformer Design

Inductance (nH)	p	S1	S2	s3	s4
p	10382	2592	2592	2592	2592
S1	2592	833	607	556	607
S2	2592	607	833	607	556
S3	2592	556	607	833	607
S4	2592	607	556	607	833

L11= 10382 nH; L12 = 2592 nH; L22 = 650 nH;

Here n1 =32; n2 =8

$$\text{Magnetizing Inductance, } \mathrm{LM} = \mathrm{L12} * \frac{\mathrm{n1}}{\mathrm{n2}} = 2592\ * \frac{32}{8} = 10378\ \mathrm{nH}$$

$$\text{Leakage Inductance on primary},\ \text{Ll1} = \text{L11} - \text{L12} * \frac{\text{n1}}{\text{n2}} = 14\ \text{nH}$$

$$\text{Leakage Inductance on secondary},\ \text{Ll2} = \text{L22} - \text{L12} * \frac{\text{n2}}{\text{n1}} = 2.75\ \text{nH}$$

$$\text{effective turns ratio},\ \text{ne} = \sqrt{\frac{\text{L11}}{\text{L22}}} = 3.99$$

The core for the constant-flux transformer can be fabricated as explained in section 2.4. As the windings of the transformer need to overlap for good coupling, the primary and secondary windings can be fabricated using DuPont pyralux tape. DuPont pyralux is a 3-layer material with kapton tape in between copper. Thus, one side of the copper can be used for primary winding, and the other side can be used for secondary winding. The kapton tape provides the insulation. Depending on the required breakdown voltage between the primary and secondary sides, thickness of the kapton tape can be decided.

For measuring the dc resistance of the primary and secondary sides, primary and secondary windings are separately fabricated using DuPont pyralux. Copper on one side of pyralux is completely etched. From a 3D drawing of the distributed windings of the primary and secondary sides (separately), a 2D model is made by flipping all the surfaces to the same plane such that by folding the extended patterns, the 3D model can be re-created. The steps in the fabrication of primary and secondary windings are shown in Fig. 50, Fig 51, Fig. 52, and Fig. 53.

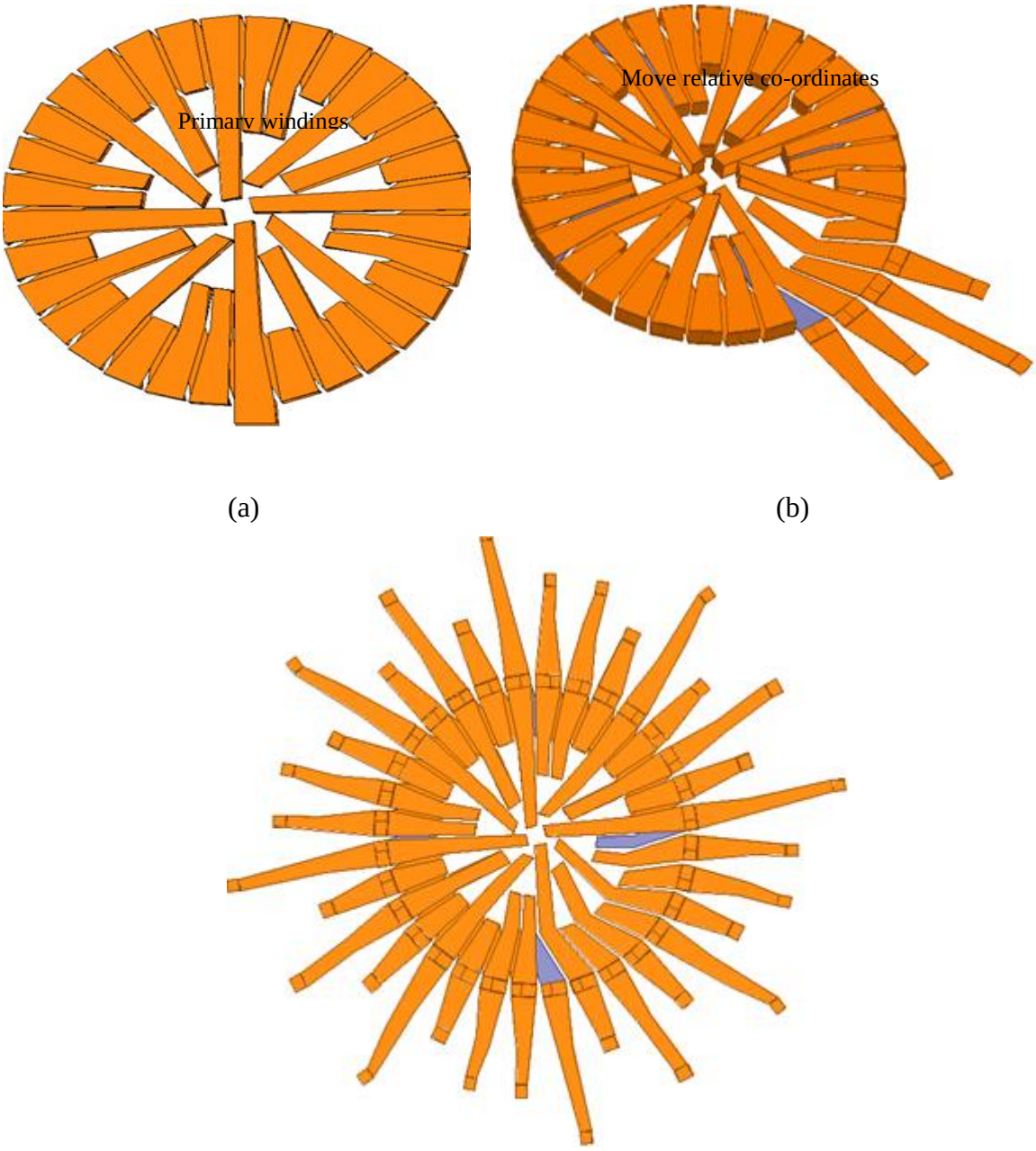

Fig. 50. Steps in the fabrication of distributed winding with 32 turns; (a) 3D model of the distributed winding; (b) Position of the co-ordinates is moved to flip open each surface ; (c) 2D model of the flipped open 3D drawing of the distributed windings.

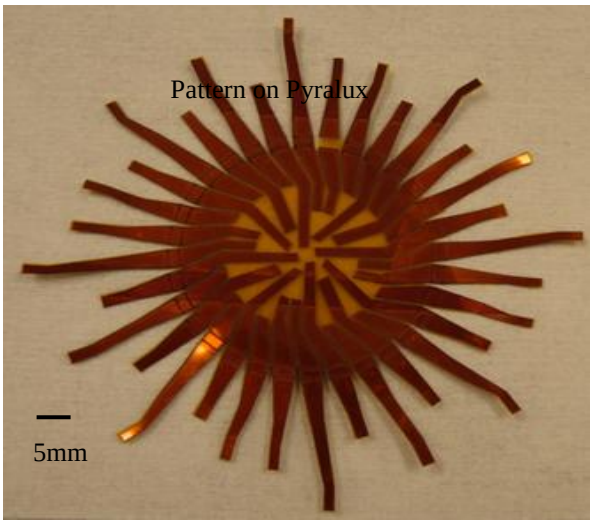

Fig 51. Pattern etched on one side of DuPont pyralux tape of primary side of constant-flux transformer with 32 turns.

(a) (b)

Fig. 52. (a) Top and (b) Bottom sides of the primary winding formed from the DuPont pyralux pattern soldered using eutectic solder (Sn32Pb68).

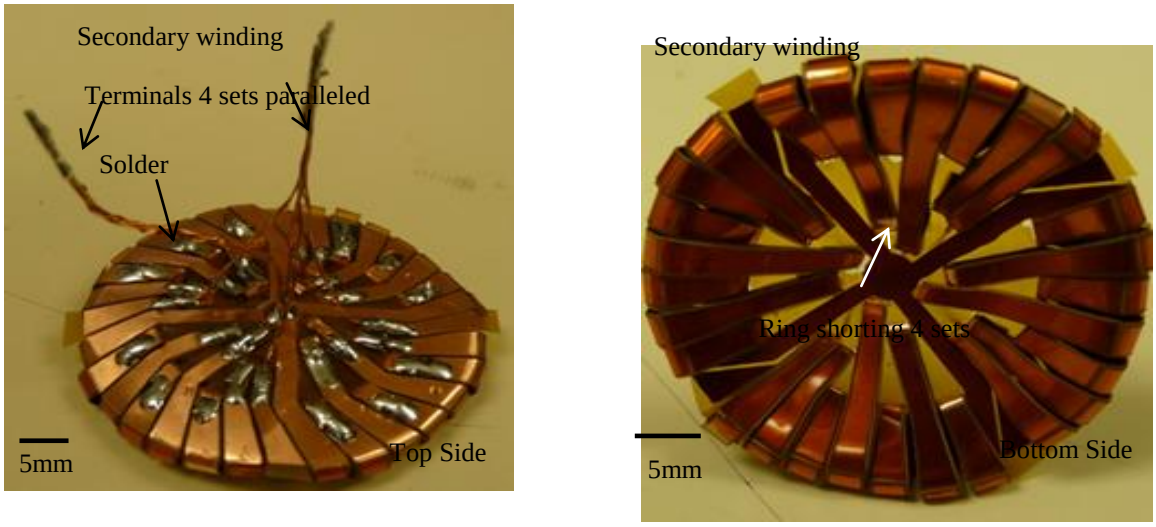

(a) (b)

Fig. 53. (a) Top and (b) Bottom sides of the secondary winding formed from the DuPont pyralux pattern with the ring on bottom side connecting four sets of windings in parallel

TABLE XXI lists the DCR of primary and secondary windings of the fabricated constant-flux transformer.

TABLE XXI.
Measured and Simulated Values of DCR and Inductance on Primary and Secondary Windings

		Primary	Secondary
Number of Turns		32	8 (4 sets in parallel)
Thickness of copper		70 µm	70 µm
DCR	Simulated	80 mΩ	6 mΩ
	Measured	100 mΩ	9 mΩ

8 CONCLUSION

In this thesis a constant-flux inductor/transformer is designed to have a core and winding configuration to achieve a desirable distribution of the magnetic field to store the maximum amount of energy throughout the core volume. Constant-flux and constant-width inductors were discussed in detail. To design an inductor with high inductance (energy) and low loss, it is important to choose optimum values of design parameters such as field ratio α in each cell or width of each cell of the inductor, number of cells, thickness of winding, and height of core. Depending on the application, constant-flux or constant-width inductor can be decided.

For the same maximum magnetic field intensity, the same height, the same total stored energy, and the same material, the footprint area of a three-cell constant-flux toroidal inductor is 1.48 times less than that of an equivalent conventional toroidal inductor. The core loss is at least 1%, and the winding loss is at least 10% smaller in constant-flux inductor. For the same footprint area/volume, a constant-flux inductor stores four times more energy than the conventional toroidal inductor.

The concept of constant-flux inductor was verified using discrete cores. The measured, calculated and simulated inductances were within 3% of each other. A constant-flux inductor for a high-current, high-power application carrying 180 A peak current for operating frequency of 20 KHz was designed to show that the design procedure can be used for designing low and high-power magnetic components. The height of the constant-flux inductor was 20% less than the commercial product of same energy, DCR, and footprint area.

A CFI was designed, simulated, and fabricated using Micrometal-8 with relative permeability of ~ 35 and Bmax = 3600 Gauss. The measured inductance was 1.2 μH. Using 2 round wires of AWG 22 in parallel, the DCR was 8 mΩ with a compromise on height (4.5 mm)

owing to bulging of the thick conductors and overlapping. Using flat wire of 0.97 mm width and 0.24 mm thickness, the DCR was measured as 14.4 mΩ while the height was 2.5 mm.

The construction of the constant-flux transformer for a given leakage and magnetizing inductance using inductance matrix was discussed. A design detail of a constant-flux transformer was discussed for a magnetizing inductance of 600 nH, a leakage inductance of 100 nH, all referred to the secondary side. Using DuPont pyralux, the distributed windings for primary and secondary was fabricated separately. Dc resistance was 100 mΩ on primary side and 9 mΩ on the secondary.

9 FUTURE WORK

The constant-flux inductor designed to be equivalent to the commercially available inductor has a larger DCR for smaller height or vice versa. In order to meet the DCR and have a smaller height, a low-temperature, co-fired ceramic (LTCC) process needs to be employed. In this process, the conductor, silver paste (DuPont 7740), is filled in the slot and printed on the surface. The conductor paste can be fired along with the LTCC green tape (ESL 40010). The surface conductors can be widened to cover the entire surface of the core. Printing multiple times can vary the thickness of the paste. This process of co-firing the green tape and conductor helps control the height and DCR.

A combination of a constant-flux and constant-width inductor or varying field ratio α inductor can be used in the design to store more energy in the outer cells. Also, instead of the toroidal shape for the cells, "squaroid" can be used, which helps store energy even at the corners.

For the constant-flux transformer, the primary windings and the distributed core can be co-fired using LTCC – ESL 40010 and DuPont 7740. The secondary winding can be made using the DuPont pyralux circuit, as explained in chapter 4. In order to achieve the required breakdown voltage between the two, the transformer can be dipped into epoxy/ encapsulant with high breakdown voltage.

APPENDIX A: STEPS TO DRAW THE WINDINGS OF A DISTRIBUTED INDUCTOR IN ANSOFT MAXWELL.

Steps to draw windings for a toroidal inductor using Ansoft Maxwell 12.[35]

Step 1: Obtain the dimensions and number of turns of the structure.

Step 2: Open a 3D project in Ansoft Maxwell 12.

Step 3: Draw the core/cell by drawing cylinders with radius of minimum and maximum radius of the cell. The height of the cylinder is the height of the core/cell. Subtract the smaller cylinder from the larger cylinder.

Step4: Assign material properties to the core.

Step 5: To draw the windings of the cylinder, draw the outline of the slot on one surface, and sweep it along the height to form the conductor in the slot.

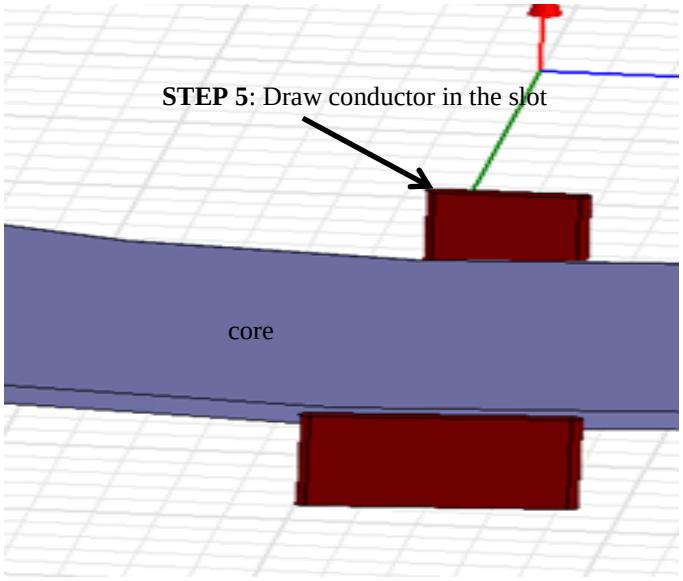

Fig. 54 Step 5: Draw conductor in the slots between the core cells.

Step 6: Copy, paste, and rotate the conductor in the outer slot by the slot angle (= 360 deg/total number of ampere-turns). Connect the conductor in the inner slot with the conductors in the outer slots by drawing conductor on the surface (sheet) and sweeping it for thickness of the conductor on top and on bottom, forming one-ampere turn around the cell.

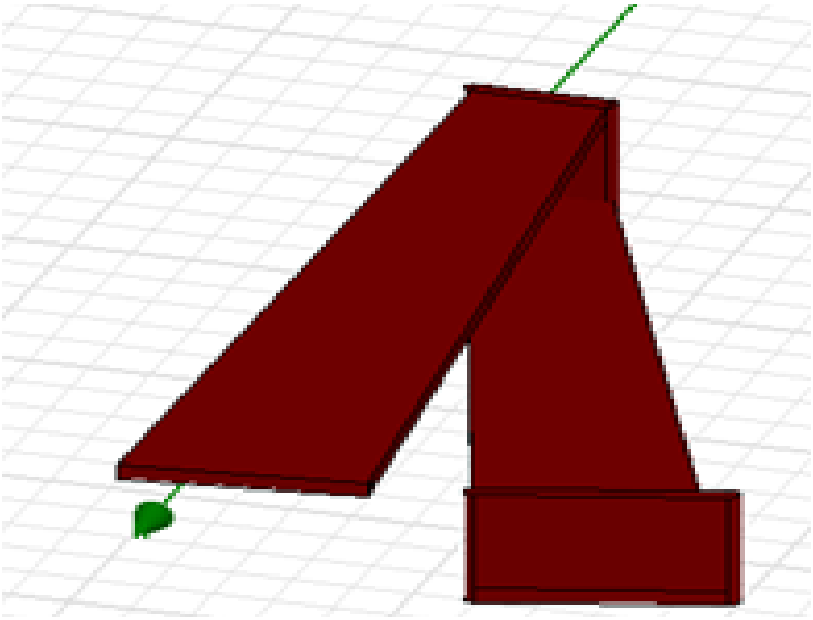

Fig. 55 Connect the conductor in the slots by drawing conductor on surface- forms one turn.

Step 7: Duplicate the one-turn to the desired number of turns with angle of rotation being slot angle.

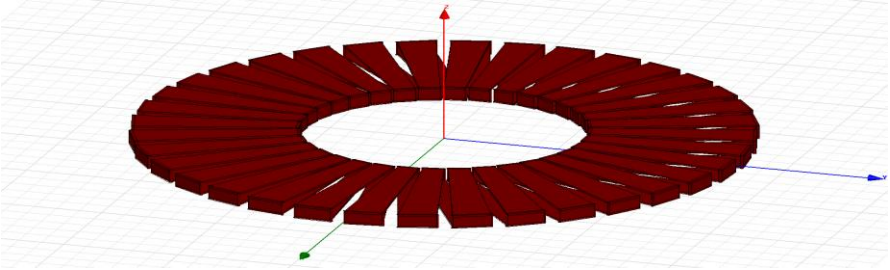

Fig. 56 Duplicate one turn to 36 with an angle of 10 deg per turn. For the constant-flux inductor, follow same steps for each cell. Instead of sweeping by 360 deg, copy and rotate one-turn to the required angle.

Step 8: Remove the conductor on the surface from one of the turns. Unite all the turns. This forms the winding structure.

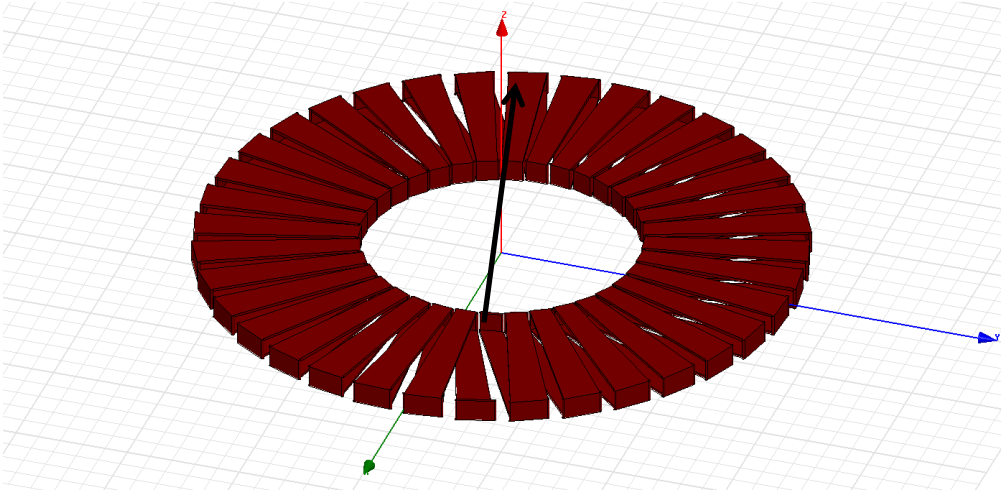

Fig. 57: Remove conductor on surface for one turn for terminal and unite.

Step 9: Excitation is given to the open faces of conductor in the slot from where the surface conductor was removed.

Step 10: Give “region” as boundary condition.

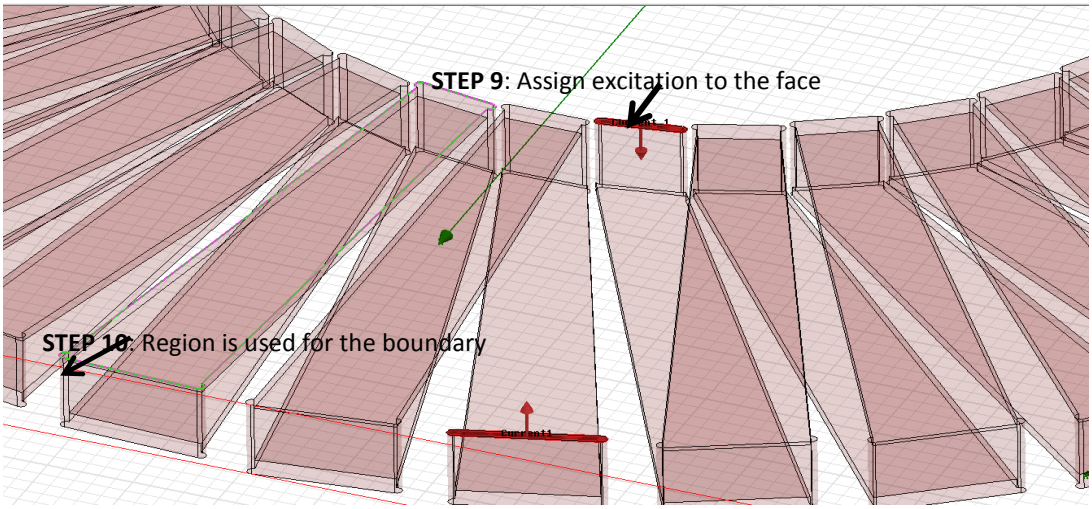

Fig. 58**:** Assign excitation to the face. Region is used for the boundary.

Step 11: Add a solution step for analysis and analyze all.

Step 12: To obtain a line plot of magnetic flux density or energy in the core, draw a line in the desired region. In the results section, add a rectangular plot and select the field and the line for the plot.

APPENDIX B: MATLAB CODES

Matlab codes mentioned in section 4.1

GUI:

```
function varargout = gui_1(varargin)
gui_Singleton = 1;
gui_State = struct('gui_Name',       mfilename, ...
    'gui_Singleton',  gui_Singleton, ...
    'gui_OpeningFcn', @gui_1_OpeningFcn, ...
    'gui_OutputFcn',  @gui_1_OutputFcn, ...
    'gui_LayoutFcn',  [] , ...
    'gui_Callback',   []);
if nargin && ischar(varargin{1})
    gui_State.gui_Callback = str2func(varargin{1});
end

if nargout
    [varargout{1:nargout}] = gui_mainfcn(gui_State, varargin{:});
else
    gui_mainfcn(gui_State, varargin{:});
end
function gui_1_OpeningFcn(hObject, eventdata, handles, varargin)
 handles.output = hObject;
 guidata(hObject, handles);
function varargout = gui_1_OutputFcn(hObject, eventdata, handles)
varargout{1} = handles.output;
function L_in_Callback(hObject, eventdata, handles)
input = str2num(get(hObject,'String'));
 if (isempty(input))
    set(hObject,'String','0')
 end
guidata(hObject, handles);

function L_in_CreateFcn(hObject, eventdata, handles)
if ispc && isequal(get(hObject,'BackgroundColor'),
get(0,'defaultUicontrolBackgroundColor'))
```

```
    set(hObject,'BackgroundColor','white');
end
function Ipeak_in_Callback(hObject, eventdata, handles)
 input = str2num(get(hObject,'String'));
 if (isempty(input))
    set(hObject,'String','0')
end
guidata(hObject, handles);
function Ipeak_in_CreateFcn(hObject, eventdata, handles)

if ispc && isequal(get(hObject,'BackgroundColor'),
get(0,'defaultUicontrolBackgroundColor'))
    set(hObject,'BackgroundColor','white');
end

function Irms_in_Callback(hObject, eventdata, handles)
input = str2num(get(hObject,'String'));

if (isempty(input))
    set(hObject,'String','0')
end
guidata(hObject, handles);

function Irms_in_CreateFcn(hObject, eventdata, handles)
if ispc && isequal(get(hObject,'BackgroundColor'),
get(0,'defaultUicontrolBackgroundColor'))
    set(hObject,'BackgroundColor','white');
end

function Rmax_in_Callback(hObject, eventdata, handles)
input = str2num(get(hObject,'String'));
%checks to see if input is empty. if so, default input1_editText to zero
if (isempty(input))
    set(hObject,'String','0')
end
guidata(hObject, handles);
```

```
% --- Executes during object creation, after setting all properties.
function Rmax_in_CreateFcn(hObject, eventdata, handles)
if ispc && isequal(get(hObject,'BackgroundColor'),
get(0,'defaultUicontrolBackgroundColor'))
    set(hObject,'BackgroundColor','white');
end

function hmax_in_Callback(hObject, eventdata, handles)
input = str2num(get(hObject,'String'));

if (isempty(input))
    set(hObject,'String','0')
end
guidata(hObject, handles);

% --- Executes during object creation, after setting all properties.
function hmax_in_CreateFcn(hObject, eventdata, handles)

if ispc && isequal(get(hObject,'BackgroundColor'),
get(0,'defaultUicontrolBackgroundColor'))
    set(hObject,'BackgroundColor','white');
end

function mat_in_Callback(hObject, eventdata, handles)
input = str2num(get(hObject,'String'));

%checks to see if input is empty. if so, default input1_editText to zero
if (isempty(input))
    set(hObject,'String','0')
end
guidata(hObject, handles);

% --- Executes during object creation, after setting all properties.
function mat_in_CreateFcn(hObject, eventdata, handles)
if ispc && isequal(get(hObject,'BackgroundColor'),
get(0,'defaultUicontrolBackgroundColor'))
    set(hObject,'BackgroundColor','white');
end
```

```
function f_in_Callback(hObject, eventdata, handles)
input = str2num(get(hObject,'String'));

if (isempty(input))
    set(hObject,'String','0')
end
guidata(hObject, handles);

% --- Executes during object creation, after setting all properties.
function f_in_CreateFcn(hObject, eventdata, handles)
if ispc && isequal(get(hObject,'BackgroundColor'),
get(0,'defaultUicontrolBackgroundColor'))
    set(hObject,'BackgroundColor','white');
end

function ucore_in_Callback(hObject, eventdata, handles)
  input = str2num(get(hObject,'String'));

if (isempty(input))
    set(hObject,'String','0')
end
guidata(hObject, handles);

% --- Executes during object creation, after setting all properties.
function ucore_in_CreateFcn(hObject, eventdata, handles)
if ispc && isequal(get(hObject,'BackgroundColor'),
get(0,'defaultUicontrolBackgroundColor'))
    set(hObject,'BackgroundColor','white');
end

function Bmax_in_Callback(hObject, eventdata, handles)
input = str2num(get(hObject,'String'));

if (isempty(input))
    set(hObject,'String','0')
end
```

```
guidata(hObject, handles);

% --- Executes during object creation, after setting all properties.
function Bmax_in_CreateFcn(hObject, eventdata, handles)
if ispc && isequal(get(hObject,'BackgroundColor'),
get(0,'defaultUicontrolBackgroundColor'))
    set(hObject,'BackgroundColor','white');
end

function DCR_in_Callback(hObject, eventdata, handles)
input = str2num(get(hObject,'String'));

if (isempty(input))
    set(hObject,'String','0')
end
guidata(hObject, handles);

% --- Executes during object creation, after setting all properties.
function DCR_in_CreateFcn(hObject, eventdata, handles)
if ispc && isequal(get(hObject,'BackgroundColor'),
get(0,'defaultUicontrolBackgroundColor'))
    set(hObject,'BackgroundColor','white');
end

function k_in_Callback(hObject, eventdata, handles)
input = str2num(get(hObject,'String'));

if (isempty(input))
    set(hObject,'String','0')
end
guidata(hObject, handles);
% --- Executes during object creation, after setting all properties.
function k_in_CreateFcn(hObject, eventdata, handles)
if ispc && isequal(get(hObject,'BackgroundColor'),
get(0,'defaultUicontrolBackgroundColor'))
    set(hObject,'BackgroundColor','white');
end
```

```
function alpha_in_Callback(hObject, eventdata, handles)
input = str2num(get(hObject,'String'));

if (isempty(input))
    set(hObject,'String','0')
end
guidata(hObject, handles);


% --- Executes during object creation, after setting all properties.
function alpha_in_CreateFcn(hObject, eventdata, handles)
if ispc && isequal(get(hObject,'BackgroundColor'),
get(0,'defaultUicontrolBackgroundColor'))
    set(hObject,'BackgroundColor','white');
end

function beta_in_Callback(hObject, eventdata, handles)
input = str2num(get(hObject,'String'));

if (isempty(input))
    set(hObject,'String','0')
end
guidata(hObject, handles);
% --- Executes during object creation, after setting all properties.
function beta_in_CreateFcn(hObject, eventdata, handles)
if ispc && isequal(get(hObject,'BackgroundColor'),
get(0,'defaultUicontrolBackgroundColor'))
    set(hObject,'BackgroundColor','white');
end

function coreloss_in_Callback(hObject, eventdata, handles)
input = str2num(get(hObject,'String'));

if (isempty(input))
    set(hObject,'String','0')
end
```

```
guidata(hObject, handles);
% --- Executes during object creation, after setting all properties.
function coreloss_in_CreateFcn(hObject, eventdata, handles)
if ispc && isequal(get(hObject,'BackgroundColor'),
get(0,'defaultUicontrolBackgroundColor'))
    set(hObject,'BackgroundColor','white');
end
function thickness_in_Callback(hObject, eventdata, handles)
input = str2num(get(hObject,'String'));

if (isempty(input))
    set(hObject,'String','0')
end
guidata(hObject, handles);

% --- Executes during object creation, after setting all properties.
function thickness_in_CreateFcn(hObject, eventdata, handles)
if ispc && isequal(get(hObject,'BackgroundColor'),
get(0,'defaultUicontrolBackgroundColor'))
    set(hObject,'BackgroundColor','white');
end

function voltage_in_Callback(hObject, eventdata, handles)
input = str2num(get(hObject,'String'));

if (isempty(input))
    set(hObject,'String','0')
end
guidata(hObject, handles);
% --- Executes during object creation, after setting all properties.
function voltage_in_CreateFcn(hObject, eventdata, handles)
if ispc && isequal(get(hObject,'BackgroundColor'),
get(0,'defaultUicontrolBackgroundColor'))
    set(hObject,'BackgroundColor','white');
end
```

```
function angle_in_Callback(hObject, eventdata, handles)
input = str2num(get(hObject,'String'));

if (isempty(input))
    set(hObject,'String','0')
end
guidata(hObject, handles);

% --- Executes during object creation, after setting all properties.
function angle_in_CreateFcn(hObject, eventdata, handles)
if ispc && isequal(get(hObject,'BackgroundColor'),
get(0,'defaultUicontrolBackgroundColor'))
    set(hObject,'BackgroundColor','white');
end

% --- Executes on button press in cal_push.
function cal_push_Callback(hObject, eventdata, handles)
L_1 = str2num(get(handles.L_in,'String'));
Ipeak_1 = str2num(get(handles.Ipeak_in,'String'));
Irms_1 = str2num(get(handles.Irms_in,'String'));
Rmax_1 = str2num(get(handles.Rmax_in,'String'));
hmax_1 = str2num(get(handles.hmax_in,'String'));
mat_1 = str2num(get(handles.mat_in,'String'));
f_1 = str2num(get(handles.f_in,'String'));
Bmax_1 = str2num(get(handles.Bmax_in,'String'));
ucore_1 = str2num(get(handles.ucore_in,'String'));
DCR_1 = str2num(get(handles.DCR_in,'String'));
thickness_1 = str2num(get(handles.thickness_in,'String'));
%voltage_1 = str2num(get(handles.voltage_in,'String'));
angle_1 = str2num(get(handles.angle_in,'String'));
k_1 = str2num(get(handles.k_in,'String'));
alpha_1 = str2num(get(handles.alpha_in,'String'));
beta_1 = str2num(get(handles.beta_in,'String'));
coreloss_1 = str2num(get(handles.coreloss_in,'String'));
max_alpha_1=str2num(get(handles.max_alpha_in,'String'));
min_alpha_1=str2num(get(handles.min_alpha_in,'String'));
min_cell_1=str2num(get(handles.min_cell_in,'String'));
max_cell_1=str2num(get(handles.max_cell_in,'String'));
```

```
[Output]=check(L_1, Ipeak_1, Irms_1, Rmax_1, hmax_1, mat_1, f_1, Bmax_1,
ucore_1, DCR_1,thickness_1,  angle_1, k_1, alpha_1, beta_1,
coreloss_1,min_alpha_1, max_alpha_1, min_cell_1, max_cell_1); %calls the
function check to design the Distributed Inductor

if (Output.flag==1)
    set(handles.mess,'String',Output.mess);

else
    set(handles.mess,'String',Output.mess);
end
    Lout=num2str(Output.Lm);
    Rcopperout=num2str(round(Output.Rcopper*1000)/1000);
    Pcopperout=num2str(round(Output.Pcopper*1000)/1000);
    Pcoreout=num2str(round(Output.Pcore*1000)/1000);
    ucoreout=num2str(round(Output.ucore*1000)/1000);
    alphaout=num2str(Output.alpha);
    Hmaxout=num2str(Output.height);
    PracR_round=num2str(Output.PracR_round);
    PracR_flat=num2str(Output.PracR_flat);
    core_height=num2str(Output.core_height);
    overall_fp=num2str(Output.overall_fp);
    overall_fp2=num2str(Output.overall_fp);
    width_flat=num2str(Output.width_flat);
    Length_DI=num2str(Output.Length_DI);
    N_DI=num2str(Output.N_DI);
    QF_DI=num2str(Output.QF_DI);

    set(handles.L_out,'String',Lout);
    set(handles.Rcopper_out,'String',Rcopperout);
    set(handles.Pcopper_out,'String',Pcopperout);
    set(handles.Pcore_out,'String',Pcoreout);
    set(handles.Hmax_out,'String',Hmaxout);
    set(handles.ucore_out,'String',ucoreout);
    set(handles.alpha_out,'String',alphaout);
    set(handles.Length_DI,'String',Length_DI);
```

```
    set(handles.PracR_flat,'String',PracR_flat);
    set(handles.core_height,'String',core_height);
    set(handles.overall_fp,'String',overall_fp);
    set(handles.overall_fp2,'String',overall_fp2);
    set(handles.width_flat,'String',width_flat);
   set(handles.N_DI,'String',N_DI);
   set(handles.QF_DI,'String',QF_DI);
    for i=1:Output.a;
        eval(['set(handles.cell_' num2str(i) ','''String''',' num2str(i) ')']);
        eval(['set(handles.Rmax_' num2str(i) ','''String''', Output.Rmax'
num2str(i) ')']);
        eval(['set(handles.Rmin_' num2str(i) ','''String''', Output.Rmin'
num2str(i) ')']);
        eval(['set(handles.n_' num2str(i) ','''String''', Output.n' num2str(i)
')']);
         eval(['set(handles.draw_Rmax_' num2str(i) ','''String''',
Output.Rmaxdraw' num2str(i) ')']);
          eval(['set(handles.draw_Rmin_' num2str(i) ','''String''',
Output.Rmindraw' num2str(i) ')']);
    end
Lcc2=num2str(Output.Lcc);
Rcmin=num2str(Output.cRmin);
Rcmax=num2str(Output.cRmax);

Ncc2=num2str(Output.Ncc);
rfpa=num2str(Output.fpac);
alphac=num2str(Output.calpha);
QF_c=num2str(Output.QF_c);
length_c=num2str(Output.length_c);
DCR_round=num2str(Output.DCR_round);
DCR_flat=num2str(Output.DCR_flat);
Copper_loss_c=num2str(Output.Copper_loss_c);
pcorec=num2str(Output.pcorec);
core_height_c=num2str(Output.core_height_c);
inductor_height_c=num2str(Output.inductor_height_c);
fp_1=num2str(Output.fp_1);
fp_2=num2str(Output.fp_2);
```

```
set(handles.Lcc,'String',Lcc2);
    set(handles.Rcmin,'String',Rcmin);
    set(handles.Rcmax,'String',Rcmax);

    set(handles.Ncc,'String',Ncc2);
    set(handles.fpa,'String',rfpa);
    set(handles.alphac,'String',alphac);
    set(handles.core_height_c,'String',core_height_c);
    set(handles.length_c,'String',length_c);
    set(handles.DCR_round,'String',DCR_round);
    set(handles.DCR_flat,'String',DCR_flat);
    set(handles.Copper_loss_c,'String',Copper_loss_c);
    set(handles.pcorec,'String',pcorec);
    set(handles.QF_c,'String',QF_c);
    set(handles.inductor_height_c,'String',inductor_height_c);
    set(handles.fp_1,'String',fp_1);
    set(handles.fp_2,'String',fp_2);
guidata(hObject, handles);
% --- Executes on button press in new.
function new_Callback(hObject, eventdata, handles)

%inputs to zero
Input.L=0;
Input.Ipeak=0;
Input.Irms=0;
Input.mat=1;
Input.hmax=0;
Input.Rmax=0;
Input.v=0;
Input.alpha=0;
Input.beta=0;
Input.k=0;
Input.coreloss=0;
Input.thickness=0;
Input.DCR=0;
Input.f=0;
Input.maxalpha=0.99;
Input.minalpha=0.6;
```

```
Input.maxcell=5;
Input.mincell=4;

set(handles.L_in,'String',Input.L);
set(handles.Ipeak_in,'String',Input.Ipeak);
set(handles.Rmax_in,'String',Input.Rmax);
set(handles.hmax_in,'String',Input.hmax);
set(handles.mat_in,'String',Input.mat);
set(handles.voltage_in,'String',Input.v);
set(handles.DCR_in,'String',Input.DCR);
set(handles.thickness_in,'String',Input.thickness);
set(handles.coreloss_in,'String',Input.coreloss);
set(handles.k_in,'String',Input.k);
set(handles.alpha_in,'String',Input.alpha);
set(handles.beta_in,'String',Input.beta);
set(handles.Irms_in,'String',Input.Irms);
set(handles.f_in,'String',Input.f);
set(handles.max_alpha_in,'String',Input.maxalpha);
set(handles.max_cell_in,'String',Input.maxcell);
set(handles.min_alpha_in,'String',Input.minalpha);
set(handles.min_cell_in,'String',Input.maxcell);

%output to zero
Output.mess= ' ';
set(handles.mess,'String',Output.mess);
Output.Lm=0;
Output.Rcopper=0;
Output.Pcopper=0;
Output.Pcore=0;
Output.ucore=0;
Output.alpha=0;
Output.height=0;
Output.a=7;
Output.PracR_round=0;
Output.PracR_flat=0;
Output.parallel=0;
for i=1:Output.a;
    eval(['Output.cell' num2str(i) '='' '' ' ]);
```

```
    eval(['Output.Rmax' num2str(i) '='' '' ' ]);
    eval(['Output.Rmin' num2str(i) '='' '' ']);
    eval(['Output.n' num2str(i) '='' '' ']);
    eval(['Output.Rmaxdraw' num2str(i) '='' '' ' ]);
    eval(['Output.Rmindraw' num2str(i) '='' '' ' ]);
end

Lout=(Output.Lm);
Rcopperout=Output.Rcopper;
Pcopperout=(Output.Pcopper);
Pcoreout=(Output.Pcore);
ucoreout=(Output.ucore);
alphaout=(Output.alpha);
Hmaxout=(Output.height);
PracRout_round=(Output.PracR_round);
PracRout_flat=(Output.PracR_flat);
parallel_out=(Output.parallel);
set(handles.L_out,'String',Lout);
set(handles.Rcopper_out,'String',Rcopperout);
set(handles.Pcopper_out,'String',Pcopperout);
set(handles.Pcore_out,'String',Pcoreout);
set(handles.Hmax_out,'String',Hmaxout);
set(handles.ucore_out,'String',ucoreout);
set(handles.alpha_out,'String',alphaout);
set(handles.PracR_round,'String',PracRout_round);
set(handles.PracR_flat,'String',PracRout_flat);
set(handles.parallel,'String',parallel_out);
for i=1:Output.a;
    eval(['set(handles.cell_' num2str(i) ',''String'','' '' )']);
    eval(['set(handles.Rmax_' num2str(i) ',''String'', Output.Rmax'
num2str(i) ')']);
    eval(['set(handles.Rmin_' num2str(i) ',''String'', Output.Rmin'
num2str(i) ')']);
    eval(['set(handles.n_' num2str(i) ',''String'', Output.n' num2str(i)
')']);
    eval(['set(handles.draw_Rmax_' num2str(i) ',''String'', Output.Rmaxdraw'
num2str(i) ')']);
```

```
    eval(['set(handles.draw_Rmin_' num2str(i) ','''String''', Output.Rmindraw'
num2str(i) ')']);
end
%Conventional
Lcc=0;
Rcmin=0;
Rcmax=0;
Ncc=0;
rfpa=0;
alphac=0;
set(handles.Lcc,'String',Lcc);
    set(handles.Rcmin,'String',Rcmin);
    set(handles.Rcmax,'String',Rcmax);

    set(handles.Ncc,'String',Ncc);
    set(handles.fpa,'String',rfpa);
    set(handles.alphac,'String',alphac);
    set(handles.pcorec,'string',pcorec);
guidata(hObject, handles);




function max_alpha_in_Callback(hObject, eventdata, handles)
input = str2num(get(hObject,'String'));

if (isempty(input))
    set(hObject,'String','0')
end
guidata(hObject, handles);

function max_alpha_in_CreateFcn(hObject, eventdata, handles)
if ispc && isequal(get(hObject,'BackgroundColor'),
get(0,'defaultUicontrolBackgroundColor'))
    set(hObject,'BackgroundColor','white');
end

function min_alpha_in_CreateFcn(hObject, eventdata, handles)
```

```
input = str2num(get(hObject,'String'));

if (isempty(input))
    set(hObject,'String','0')
end
guidata(hObject, handles);

function max_cell_in_Callback(hObject, eventdata, handles)
input = str2num(get(hObject,'String'));

if (isempty(input))
    set(hObject,'String','0')
end
guidata(hObject, handles);

function max_cell_in_CreateFcn(hObject, eventdata, handles)

if ispc && isequal(get(hObject,'BackgroundColor'),
get(0,'defaultUicontrolBackgroundColor'))
    set(hObject,'BackgroundColor','white');
end



function min_cell_in_Callback(hObject, eventdata, handles)
input = str2num(get(hObject,'String'));

if (isempty(input))
    set(hObject,'String','0')
end
guidata(hObject, handles);


function min_cell_in_CreateFcn(hObject, eventdata, handles)

if ispc && isequal(get(hObject,'BackgroundColor'),
get(0,'defaultUicontrolBackgroundColor'))
    set(hObject,'BackgroundColor','white');
```

```
end

function min_alpha_in_Callback(hObject, eventdata, handles)
```

Check:

```
% Inputs are taken from GUI;
% Energy=> Inductance, Voltage; Copper Loss; Core loss are calculated
% Quality factor is determimed

function [Output]=check(L_1, Ipeak_1, Irms_1, Rmax_1, hmax_1, mat_1, f_1,
Bmax_1, ucore_1, DCR_1,thickness_1,  angle_1, k_1, alpha_1, beta_1,
coreloss_1,min_alpha_1, max_alpha_1, min_cell_1, max_cell_1) %calls the
function check to design the Distributed Inductor

%storing Inputs
u0=4e-7*pi;
p=1.72e-8;

Lwant=L_1;
Idc=Irms_1; %dc current
Ipeak=Ipeak_1/2;
Ipeak2=Idc+Ipeak;
Irms=(Ipeak2)/1.414;
%v= voltage_1;
angle=angle_1;

Ewant=0.5*Lwant*Ipeak2^2;

Rmaxwant=(Rmax_1-thickness_1)*0.001/2;
Rwant=15e-3:1e-3:Rmaxwant; % you can change the starting maximum radius

hmaxwant=(hmax_1-2*thickness_1)*0.001;
height=15e-3:0.5e-3:hmaxwant;%you can change the starting maximum height
%hmaxwant=hmax_1;%input

material=mat_1;
Nmincell=min_cell_1; %min number of cells
Ncell=max_cell_1; % maximum number of cells
```

```
alpha=min_alpha_1:0.05:max_alpha_1;

f=f_1*1000000; %frequency of operation
DCR_want=DCR_1*0.001; % DCR wanted
t=thickness_1*0.001;

if t==0
    tcu=0.1319/sqrt(f); % thickness of coper wrt skin epth
else
    tcu=t;
end
%1= LTCC 50; 2= 4F1; 3= Koool Mu u<60; 4 Kool Mu u>60;

if material ==1
    Bmax=0.015;
    %     Bmax=0.0075;
    %     Bmax=0.010;
    beta=2.715;
    K=0.1094;
    al=1.296;
    f_p=f/1000000; %in MHz
    Bmaxp=Bmax*1000; % in mT
    ucore=[50];

%ucore=[1,2,3,4,5,6,7,8,9,10,11,12,13,14,15,16,17,18,19,20,21,22,23,24,25,26,
27,28,29,30];
elseif material==2
    f=3e6;
    Bmax=0.02;
    beta=2.902;
    K=0.0292;
    al=1.599;
    f_p=f/1000000; %in MHz
    Bmaxp=Bmax*1000; %in mT
    ucore=[80];
elseif material ==3
    Bmax=0.36;
```

```
    ucore=[1:0.1:100];
    beta=0;
    K=0;
    al=0;
    f_p=f/1000000; %in MHz
    Bmaxp=Bmax*1000; % in mT

elseif material ==0
    Bmax=Bmax_1;
    ucore=[ucore_1];
    beta=beta_1;
    K=k_1;
    al=alpha_1;
    f_p=f/1000000; %in MHz
    Bmaxp=Bmax*1000; % in mT

elseif material ==4
    Bmax=Bmax_1;
    ucore=[ucore_1];
    beta=2;
    K=120;
    al=1.46;
    f_p=f/1000; %in KHz
    Bmaxp=Bmax; % in KGauss
end
if coreloss_1==0 % if core loss need no be considered
    beta=0;
    K=0;
    al=0;
end
v=0;
if v>0 % if transformer volta second balance is used
    slot=2*tcu+0.150e-3; %2 windings of equal thickness considered, Gap
between the windings and winding and slot edge is approximated  to 0.05um.
    vmin=v*0.9;
    vmax=v*1.1;
else % if desiging Inductor, voltsecond is not considered
    slot=tcu+0.10e-3;
```

```
    vmin=0;
    vmax=10000;
end
slot=0.5e-3;
flag=0;
flag2=0;
k=0;
for Rout=1:size(Rwant,2)
    Rmaxwant=Rwant(Rout);

    for uIndex=1:size(ucore,2)
        u=ucore(uIndex)*u0;
        Hmax=Bmax/u; %fixing the max H

        for hIndex=1:size(height,2)
            h=height(hIndex);
            Rside_hconstant=(p*h/(2*pi*tcu));
            E_hconstant=u*pi*h*Hmax^2;
            v_hconstant=4*f*h*Bmax;

            for aIndex=1:size(alpha,2)
                a=alpha(aIndex);
                %initiaizing all the values
                Rcon=0;
                Rside=0;
                Vcore=0;
                Pcopper=0;
                Pcore=0;
                Rmax=Rmaxwant;
                rmin=Rmax*a;
                Rmin=rmin;
                E=0;
                Voltage=0;
                L=0;
                i=1;
                N=round(Hmax*2*pi*Rmin/Ipeak2);
                n=N;
                Rcopper=0;
```

```
                count=0;
                length_1=0;
                while(Rmin>1.1*tcu) %the limit of 1.1 chosen so that it fits
the conductor

                    R_1(Rout,uIndex,hIndex,aIndex,i)=Rmax;
                    Rmin_1(Rout,uIndex,hIndex,aIndex,i)=Rmin;
                    N_1(Rout,uIndex,hIndex,aIndex,i)=N;
                    n_1(Rout,uIndex,hIndex,aIndex,i)=n;
                    Rmaxdraw(Rout,uIndex,hIndex,aIndex,i)=1.20*Rmax; % 20%
shrinkage is considered
                    Rmindraw(Rout,uIndex,hIndex,aIndex,i)=1.20*Rmin;

                    if(i>1)
                        n=N_1(Rout,uIndex,hIndex,aIndex,i-1)-
N_1(Rout,uIndex,hIndex,aIndex,i);
                        n_1(Rout,uIndex,hIndex,aIndex,i-1)=n;

Rside=Rside_hconstant*(n^2/(Rmin_1(Rout,uIndex,hIndex,aIndex,i-1)-(slot/2)));
                    end
                    if(i==1)
                        Rside=Rside_hconstant*(n^2/(Rmax+(slot/2)));
%resistance due toconuctor in via
                    end

                    E=E+E_hconstant*((Rmin)^2*log(Rmax/Rmin)); %energy in
each cell is added
                    Voltage=Voltage + v_hconstant*n*(Rmaxwant-Rmin);


                    % Ideal Copper loss

                    Rcon=(N^2*log((Rmax+tcu)/(Rmin-tcu))*p/(pi*tcu)); %
resistance due to conductor on surface
                    Rcopper=Rcopper+Rcon+Rside;

                    Hmaxp=Bmaxp/u;
```

```
                    % Core loss
                    if (material ==1 || material ==2 )

Pcore=Pcore+1000*K*2*pi*h*(f_p^al)*(u*Hmax*Rmin*10^3)^beta*(Rmax^(2-beta)-
Rmin^(2-beta))/(2-beta);
                    else
                        if beta ==2

%Pcore=Pcore+K*2*pi*h*(f_p^al)*(u*Hmaxp*Rmin)^beta*10^(beta+6)*(log(Rmax/Rmin
))/1000;

Pcore=Pcore+K*2*pi*h*(f_p^al)*(u*Hmaxp*Rmin)^beta*(log(Rmax/Rmin))*1000;
                        else

Pcore=Pcore+K*(2*pi)*h*(f_p^al)*(u*Hmaxp*Rmin)^beta*10^(beta+6)*(Rmax^(2-
beta)-Rmin^(2-beta))/(1000*(2-beta));
                        end
                    end

                    Vcore=Vcore+pi*h*(Rmax^2-Rmin^2);
                    L=E*2/Ipeak2^2;
                    %if L is in the required range,store the values and
calculate Q
                    if(L>0.95*Lwant && L<1.05*Lwant && i>=Nmincell &&
i<=Ncell && Voltage >vmin && Voltage <vmax && Rcopper<1.1*DCR_want &&
N_1(Rout,uIndex,hIndex,aIndex,1)<100)% use condition on total turns if given
inproblem statement
                        flag=1; %if match is found, flag is set to 1 else
flag is 0
                        E_1(Rout,uIndex,hIndex,aIndex)=E;
                        n=N;
                        n_1(Rout,uIndex,hIndex,aIndex,i)=n;
                        if n==0
                            break;
                        end
                        k=k+1;
                        height_plot(k)=h;
                        u_plot(k)=u/(4e-7*pi);
```

```
                        N_plot(k)=N_1(Rout,uIndex,hIndex,aIndex,1);
                        for a=1:i
                            length_1=length_1
+2*n_1(Rout,uIndex,hIndex,aIndex,a)*(R_1(Rout,uIndex,hIndex,aIndex,1)-
Rmin_1(Rout,uIndex,hIndex,aIndex,a));
                            Area_round=pi*(tcu/2)^2;

width=0.8*2*pi*(Rmin_1(Rout,uIndex,hIndex,aIndex,a)/(N_1(Rout,uIndex,hIndex,a
Index,a)));
                            Area_flat=width*tcu;
                        end

length_1=length_1+2*h*N_1(Rout,uIndex,hIndex,aIndex,1);
                        length_11(Rout,uIndex,hIndex,aIndex)=length_1;
                        length_plot(k)=length_1;
                        Area_round=pi*(tcu/2)^2;

                        Rcopper=p*length_1/(Area_round);
                        Rcopper_1(Rout,uIndex,hIndex,aIndex)=Rcopper;
                        Pcopper=Rcopper*Irms^2;
                        Pcopper_1(Rout,uIndex,hIndex,aIndex)=Pcopper;
                        Lm_1(Rout,uIndex,hIndex,aIndex)=L;
                        Pcoremax=1000*K*(f_p^al)*(Bmaxp^beta)*pi*h*(Rmax^2);
                        Pcore_1(Rout,uIndex,hIndex,aIndex)=Pcore;
                        E_1(Rout,uIndex,hIndex,aIndex)=E;
                        Q=E*2*pi*f/(Pcore+Pcopper); % Quality factor is used
for optimization
                        Q_1(Rout,uIndex,hIndex,aIndex)=Q;
                        Lcheck=0;
                        %
length_1(Rout,uIndex,hIndex,aIndex)=length_1(Rout,uIndex,hIndex,aIndex)+(R_1(
Rout,uIndex,hIndex,aIndex,1)-Rmin_1(Rout,uIndex,hIndex,aIndex,i));
                        disp(sprintf('L=%0.5g, Q=%f,
Rcopper=%0.5g,Pcopper=%0.5g, Pcore=%0.5g, ucore=%f, height=%0.5g, alpha =%f ,
', Lm_1(Rout,uIndex,hIndex,aIndex), Q_1(Rout,uIndex,hIndex,aIndex),
Rcopper_1(Rout,uIndex,hIndex,aIndex),Pcopper_1(Rout,uIndex,hIndex,aIndex),Pco
re_1(Rout,uIndex,hIndex,aIndex),ucore(uIndex),height(hIndex),
alpha(aIndex)));
```

```
                        for acc=1:i
                            disp(sprintf('R0=%f, Ri=%f,N=%f,
n=%f',R_1(Rout,uIndex,hIndex,aIndex,acc),Rmin_1(Rout,uIndex,hIndex,aIndex,acc
),N_1(Rout,uIndex,hIndex,aIndex,acc),n_1(Rout,uIndex,hIndex,aIndex,acc)));

Lcheck=Lcheck+u*height(hIndex)*N_1(Rout,uIndex,hIndex,aIndex,acc)^2*log(R_1(R
out,uIndex,hIndex,aIndex,acc)/Rmin_1(Rout,uIndex,hIndex,aIndex,acc))/(2*pi);
                        end
                        disp(sprintf('l=%0.5g',Lcheck));

                        Rm_1(Rout,uIndex,hIndex,aIndex)=Rmax;
                        hm_1(Rout,uIndex,hIndex,aIndex)=h;
                        count=count+1;
                        break;


                    elseif(L>1.05*Lwant)
                        break;

                    else
                        %go to next inner cell
                        Rmax=Rmin-slot;
                        Rmin=Rmax*a;
                        N=round(Hmax*2*pi*Rmin/Ipeak2);
                        i=i+1;

                    end
                end
                E_1(Rout,uIndex,hIndex,aIndex)=E;
                cellno(Rout,uIndex,hIndex,aIndex)=i;
                Ll_1(Rout,uIndex,hIndex,aIndex)=E*2/Ipeak2^2;

            end
        end
    end
end

Output.flag=flag;
```

```
if (flag==0)
    mess='No Design found. Please change the Input parameters.';
    Output.mess=mess;

    Output.Lm =0;
    Output.Q=0;
    Output.Rcopper=0;
    Output.Pcopper=0;
    Output.Pcore=0;
    Output.ucore=0;
    Output.height=0;
    Output.alpha=0;

    Output.a=7;
    for i=1:Output.a;
        eval(['Output.cell' num2str(i) '= '' '' ' ]);
        eval(['Output.Rmax' num2str(i) '= '' '' ' ]);
        eval(['Output.Rmin' num2str(i) '= '' '' ']);
        eval(['Output.n' num2str(i) '= '' '' ']);
        eval(['Output.Rmaxdraw' num2str(i) '= '' '' ']);
        eval(['Output.Rmindraw' num2str(i) '= '' '' ']);
    end
else
    mess='Optimized Design for Constant Alpha ';
    Output.mess=mess;
    qr=numel(Q_1);
    pqr=0;
    while pqr<qr
        pqr=pqr+1;

        [max_val,positionr]=max(Q_1(:));
        [rn,un,hn,an]=ind2sub(size(Q_1),positionr);
        if(max_val==0)
            break;
        else
            l=cellno(rn,un,hn,an);
            Lcheck=0;
            Output.Lm =Lm_1(rn,un,hn,an);
```

```
            Output.QF_DI=Q_1(rn,un,hn,an);
            Output.Rcopper=Rcopper_1(rn,un,hn,an)*1000;
            Output.Pcopper=Pcopper_1(rn,un,hn,an);
            Output.Pcore=Pcore_1(rn,un,hn,an);
            Output.ucore=ucore(un);
            Output.height=height(hn)*1000;
            Output.alpha=alpha(an);

            disp(sprintf('Distributed Inductor with highest Q factor '));
            disp(sprintf('L=%0.5g, Q=%f, Rcopper=%0.5g,
Pcopper=%0.5g,Pcore=%0.5g, ucore=%f, height=%0.5g, alpha =%f , ',
Lm_1(rn,un,hn,an),
Q_1(rn,un,hn,an),Rcopper_1(rn,un,hn,an),Pcopper_1(rn,un,hn,an),Pcore_1(rn,un,
hn,an),ucore(un),height(hn), alpha(an)));
            length=2*N_1(rn,un,hn,an,1)*height(hn);

            for a=1:l
                length=length +2*n_1(rn,un,hn,an,a)*(R_1(rn,un,hn,an,1)-
Rmin_1(rn,un,hn,an,a));
                Area_round=pi*(tcu/2)^2;
                width=0.8*2*pi*(Rmin_1(rn,un,hn,an,l)/(N_1(rn,un,hn,an,l)));
                Area_flat=width*tcu;
            end
            PracR_round=p*length/Area_round;
            Rcopper2=Rcopper_1(rn,un,hn,an);
            thickness_flat=p*length/(width*DCR_want);

            parallel= PracR_round/Rcopper_1(rn,un,hn,an);
            core_height=height(hn)+ 2*thickness_flat;
            for a=1:l
                disp(sprintf('R0=%0.5g, Ri=0.5g,N=%f,
n=%f',R_1(rn,un,hn,an,a),Rmin_1(rn,un,hn,an,a),N_1(rn,un,hn,an,a),n_1(rn,un,h
n,an,a)));
                %                disp(sprintf('length= %g, Area=%g,
PracR=%g',length,Area_round,PracR));
                eval(['Output.Rmax' num2str(a) '=R_1(rn,un,hn,an,a)*1000']);
                eval(['Output.Rmin' num2str(a)
'=Rmin_1(rn,un,hn,an,a)*1000']);
```

```
                eval(['Output.n' num2str(a) '=n_1(rn,un,hn,an,a)']);
                eval(['Output.N' num2str(a) '=N_1(rn,un,hn,an,a)']);
                eval(['Output.Rmaxdraw' num2str(a)
'=Rmaxdraw(rn,un,hn,an,a)*1000']);
                eval(['Output.Rmindraw' num2str(a)
'=Rmindraw(rn,un,hn,an,a)*1000']);
                turns(a)=n_1(rn,un,hn,an,a);
                Radius(a)=Rmin_1(rn,un,hn,an,a);
                OuterR=R_1(rn,un,hn,an,1);
                %
Lcheck=Lcheck+u*height(i)*N_1(rn,un,hn,an,a)^2*log(R_1(rn,un,hn,an,a)/Rmin_1(
rn,un,hn,an,a))/(2*pi);
            end
        end
        break;
    end

    NN=N_1(rn,un,hn,an,1);
    Output.a=a;
    Output.PracR_round=PracR_round*1000;
    Output.PracR_flat=thickness_flat*1000;
    Output.width_flat=width*1000;
    Output.core_height=core_height*1000;
    Output.overall_fp=(2*R_1(rn,un,hn,an,1)+2*thickness_flat)*1000;
    Output.overall_fp2=Output.overall_fp;
    Output.N_DI=N_1(rn,un,hn,an,1);
    Output.Length_DI=length*1000;
    slots(turns,NN,angle,l,Radius); %calls the function Slots to plot the
slot vs angle
    % Constant width uses the maximum and minimum radius and height
    % and ucore from the constant alpha optimized case
    %conventional
    Ca=1:0.1:100;
    xa=0.1:0.01:1;
    alpha_check=1;
    ncc=N_1(rn,un,hn,an,1);
    rcc=Rmin_1(rn,un,hn,an,1);
    u=ucore(un)*u0;
```

```
    for caIndex=1:size(Ca,2)
        ca=Ca(caIndex)*0.001;
        for xIndex=1:size(xa,2)
            x=xa(xIndex);
            Ncc=(N_1(rn,un,hn,an,1)*ca/Rmin_1(rn,un,hn,an,1));

            Ec=ucore(un)*u0*height(hn)*Ipeak2^2*Ncc^2*log(1/x)/(4*pi);
            Lc=ucore(un)*u0*height(hn)*Ncc^2*log(1/x)/(2*pi);
            Hmaxp=Bmaxp/(ucore(un)*u0);
            if (Lc>0.99*Lwant && Lc<1.01*Lwant)
                rrr=((2*R_1(rn,un,hn,an,1))+2*thickness_flat)^2;
                fp_c=2*(ca/x)+2*thickness_flat;
                fpac=fp_c^2;
                rfpac=fpac/rrr;

                %Core loss
                pcore_c=0;

Pcorec=K*2*pi*height(hn)*(f_p^al)*(u*Hmaxp*ca)^beta*(log(1/x))*1000;
                Rcorec=pcore_c/Ipeak^2;
                Rcorec_1(alpha_check)=Rcorec;
                length_c=2*Ncc*((ca/x)-ca)+2*(Ncc*height(hn));
                Area_round=pi*(tcu/2)^2;
                Area_flat=width*thickness_flat;
                DCR_round=1.72e-8*length_c/(Area_round);
                DCR_flat=1.72e-8*length_c/(Area_flat);
                culoss=p*log(1/x)*Ncc^2/(pi*tcu);
                Rsidec=(p*height(hn)/(2*pi*tcu))*(Ncc^2 * (ca/x)+Ncc*ca);
                Rcopperc=culoss+Rsidec;
                Pcopperc=DCR_round*Irms^2;
                induc_height=height(hn)+2*thickness_flat;
                fp_c=2*(ca/x)+2*thickness_flat;
                Qcc=2*pi*f*Ec/(Pcopperc+pcore_c);
                Qcc_1(alpha_check)=Qcc;
                alphac(alpha_check)=x;
                rminc(alpha_check)=ca;
                Rmaxc(alpha_check)=ca/x;
                rfpa_1(alpha_check)=rfpac;
```

```
            Qcc_1(alpha_check)=Qcc;
            Lcc_1(alpha_check)=Lc;
            Ncc_1(alpha_check)=round(Ncc);
            Rcopperc_1(alpha_check)=Rcopperc;
            Pcopperc_1(alpha_check)=Pcopperc;
            Pcorec_1(alpha_check)=Pcorec;
            length_c_1(alpha_check)=length_c*1000;
           DCR_round_1(alpha_check)=DCR_round*1000;
           DCR_flat_1(alpha_check)=DCR_flat*1000;
           induc_height_1(alpha_check)=induc_height*1000;
           fpcc_1(alpha_check)=fp_c*1000;
            alpha_check=alpha_check+1;
            break;
        end

    end
end
qq=numel(rfpa_1);
pqq=0;
while pqq<qq
    pqq=pqq+1;

    [min_val,positionr]=min(rfpa_1(:));
    [mi]=ind2sub(size(rfpa_1),positionr);
    if min_val~=0
        Output.cRmin=rminc(mi)*1000;
        Output.cRmax=Rmaxc(mi)*1000;
        Output.cucore= ucore(un);
        Output.core_height_c= height(hn)*1000;
        Output.length_c= length_c_1(mi);
        Output.DCR_round= DCR_round_1(mi);
        Output.DCR_flat= DCR_flat_1(mi);
        Output.Copper_loss_c= Pcopperc_1(mi);
        Output.pcorec= Pcorec_1(mi);
        Output.QF_c= Qcc_1(mi);
        Output.inductor_height_c= induc_height_1(mi);
        Output.fp_1= fpcc_1(mi);
        Output.fp_2= fpcc_1(mi);
```

```
            Output.Ncc=Ncc_1(mi);
            Output.fpac=rfpa_1(mi);
            Output.calpha=alphac(mi);
            Output.Lcc=Lcc_1(mi);
            %Output.pcorec=pcorec_1(mi);

            disp(sprintf('Conventional Toroid with least foot print area'));
            disp(sprintf(' alpha=%f, rmin=%f,  Rmax=%f,fpac_1=%0.5g, Ncc=%f,
height =%f, ucore =%f, LLcc=%0.5g, Qcc=%f\n core=%f r=%f',
alphac(mi),rminc(mi), Rmaxc(mi),rfpa_1(mi),Ncc_1(mi), height(hn),
ucore(un),Lcc_1(mi),Qcc_1(mi),Pcorec_1(mi),Pcopperc_1(mi) ));
            break;


        end
    end
end
```

Slots:

```
function slots(turns,NN,angle,l,Radius)
i=l;
N=NN;
%      OR=OuterR;
     stepValue = angle/N;
            slotN = stepValue: stepValue:angle;
             prevSlot = [];
figure;
            H=gca;
            YTickValues=[];
            for count=i:-1:1
                YTickValues=[YTickValues Radius(count)];
            end
     %       YTickValues=[YTickValues OuterR];
           XTickValues=slotN;
          set(H, 'XTickMode', 'manual', 'YTickMode', 'manual', 'XTick',
XTickValues ,'YTick', YTickValues); grid on; hold on;
            for count=i:-1:1
                R(count)=Radius(count);
```

```
            n=turns(count);
            slot_s=FindSlots(n, prevSlot, stepValue, slotN,angle);
           % slot(count)=slot_s;
            plot(slot_s,R(count)*ones(size(slot_s)),'s');
            prevSlot = [prevSlot slot_s];

        end
```

FindSlotS:

```
function finalSlots = FindSlots(n, prevSlots, offsetValue, slotN, angle)
stepValue = angle/n;
slots = stepValue: stepValue: angle;

for jkl = 1: length(slots)
    [minVal minIndex] = min(abs(slotN - slots(jkl)));
    finalSlots(jkl) = slotN(minIndex);
    while(~isempty(find(abs(prevSlots - finalSlots(jkl)) == 0)))
        finalSlots(jkl) = mod(finalSlots(jkl) + offsetValue, angle);
    end
    prevSlots = [prevSlots finalSlots(jkl)];
end
```

REFERENCES

[1] D. M. Robert W Erickson, "Basic Magnetics Theory," in *Fundamentals of Power Electronics,* 2 ed.: Springer, 2001, pp. 491-585.

[2] A. F. Goldberg and M. F. Schlecht, "The relationship between size and power dissipation in a 1-10 MHz transformer," *Power Electronics, IEEE Transactions,* vol. 7, pp. 63-74, 1992.

[3] E.C.Snelling, *Soft Ferrites: Properties and Applications*, 2nd ed.: Butterworths, 1988, pp. 136-157.

[4] G. Skutt and F. C. Lee, "Visualization of magnetic flux density in ferrite core structures," in *Computers in Power Electronics, 1994., IEEE 4th Workshop on,* 1994, pp. 307-312.

[5] L. Qiang and F. C. Lee, "High Inductance Density Low-Profile Inductor Structure for Integrated Point-of-Load Converter," in *Applied Power Electronics Conference and Exposition, 2009. APEC 2009. Twenty-Fourth Annual IEEE,* 2009, pp. 1011-1017.

[6] E. Herbert, "Flat Matrix Transformers," U.S. Patent 4 665 357, May 12, 1987.

[7] K. D. T. Ngo, E. Alpizar, and J. K. Watson, "Modeling of losses in a sandwiched-winding matrix transformer," *Power Electronics, IEEE Transactions on,* vol. 10, pp. 427-434, 1995.

[8] E. J. Osegueda and K. D. T. Ngo, "Analysis and design of perforated-plate matrix transformers," in *Power Electronics Specialists Conference, 1992. PESC '92 Record., 23rd Annual IEEE,* 1992, pp. 1393-1400 vol.2.

[9] S. Kirli, K. D. T. Ngo, W. M. Polivka, and M. M. Walters, "Inductance modeling for a mode-2 perforated-plate matrix inductor/transformer," in *Power Electronics Specialists Conference, 1993. PESC '93 Record., 24th Annual IEEE,* 1993, pp. 1130-1136.

[10] R. S. Lai, K. D. T. Ngo, and J. K. Watson, "Steady-state analysis of the symmetrical push-pull power converter employing a matrix transformer," *Power Electronics, IEEE Transactions on,* vol. 7, pp. 44-53, 1992.

[11] K. D. T. Ngo, E. Alpizar, and J. K. Watson, "Modeling of magnetizing inductance and leakage inductance in a matrix transformer," *Power Electronics, IEEE Transactions on,* vol. 8, pp. 200-207, 1993.

[12] M. H. A. H. Feingold, R. L. Wahlers, M. A. Stein, "Materials for Capacitive and Inductive Components Integrated with Commercially Available LTCC Systems," presented at the IMAPS 2003, 2003.

[13] M. S. Rylko, K. J. Hartnett, J. G. Hayes, and M. G. Egan, "Magnetic Material Selection for High Power High Frequency Inductors in DC-DC Converters," in *Applied Power Electronics Conference and Exposition, 2009. APEC 2009. Twenty-Fourth Annual IEEE*, 2009, pp. 2043-2049.

[14] H. Yehui, G. Cheung, L. An, C. R. Sullivan, and D. J. Perreault, "Evaluation of magnetic materials for very high frequency power applications," in *Power Electronics Specialists Conference, 2008. PESC 2008. IEEE*, 2008, pp. 4270-4276.

[15] K. W. E. Cheng and P. D. Evans, "Optimisation of high frequency inductor design of series resonant converter," in *Power Electronics Specialists Conference, 1992. PESC '92 Record., 23rd Annual IEEE*, 1992, pp. 1416-1422 vol.2.

[16] J. A. Ferreira, "Improved analytical modeling of conductive losses in magnetic components," *Power Electronics, IEEE Transactions on*, vol. 9, pp. 127-131, 1994.

[17] J. D. Lavers and V. Bolborici, "Loss comparison in the design of high frequency inductors and transformers," *Magnetics, IEEE Transactions on*, vol. 35, pp. 3541-3543, 1999.

[18] C. R. Sullivan, L. Weidong, S. Prabhakaran, and L. Shanshan, "Design and Fabrication of Low-Loss Toroidal Air-Core Inductors," in *Power Electronics Specialists Conference, 2007. PESC 2007. IEEE*, 2007, pp. 1754-1759.

[19] Available: http://www2.dupont.com/MCM/en_US/assets/downloads/prodinfo/7740.pdf

[20] Available: http://www.home.agilent.com/agilent/product.jspx?cc=US&lc=eng&nid=-33831.536879654&&cc=US&lc=eng

[21] Available: http://www.coilws.com/images/E70340-010%20Rev%20D1-Web.pdf

[22] Available: http://www.micrometals.com/

[23] Available: http://www.mag-inc.com/

[24] G. S. J. Bielawski, Midcom, Inc. & A. H. Feingold, C. Y. D. Huang, M. R. Heinz, R. L. Wahlers, , "Low Profile Transformers Using Low Temperature Co-Fire Magnetic Tape," presented at the IMAPS 2003, 2003.

[25] W. Laili, P. Yunqing, Y. Xu, S. Bo, W. Zhaoan, and Z. Guopeng, "Evaluation of LTCC capacitors and inductors in DC/DC converters," in *Applied Power Electronics Conference and Exposition (APEC), 2010 Twenty-Fifth Annual IEEE*, 2010, pp. 2060-2065.

[26] M. H. Lim, J. Dong, J. D. van Wyk, T. C. Lee, and K. D. T. Ngo, "Shielded LTCC Inductor as Substrate for Power Converter," in *Power Electronics Specialists Conference, 2007. PESC 2007. IEEE*, 2007, pp. 1605-1611.

[27] M. H. Lim, Z. Liang, and J. D. v. Wyk, "An improved low profile integratable LTCC power inductor for microprocessor power delivery applications," *Integrated Power Systems (CIPS), 2006 4th International Conference on*, pp. 1-6, 2006.

[28] M. H. Lim, J. D. van Wyk, F. C. Lee, and K. D. T. Ngo, "A Class of Ceramic-Based Chip Inductors for Hybrid Integration in Power Supplies," *Power Electronics, IEEE Transactions on*, vol. 23, pp. 1556-1564, 2008.

[29] M. H. F. Lim, Z. Liang, and J. D. van Wyk, "Low profile integratable inductor fabricated based on LTCC technology for microprocessor power delivery applications," in *Applied Power Electronics Conference and Exposition, 2006. APEC '06. Twenty-First Annual IEEE*, 2006, p. 7 pp.

[30] L. wang, Y. Pei, X. Yang, and Z. Wang, "Design of Ultra-thin LTCC Coupled Inductors for Compact DC/DC Converters," *Power Electronics, IEEE Transactions on*, vol. PP, pp. 1-1, 2011.

[31] M. Mingkai, L. Qiang, D. Gilham, F. C. Lee, and K. D. T. Ngo, "New core loss measurement method for high frequency magnetic materials," in *Energy Conversion Congress and Exposition (ECCE), 2010 IEEE*, 2010, pp. 4384-4389.

[32] M. Nigam and C. R. Sullivan, "Multi-layer folded high-frequency toroidal inductor windings," in *Applied Power Electronics Conference and Exposition, 2008. APEC 2008. Twenty-Third Annual IEEE*, 2008, pp. 682-688.

[33] K. Chan-Young, K. Hee-Jun, and K. Jong-Ryoul, "An integrated LTCC inductor," *Magnetics, IEEE Transactions on*, vol. 41, pp. 3556-3558, 2005.

[34] M. H. F. Lim and J. D. van Wyk, "Applying the Steinmetz Model to Small Cores in LTCC Ferrite for Integration Applications," in *Applied Power Electronics Conference and Exposition, 2009. APEC 2009. Twenty-Fourth Annual IEEE*, 2009, pp. 1027-1033.

[35] Available: http://www.ansys.com/Products/Simulation+Technology/Electromagnetics/Electromechanical+&+Power+Electronics+&+Mechatronics/ANSYS+Maxwell